

**UNIVERSIDADE DE SÃO PAULO
INSTITUTO DE QUÍMICA**

Programa de Pós-Graduação em Química

JHONATAN LUIZ FIORIO

**Catalysis at gold-ligand interfaces: a frustrated
Lewis pair mechanism for selective reduction
reactions**

Versão corrigida da Tese defendida

São Paulo

Data do Depósito na SPG:

04/10/2019

JHONATAN LUIZ FIORIO

**Catalysis at gold-ligand interfaces: a frustrated
Lewis pair mechanism for selective reduction
reactions**

*A thesis submitted to the Institute of
Chemistry of the University of São Paulo for
the degree of Doctor of Science*

Advisor: Profa. Dra. Liane Marcia Rossi

São Paulo

2019

Autorizo a reprodução e divulgação total ou parcial deste trabalho, por qualquer meio convencional ou eletrônico, para fins de estudo e pesquisa, desde que citada a fonte.

Ficha Catalográfica elaborada eletronicamente pelo autor, utilizando o programa desenvolvido pela Seção Técnica de Informática do ICMC/USP e adaptado para a Divisão de Biblioteca e Documentação do Conjunto das Químicas da USP

Bibliotecária responsável pela orientação de catalogação da publicação:
Marlene Aparecida Vieira - CRB - 8/5562

F519c Fiorio, Jhonatan Luiz
Catalysis at gold-ligand interfaces: a frustrated Lewis pair mechanism for selective reduction reactions / Jhonatan Luiz Fiorio. - São Paulo, 2019.
192 p.

Tese (doutorado) - Instituto de Química da Universidade de São Paulo. Departamento de Química Fundamental.

Orientador: Rossi, Liane Marcia

1. gold nanoparticles. 2. ligand effect. 3. hydrogenation. 4. alkynes. 5. nitrogen-doped carbon.
I. T. II. Rossi, Liane Marcia, orientador.

To my family, for their endless love, continuous support and
encouragement.

ACKNOWLEDGMENTS

First of all, I would like to thank my supervisor, Prof. Liane M. Rossi, who gave me a brilliant opportunity to work in her group. Apart from owning outstanding knowledge of chemistry and passion for research, Liane showed kindness and patience and proved to be a very caring leader, whose support, advice and encouragement constantly guided me on the long road of this project.

I thank Prof. Núria López from ICIQ - Spain, as her help, discussions, and co-operation were invaluable for this work. I would like also to thank Prof. A. Stephen K. Hashmi for accepting me and all the support during my stay in his group in Heidelberg. I also thank Prof. Pedro H. C. Camargo, Prof. Renato V. Gonçalves, Dr. Érico T. Neto and Dr. Matthias Rudolph for a great collaborative experience.

I also express my gratitude to past and present members of Prof. Rossi's and Prof. Hashmi's group not only colleagues but also friends and everyone else who has made my life interesting and fun during these years. My special thanks go to my good friends Dr. Fernanda P. Silva, Dr. Marco A. S. Garcia, Tiago Rosa, Nágila E. C. Maluf and Danielle K. Kikuchi, for their unconditional support creating a relaxed work environment and enhancing the Ph.D. experience. I am also grateful to my friends/brothers Matheus Bofinger, Eduardo Duarte and Fabiano Bueno for the unconditional friendship, for their support during tough times and the opportunity to keep on exchanging fundamental knowledge for my life. During my internship in Heidelberg, I met

one of the most brilliant people in the world, my BFF Shaista Tahir. Thank you for the great and productive talks in the coffee room. I learned a lot from you. I also got to know two “crazy women”, that have cheer up my days in Germany, a big thanks to Rita and Honey, I love you girls. I also would like to thank Eduardo C. M. Barbosa who has helped, encouraged and supported me and shared both tough and bright moments during this journey.

I am thankful for the help and support of technical staff at the University of São Paulo and Heidelberg University, without which none of this research would have been possible. I am forever grateful to Suzana C. do Rosário, Petra Krämer, and Alexander Flatow. I would especially like to thank Fabiane C. Fogo besides helping in daily lab organization, she has become a great friend who has always helped either with comforting words or making me laugh with her adventures.

I acknowledge LNLS – Brazilian Synchrotron Light Laboratory, CNPEM/MCTI for the SXS experimental facilities and LNNano - Brazilian Nanotechnology National Laboratory, CNPEM/MCTI for the TEM facilities. I also thank the Brazilian government agencies FAPESP (Grant 2016/16738-7), CNPq, and CAPES for financial support. I also thank CAPES for the Ph.D. fellowship in Brazil (Grant 33002010191P0) and CAPES-DAAD-CNPQ that provided a Ph.D. fellowship (Grant 88887.161404/2017-00) during the time in Germany.

Last but actually most important, I am very grateful for my loving family. Without their advice, support and love I wouldn't even be close to where I am right now.

*“What screws us up most in life is the picture in our heads of how it’s
supposed to be”*

Socrates

RESUMO

Fiorio, J.L. **Catalise na interface ouro-ligante: pares de Lewis frustrados aplicados em reações de redução seletivas**. 2019. 192 p. Tese (Doutorado) - Programa de Pós-Graduação em Química. Instituto de Química, Universidade de São Paulo, São Paulo.

A interação dos ligantes orgânicos com nanopartículas de metal certamente tem um papel muito importante para aplicações em catálise, bem como outros processos envolvendo ligantes que podem ativar ou envenenar a superfície de nanopartículas metálicas. Até agora, muito pouco foi estudado sobre o papel dos ligantes orgânicos utilizados na preparação de nanopartículas para aplicações em catálise ou adição na reação para ativar o catalisador. Nesta tese, foram estudadas estratégias para a síntese de nanopartículas metálicas, seu uso como componentes para a preparação de catalisadores suportados e processos de ativação e desativação envolvendo ligantes empregados como estabilizantes ou propositalmente adicionados ao meio de reação ou suporte para estimular novas reatividades e seletividade em reações de interesse industrial, como reações de hidrogenação. Aqui, o conceito de pares de Lewis frustrados (FLPs) foi expandido para o seu análogo de superfície formado pela combinação de nanopartículas (NPs) de ouro e bases de Lewis, como aminas ou fosfinas, criando um novo canal para a clivagem heterolítica de H₂ e, assim, realizando reações seletivas de hidrogenação com ouro. Uma primeira abordagem para melhorar a atividade catalítica das nanopartículas de ouro foi analisar o efeito de bases contendo nitrogênio. As nanopartículas de ouro inicialmente inativas tornaram-se altamente ativas para a hidrogenação seletiva de alquino em *cis-alquenos*. A hidrogenação prosseguiu foi factível e totalmente seletiva usando H₂ como fonte de hidrogênio e sob condições relativamente amenas (80 °C, 6 bar de H₂). Nossos estudos também revelaram que a presença de estabilizantes pode bloquear a adsorção da base na superfície do ouro, impedindo a formação da interface FLPs e, portanto, levando a baixa atividade catalítica. Quando os estabilizantes foram removidos da superfície do catalisador e um ligante foi adicionado, o FLPs é formado sendo a atividade catalítica aprimorada. Além disso, demonstramos o uso bem-sucedido de ligantes organofosforados atuando como ativadores de Au NPs em uma série de importantes reações de redução, como, epóxidos, N-óxidos, sulfóxidos e alquinos. Além disso, a escolha do ligante fosforado resultou em uma diminuição na quantidade necessária para alcançar alta conversão mantendo a seletividade inalterada. A relação ligante/metal diminuiu de 100/1 (amina/Au) para 1/1 (fosfito/Au). A síntese de nanopartículas de ouro suportadas em carbono dopado com nitrogênio foi utilizada como método alternativo para a síntese de um catalisador heterogêneo de ouro ativo para hidrogenações seletivas. A principal vantagem em relação aos estudos anteriores foi evitar a adição de ligantes externos, em grande excesso, para a ativação de superfícies de ouro via FLP, tornando todo o processo ambiental e economicamente atraente.

Keywords: nanopartículas de ouro, efeito de ligante, hidrogenação, alquinos alquenos, carbono dopado com nitrogênio.

ABSTRACT

Fiorio, J.L. **Catalysis at gold-ligand interfaces: a frustrated Lewis pair mechanism for selective reduction reactions**. 2019. 192 p. PhD Thesis - Graduate Program in Chemistry. Instituto de Química, Universidade de São Paulo, São Paulo.

The interaction of the organic ligands with metal nanoparticle has a very important role for applications in catalysis, as well as other processes involving ligands that can activate or poison the surface of metal nanoparticles. Very little has been studied so far on the role of organic ligands used either in the preparation of nanoparticles for applications in catalysis or addition in the reaction to activate the catalyst. In this thesis, we have studied strategies for the synthesis of metal nanoparticles, their use as components for the preparation of supported catalysts and activation and deactivation processes involving the ligands used as stabilizers or purposely added to the reaction medium or support for stimulate new reactivity and selectivity in reactions of industrial interest, such as hydrogenation. Here, the concept of frustrated Lewis pairs (FLPs) has been expanded to surface-FLP analogous formed by combining gold nanoparticles (NPs) and Lewis bases, such as amines or phosphines, creating a new channel for the heterolytic cleavage of H₂, and thereby performing selective hydrogenation reactions with gold. A first approach to improve the catalytic activity of gold nanoparticles was to analyze the effect of nitrogen-containing bases. The starting inactive gold nanoparticles became highly active for the selective hydrogenation of alkyne into *cis*-alkenes. The hydrogenation proceeded smoothly and fully selective using H₂ as the hydrogen source and under relatively mild conditions (80 °C, 6 bar H₂). Our studies also have revealed that the presence of capping ligands blocks the adsorption of the amine to the gold surface, avoiding the FLPs interface and thereby leading to low catalytic activity. When the capping ligands were removed from the catalyst surface and an amine ligand was added, the FLPs interface is recovered and an enhanced catalytic activity was observed. Furthermore, we have demonstrated the successful use of simple organophosphorus ligands to boost the catalytic activity of Au NPs for a range of important reduction reactions, namely, epoxides, N-oxides, sulfoxides, and alkynes. Furthermore, the choice of phosphorus-containing ligands resulted in a decrease in the amount necessary to reach high conversion and selectivity in comparison with our previous study with N-containing ligands. The ligand-to-metal ratio decreased from 100 (amine/Au) to 1 (phosphite/Au). The synthesis of gold nanoparticles supported on N-doped carbon supports was used as an alternative method for the synthesis of a heterogeneous active gold catalyst for selective hydrogenations. The main advantage with respect to previous studies was to avoid the addition of external ligands, in large excess, for the activation of gold surfaces via FLP, making the whole process environmentally and economically attractive.

Keywords: gold nanoparticles, ligand effect, hydrogenation, alkynes, alkenes, nitrogen-doped carbon.

ABBREVIATION GLOSSARY

NP(s) – Nanoparticle(s)

TON – Turnover Number

TOF – Turnover Frequency

TEM – Transmission Electron Microscopy

EDX – Energy Dispersive X-Ray

HAADF – High Angle Annular Dark Field

FAAS – Flame atomic absorption spectroscopy

DRS/DR UV-vis – Diffuse reflectance UV-vis

GC – Gas Chromatography

XRD – X-ray Diffraction

JCPDS-ICDD – Joint Committee on Powder Diffraction Standards International
Centre for Diffraction Data

XPS – X-ray Photoelectron Spectroscopy

IR – Infrared Spectroscopy

ICP-OES – Inductively Coupled Plasma-Optical Emission Spectrometry

NMR – Nuclear magnetic resonance

DFT – Density Functional Theory

FLP – Frustrated Lewis Pairs

LA – Lewis Acid

LB – Lewis Base

PVP – Polyvinylpyrrolidone

PVA – Poly(vinyl alcohol)

STEM - Scanning transmission electron microscopy

TGA – Thermogravimetric analysis

DTG - Derivative Thermogravimetric Analysis

SUMMARY

1. INTRODUCTION	21
1.1. HYDROGENATION REACTIONS.....	21
1.2. GOLD APPLIED IN HYDROGENATION REACTIONS.....	23
1.3. FRUSTRATED LEWIS PAIRS.....	25
1.4. REFERENCES.....	28
2. OBJECTIVES	32
2.1. GENERAL OBJECTIVE	32
2.2. SPECIFIC OBJECTIVES.....	32
3. CHAPTER 1	34
3.1. MOTIVATION.....	35
3.2. RESULTS AND DISCUSSION	38
3.3. CONCLUSIONS.....	54
3.4. EXPERIMENTAL SECTION.....	55
3.4.1. Materials and Methods	55
3.4.2. Preparation of Au/SiO ₂ and Au/Fe ₃ O ₄ @SiO ₂	56
3.4.3. Preparation of Au/Support (TiO ₂ ; CeO ₂ and Al ₂ O ₃).....	57
3.4.4. General procedure for catalytic hydrogenation of alkynes.....	58
3.4.5. Recycling experiment	59
3.4.6. Scale-up hydrogenation of alkynes.....	59
3.4.7. Catalytic hydrogenation using limited amount of H ₂	60
3.4.8. Isotope H ₂ -D ₂ Exchange Reaction	60
3.4.9. Determination of the isotopic effect.....	61
3.4.10. Computational Details	61
3.5. REFERENCES.....	62

4. CHAPTER 2	71
4.1. MOTIVATION	72
4.2. RESULTS AND DISCUSSION	74
4.3. CONCLUSIONS	87
4.4. EXPERIMENTAL SECTION	88
4.4.1. Materials and Methods	88
4.4.2. Catalysts preparation	89
4.4.3. Thermal treatment to remove the ligand	91
4.4.4. Catalytic Investigations	91
4.5. REFERENCES	93
5. CHAPTER 3	98
5.1. MOTIVATION	99
5.2. RESULTS AND DISCUSSION	101
5.3. CONCLUSIONS	116
5.4. EXPERIMENTAL SECTION	117
5.4.1. Materials and Methods	117
5.4.2. Catalyst preparation	118
5.4.3. Catalytic investigations	118
5.5. REFERENCES	120
6. CHAPTER 4	128
6.1. MOTIVATION	129
6.2. RESULTS AND DISCUSSION	132
6.3. CONCLUSIONS	154
6.4. EXPERIMENTAL SECTION	155
6.4.1. Materials and methods	155
6.4.2. Catalyst preparation	157

6.4.3. Catalytic procedures	157
6.5. REFERENCES	158
7. GENERAL CONCLUSIONS	166
8. PERSPECTIVES	168
APPENDICES	169
Appendice A1. Permissions	169
Appendice A2. NMR	178
Appendice A3. Curricular Summary	190

List of Tables

Table 1. Phenylacetylene hydrogenation by Au catalysts promoted by piperazine ^a	43
Table 2. Scope of semi-hydrogenation of alkynes to alkenes using Au/SiO ₂ and piperazine B10 . ^a	46
Table 3. Hydrogenation of various alkynes using Au/SiO ₂ and piperazine ^a	47
Table 4. Reaction, ΔE , and activation energies, E_a , for heterolytic H ₂ dissociation at the N-ligand/Au(111) interface and the imaginary frequencies for the transition states, ν_i in cm ⁻¹ . All energies in eV. On the clean Au(111) surface dissociation is homolytic in nature.	51
Table 5. Hydrogenation of phenylacetylene 1a under a limited hydrogen amount. ^a	54
Table 6. Catalytic activity of Au catalysts in the hydrogenation of phenylacetylene 1a . ^a	79
Table 7. Semihydrogenation of various alkynes to alkenes. ^a	83
Table 8. Influence of organophosphorus ligands on the conversion of styrene epoxide 1a into styrene 2a catalyzed by Au/SiO ₂ . ^a	104
Table 9. Screening of reaction conditions. ^a	106
Table 10. Chemoselective reduction of epoxides to alkenes catalyzed by Au/SiO ₂ and triethylphosphite L10. ^a	110
Table 11. Selective deoxygenation of pyridine N-oxides catalyzed by Au/SiO ₂ and triethylphosphite L10. ^a	111
Table 12. Hydrogenation of sulfoxides. ^a	112
Table 13. Catalytic hydrogenation of alkynes. ^a	113
Table 14. Catalytic activity in the hydrogenation of phenylacetylene of Au@N-doped carbon catalysts obtained from Au-L1/TiO ₂ after pyrolysis at different temperatures. ^a	134
Table 15. Catalytic activity in the hydrogenation of phenylacetylene of Au@N-doped carbon catalysts obtained with different N-containing ligands, after pyrolysis at 400 °C. ^a	135

Table 16. Effect of catalysts support in the hydrogenation of phenylacetylene 1a . ^a	137
Table 17. Screening of reaction conditions in the hydrogenation of phenylacetylene 1a . ^a	138
Table 18. Au@N-doped carbon/TiO ₂ catalyst for the semihydrogenation of alkynes to alkenes. ^{a,b}	150
Table 19. Summary of results reported for semihydrogenation of alkynes with heterogeneous gold-based catalyst with and without addition of ligands.	151
Table 20. Selective hydrogenation of 1a in the presence of molecules with other reducible functional groups by Au@N-doped carbon/TiO ₂ catalyst. ^a	152
Table 21. Selective hydrogenation of other functional groups by Au@N-doped carbon/TiO ₂ catalyst. ^a	153

List of Figures

Figure 1. Scheme of hydrogenation of alkynes. (MOLNÁR; SÁRKÁNY; VARGA, 2001).....	22
Figure 2. Examples of activation of small molecules with frustrated Lewis pairs. (MELEN, 2018).....	26
Figure 3. (a) TEM image, (b) size distribution histogram and (c) UV-vis spectrum and (d) XRD pattern of Au/SiO ₂	39
Figure 4. Screening of nitrogen-containing bases for phenylacetylene 1a hydrogenation with Au/SiO ₂ catalyst. Reaction conditions: 1 mmol 1a , 0.01 mmol Au (50 mg Au/SiO ₂), 1 mmol amine, 2 mL of ethanol, 100 °C, 6 bar H ₂ , 24 h.	40
Figure 5. Catalyst recycling of the hydrogenation of phenylacetylene catalyzed by Au/Fe ₃ O ₄ @SiO ₂ catalyst. Reaction conditions: 1 mmol phenylacetylene, 0.01 mmol Au (Au/Fe ₃ O ₄ @SiO ₂), 1 mmol piperazine, 2 mL of ethanol, 80°C, 6 bar H ₂	41
Figure 6. Time course of hydrogenation of phenylacetylene catalyzed by Au/SiO ₂ with increasing amounts of piperazine: a) 0.04 mmol; b) 0.4 mmol; c) 2 mmol and d) 4 mmol. Reaction conditions: 4 mmol phenylacetylene, 0.04 mmol Au, 0.04 – 4 mmol of amine, 8 mL of ethanol, 80 °C, 6 bar H ₂	44
Figure 7. Reaction energy profiles with the corresponding configurations for the hydrogenation of 1-phenyl-1-propyne 19a . The inset corresponds to the charge distribution with respect to the neutral fragments after the first hydrogenation step. The separation between the yellow-blue colors indicates the electrostatic interactions. Yellow spheres represent Au, blue N, black C, and white H.	49
Figure 8. Transition state geometries for the hydrogenation of 1-phenyl-1-propyne 19a . Yellow spheres represent Au, blue N, black C, and white H.....	50
Figure 9. Activation energies for heterolytic H ₂ dissociation at the N-ligand/Au(111) interface.	52
Figure 10. Plot of the conversion of phenylacetylene determined using Au NPs and piperazine with H ₂ (squares) and D ₂ (circles). Reaction conditions: 4 mmol phenylacetylene, 0.04 mmol Au, 4 mmol of amine, 8 mL of ethanol, 100 °C, 6 bar H ₂ or D ₂	53
Figure 11. TEM images of nanoparticles before and after thermal treatment (a, e) Au _{PVA} /C, (b, f) Au _{PVP} /C, (c, g) Au _{Oley} /C, (d, h) Au _{Citr} /C.	74

Figure 12. Size distribution of Au NPs before and after thermal (a, e) Au _{PVA} /C, (b, f) Au _{PVP} /C, (c, g) Au _{oley} /C, (d, h) Au _{citrate} /C.	75
Figure 13. UV-vis spectra of Au NPs according to the different stabilizers.	76
Figure 14. FTIR spectra of the (a) Au _{PVA} /C, (b) Au _{PVP} /C, (c) Au _{Cit} /C, (d) Au _{Oley} /C catalysts.	77
Figure 15. a) Time course studies comparing the reaction profile of the calcined catalysts with addition of piperazine b) Au _{PVA} /C; c) Au _{PVP} /C; d) Au _{Citr} /C; e) Au _{Oley} /C; Reaction conditions: 4 mmol of alkyne, 0.5 mol% of Au, 4 mmol of piperazine, 8 mL of EtOH, 80 °C, 6 bar of H ₂	81
Figure 16. Reaction rates performance of the Au _{PVA} /C catalyst thermal treated in different temperatures.	82
Figure 17. a) Hot filtration test and b) Recycling experiments	84
Figure 18. TEM image of Au _{PVA} /C thermal treated after fifth-run reactions.	85
Figure 19. Scheme showing the differences in the activity of Au NPs with and without capping ligand.	86
Figure 20. a) Timepoint study and recycles of Au/SiO ₂ catalysts using with and without triethylphosphite L10 as ligand for the hydrogenation of styrene epoxide; b) Hot filtration test; c) TEM image and size distribution of fresh Au/SiO ₂ catalyst (Scale bar, 100 nm) and d) after the fifth reuse (Scale bar, 25 nm). Reaction conditions: 1 mmol of epoxide, 1 mol% of Au, 1 mol% of L10, 2 mL of <i>i</i> -PrOH, 100 °C, 6 bar of H ₂ , 6 h.	108
Figure 21. Hammett plot for hydrogenation of substituted alkynes catalyzed by Au/SiO ₂ and L10.	116
Figure 22. Schematic illustration of the synthesis of Au@N-doped carbon/TiO ₂ catalysts.	132
Figure 23. TGA (solid) and DTG (dashed) profile of the precursor Au-L1/TiO ₂ under N ₂	133
Figure 24. HAADF and STEM bright field images of Au-L1/TiO ₂ (a and b), and Au/TiO ₂ (d and e). The respective particle size distribution histograms (c and f). Both catalysts were prepared via pyrolysis at 400 °C for 2 h under N ₂ flow. ..	139
Figure 25. A) XRD pattern of Au-L1/TiO ₂ ; b) UV-Vis diffuse reflectance spectra (UV-Vis DRS) of Au-L1/TiO ₂ and Au/TiO ₂ . All characterized catalysts were prepared via pyrolysis at 400 °C for 2 h under N ₂ flow.	140
Figure 26. EDX spectrum from the Au@N-doped carbon catalyst.	141

- Figure 27.** (a) Bright field STEM image of a representative area of the Au@N-doped carbon catalyst (Au-L1/TiO₂ material after pyrolysis at 400 °C) and (b) corresponding EDX elemental maps. Carbon appear as the red spots deposited mostly on the yellow gold particles. (c) Au 4f XPS spectra and (d) N 1s XPS spectra for Au-L1/TiO₂ material after pyrolysis at 400 °C. 142
- Figure 28.** XPS spectra of N1s region of L1/TiO₂ (without gold) as prepared and after pyrolysis. 143
- Figure 29.** XPS spectra of N1s region of the catalyst prepared by pyrolysis at 400 °C a)Au-L2/TiO₂; b)Au-L3/TiO₂; c)Au-L4/TiO₂; d)Au-L5/TiO₂; e)Au-L6/TiO₂. 144
- Figure 30.** XPS spectra of N1s region of the Au-L1/TiO₂ material freshly-prepared and after pyrolysis at 200, 400, 600 and 800 °C under N₂. 145
- Figure 31.** (a) Time course of hydrogenation of phenylacetylene **1a** catalyzed by (b) Au@N-doped carbon/TiO₂ catalyst and (c) Au/TiO₂ catalyst; (d) Recycling experiments using the Au@N-doped carbon/TiO₂ catalyst; (e) Hot filtration test to determine homogeneous catalysis contribution in hydrogenation of **1a**. Reaction conditions: 0.14 mmol of **1a**, 2 mol% of Au, 2 mL of ethanol, 100 °C, 6 bar of H₂. 146
- Figure 32.** Catalyst recycling of the hydrogenation of phenylacetylene catalyzed by Au@N-doped carbon/TiO₂ catalyst. Reaction conditions: 1 mmol **1a**, 2 mol% of Au, 2 mL of ethanol, 100 °C, 6 bar H₂. 147
- Figure 33.** Time course of hydrogenation of phenylacetylene catalyzed by Lindlar catalyst. Reactions conditions: 4 mmol of **1a**, 0.25 mol% Pd, 4 mL of hexane, 0.2 mL of quinoline, 100 °C, 6 bar of H₂. 148
- Figure 34.** STEM bright field (a) and HAADF (b) images of the Au@N-doped carbon/TiO₂ catalyst after the tenth hydrogenation cycle. 148

1. INTRODUCTION

1.1. HYDROGENATION REACTIONS

Hydrogenation lies at the heart of many important chemical transformations. Such processes have been widely employed by industry and about 10% of all chemical reactions in multistep syntheses of pharmaceuticals, vitamins and fine chemicals are catalytic hydrogenations ranging from the upgrading of crude oil to the synthesis of a variety of pharmaceutical and agricultural chemicals. From the environmental point of view, reduction with H₂ is an atom efficient transformation and undoubtedly the cleanest method for organic molecules reduction. (SHELDON; BEKKUM, 2001)

These transformations should be highly selective, in order to preserve the target functionalities and to provide high yields of the final products. The prominent examples are hydrogenations where the target products contain a C=C functional group, such as selectivity to the alkene in partial alkyne hydrogenation, which has been defined in two different ways that can be explained by the reaction scheme in Fig. 1. (CHINCHILLA; NÁJERA, 2014) The mechanistic selectivity to the alkene is expected when $k_2 \gg k_4$. This implies that the hydrogenation of the adsorbed alkyne is favored with respect to the adsorbed alkene. However, the alkene hydrogenation rate is faster than its respective alkyne hydrogenation for most of the metals studied in the literature. Therefore, the selectivity displayed by the catalysts is mainly explained by the second nature of the selectivity, also called thermodynamic selectivity that

occurs when $k_1/k_{-1} \gg k_3/k_{-3}$. It is the ability of one metal to preferentially adsorb the alkyne moiety in the presence of the alkene and thus suppresses the consecutive hydrogen addition, which results in the production of the corresponding alkane. Also, the semihydrogenation reaction provides a practical approach for the conversion of alkynes to alkenes, a very important reaction for the removal of alkyne impurities from alkene bulk feedstocks for the polymer industry. Under industrial conditions, the mechanistic selectivity is not of prime importance due to the low alkyne content in the alkene stream. However, it would be detrimental if the alkene could adsorb competitively with the alkyne and produces the alkane. Therefore, if the thermodynamic selectivity is secured, not only the access of alkene to the surface would be hindered but as well the chemisorbed alkene would be replaced by the alkyne during the reaction. (MOLNÁR; SÁRKÁNY; VARGA, 2001)(MCCUE; ANDERSON, 2015)(JACKSON et al., 1997)(ARMBRÜSTER et al., 2010)(TROTUŞ; ZIMMERMANN; SCHÜTH, 2014)

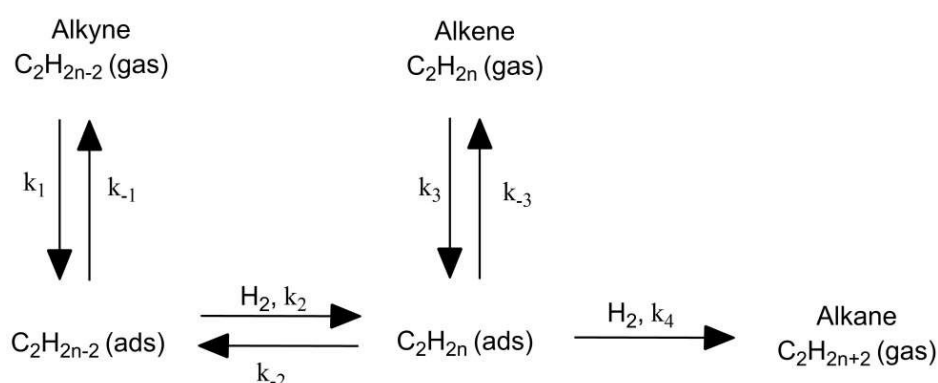


Figure 1. Scheme of hydrogenation of alkynes. (MOLNÁR; SÁRKÁNY; VARGA, 2001)

1.2. GOLD APPLIED IN HYDROGENATION REACTIONS

Bulk gold is known to be unreactive towards the dissociative adsorption of both molecular hydrogen and oxygen. Therefore, gold was considered to be inert as a catalyst. (HASHMI; HUTCHINGS, 2006) (LIU et al., 2014b)(ZHANG et al., 2012) However, in recent decades, highly dispersed nanoscale gold particles supported on metal oxides have been synthesized and found to exhibit unexpectedly high activity for some chemical reactions. (CIRIMINNA et al., 2016)(WHITTAKER et al., 2018)

Gold-based catalysts show intriguing activity for hydrogenation reactions. One can speculate that a single H atom is likely one of the most active species on gold surfaces since it is very weakly bound. This phenomenon has been observed for O on gold: model studies indicate that oxygen atoms have a weaker interaction with Au surfaces compared to other metallic surfaces, leading to extraordinary activity for selective oxidation reactions. (PAN et al., 2013)

Generally, H₂ dissociation has been considered as a key step in hydrogenation reactions. (PAN et al., 2013)(KYRIAKOU et al., 2012) Norskov and coworkers conducted density functional theory (DFT) calculations and predicted that H₂ dissociation has a high energetic barrier on an Au(111) surface.(HAMMER; NORSKOV, 1995) However, for classical gold catalysts, H₂ dissociation likely occurs at low-coordinated sites and/or the interface between the gold particles and the metal oxide support. Fujitani and coworkers observed H–D production from H₂ and D₂ by using two types of model catalysts – Au/TiO₂(110) and TiO₂/Au(111), and they provided evidence that H₂

dissociation occurs at the interface of the gold particles and TiO₂. (FUJITANI et al., 2009) The assistance of the surface properties of supports has enabled gold nanoparticles to efficiently promote hydrogenation even under liquid-phase conditions. (MITSUDOME; KANEDA, 2013)

Auxiliary ligands are usually employed as selectivity enhancers in heterogeneous catalysts;(MALLAT; BAIKER, 2000) however, very recently their capability to trigger activity in gold catalysts has been explored. The use of nitrogen-containing bases was a useful tool to boost gold-based catalysts activity, still keeping gold intrinsic selectivity, due to gold capability to preferentially adsorb the alkyne moiety even in the presence of alkene. Ren et al.(REN et al., 2012) reported a remarkable promotion effect of adsorbed quinoline molecules to the activation of H₂ over supported gold nanoparticles (mean diameter of ~2 nm) catalysts in hydrogenation reactions. Furthermore, the hydrogenation reaction could proceed smoothly under very mild conditions (even at temperatures as low as 25 °C), and various synthetically reductive functional groups remained intact. The key role of the adsorbed quinoline is to promote the heterolytic cleavage of H₂ to give metal-hydride species, occurring by a concerted effect between quinoline molecules and the supported Au NPs. Pyridine was also used as an additive to improve hydrogenation of alkynes(LI; JIN, 2014) and aldehydes(LI et al., 2014a)(LI; ZENG; JIN, 2014)(LI et al., 2015) over gold-based catalysts using molecular hydrogen. Moreover, a combination of supported Au NPs and a basic ligand, morpholine, was reported by Liang et al.(LIANG et al., 2015) to effectively catalyze the hydration of alkynes into ketone. A plausible mechanism of the reaction involves the formation of an enamine intermediate in the hydration of alkynes. Besides, the

catalyst system tolerated well sensitive functional groups (e.g., silyl ethers, ketals) or strongly coordinating group such as pyridine.

1.3. FRUSTRATED LEWIS PAIRS

The concept of frustrated Lewis pairs (FLP) was defined by Douglas W. Stephan after his fundamental work describing the first metal-free reversible activation of H₂ and the ability to catalyze hydrogenations of organic molecules. (WELCH et al., 2006) Accordingly, a frustrated Lewis pair is the prevention of classical Lewis acid and Lewis base (LA-LB) pair combination due to steric hindrance (Lewis pair segregation). The FLP reactivity is a result of the “energetic mismatch” between LA and LB rather than a result of their structure. (STEPHAN, 2016) (ARNDT; RUDOLPH; HASHMI, 2017) The concept was first introduced in order to explain the splitting of molecular hydrogen by a sterically congested Lewis acid and base pair. Although some previous observations already suggested that the cooperativity between Lewis pairs could promote metal-free transformations, it is the use of main-group FLPs for molecular hydrogen activation that led to the surge of research interest in this field. In this case, the activation of H₂ proceeds through a heterolytic cleavage, while in an oxidative addition, the dihydrogen is homolytically cleaved and the oxidation state of the metal center is increased by two. (FONTAINE; STEPHAN, 2017) (STEPHAN, 2015a) (BULLOCK; CHAMBERS, 2017)

Since then, FLPs have been shown to activate many small molecules (Figure 2). (LAM et al., 2019) The FLP pathway to activate molecules might

proceed via the frustrated Lewis pair concertedly interacting with a substrate during the transition state. This process includes a two-electron transfer from the LB to the substrate and from the substrate to the LA. The definition is also applicable to transition metal-based FLPs. In a cooperative interaction between metal center, ligand and substrate, two electrons are passed from the ligand to the substrate, while the metal center accepts two electrons from the substrate.(ARNDT; RUDOLPH; HASHMI, 2017)(FONTAINE et al., 2017)

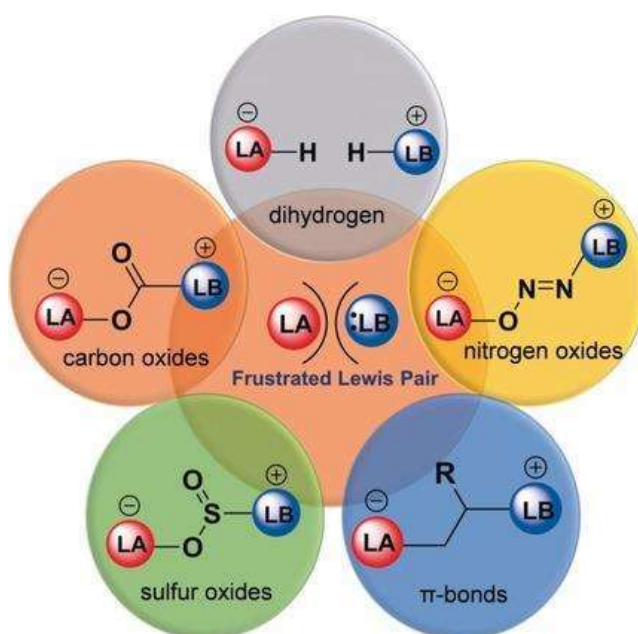


Figure 2. Examples of activation of small molecules with frustrated Lewis pairs. (MELEN, 2018)

Recently, some studies have employed the concept of FLPs to describe the activity of heterogeneous catalyst in hydrogenation reactions. These catalytic sites constructed by a solid surface and adsorbed molecules can be regarded as solid-molecule FLPs. Theoretical calculations and experimental results revealed that Au nanoparticles, with a size of 50 nm, modified with

imines and nitriles can effectively activate hydrogen molecules and even hydrogenate imines and nitriles. This catalytic behavior originates from the constructed semi-solid FLP catalysts, where Au serves as a Lewis acid and imines/nitriles are Lewis bases. Density functional theory (DFT) calculations suggested that the weak interaction between Au particles and imines/nitriles facilitated the insertion of hydrogen molecules between them. The relatively weak adsorption of imines/nitriles on the surfaces of the Au particles can also be attributed to the repulsion between the N lone pairs of the imines/nitriles and the d-band electrons of the Au surface. Using NH₃ as a probe Lewis base, the favorable orbital interaction among the Au(111) surface, H₂ and NH₃ were studied. The N lone pair and the fully filled Au d_{z²} would donate electrons to the σ^* -antibonding orbital of H₂, suggesting the Lewis basic nature of NH₃. The partially filled Au s- and p-bands would then deplete electrons from the σ -bonding orbital of H₂. As a result, these interactions weaken the H–H bond for hydrogenation. (LU et al., 2014a)

The characterization of surface FLP-like catalytic sites are still quite limited by the current technologies. Appropriate methods or techniques, which can provide a more incisive determination of the structural features of the interfacial Lewis acid–base pair-site, are essential to evaluate the catalytically active sites and to further understand their cooperative pathways with the target molecules. Although several examples of semi-solid and solid FLP catalysts have been proposed, the FLP-like performance is mainly assessed based on (1) the quenched catalytic activity upon the addition of small amounts of other small Lewis acids or Lewis bases and (2) DFT calculations. Many methods, such as Fourier transform infrared spectroscopy (FTIR), temperature-

programmed adsorption/desorption and calorimetric enthalpy of adsorption, can be employed to quantify the strength of the surface Lewis acid and Lewis base interaction. However, there is no effective descriptor to the unbonded Lewis acid/base pairs on the surface/interface of semi-solid and solid catalysts. Also, there is no theory established to predict the mechanism involved and the reactivity of such a surface-active site. Thus, the development of advanced techniques to probe surface FLP-like active centers, directly visualizing the catalytic sites, is highly desired. The obtained information would be extremely useful to understand the formation of surface FLP sites as well as to establish design guidelines for improved FLP catalysts.(MA et al., 2018)

1.4. REFERENCES

ARMBRÜSTER, M. et al. Pd–Ga Intermetallic Compounds as Highly Selective Semihydrogenation Catalysts. **Journal of the American Chemical Society**, v. 132, n. 42, p. 14745–14747, 27 out. 2010.

ARNDT, S.; RUDOLPH, M.; HASHMI, A. S. K. Gold-based frustrated Lewis acid/base pairs (FLPs). **Gold Bulletin**, v. 50, n. 3, p. 267–282, 13 set. 2017.

BULLOCK, R. M.; CHAMBERS, G. M. Frustration across the periodic table: heterolytic cleavage of dihydrogen by metal complexes. **Phil.Trans.R.Soc.A**, v. 375, n. 2101, p. 1–26, 2017.

CHINCHILLA, R.; NÁJERA, C. Chemicals from alkynes with palladium catalysts. **Chemical Reviews**, v. 114, n. 3, p. 1783–1826, 2014.

CIRIMINNA, R. et al. Industrial Applications of Gold Catalysis. **Angewandte Chemie International Edition**, v. 55, n. 46, p. 14210 –14217, 2016.

FONTAINE, F.-G.; STEPHAN, D. W. On the concept of frustrated Lewis pairs. **Philosophical Transactions of the Royal Society A: Mathematical, Physical and Engineering Sciences**, v. 375, n. 2101, p. 20170004, 2017.

FONTAINE, F. G. et al. Design principles in frustrated Lewis pair catalysis for the functionalization of carbon dioxide and heterocycles. **Coordination Chemistry Reviews**, v. 334, p. 124–135, 2017.

FUJITANI, T. et al. Hydrogen Dissociation by Gold Clusters. **Angewandte Chemie International Edition**, v. 48, n. 50, p. 9515–9518, 7 dez. 2009.

HAMMER, B.; NORSKOV, J. K. Why gold is the noblest of all the metals, **Nature**, v. 376, p. 238-240, 1995.

HASHMI, A. S. K.; HUTCHINGS, G. J. Gold Catalysis. **Angewandte Chemie International Edition**, v. 45, n. 47, p. 7896–7936, 2006.

JACKSON, S. D. et al. The effect of co-adsorbates on activity / selectivity in the hydrogenation of aromatic alkynes. **Heterogeneous Catalysis and Fine Chemicals IV**, p. 305–311, 1997.

KYRIAKOU, G. et al. Isolated Metal Atom Geometries as a Strategy for Selective Heterogeneous Hydrogenations. **Science**, v. 335, n. 6073, p. 1209–1212, 9 mar. 2012.

LAM, J. et al. FLP catalysis: main group hydrogenations of organic unsaturated substrates. **Chemical Society Reviews**, v. 48, n. 13, p. 3592–3612, 2019.

LI, G. et al. Size dependence of atomically precise gold nanoclusters in chemoselective hydrogenation and active site structure. **ACS Catalysis**, v. 4, n. 8, p. 2463–2469, 2014.

LI, G. et al. Experimental and Mechanistic Understanding of Aldehyde Hydrogenation Using Au₂₅ Nanoclusters with Lewis Acids: Unique Sites for Catalytic Reactions. **Journal of the American Chemical Society**, v. 137, n. 45, p. 14295–14304, 18 nov. 2015.

LI, G.; JIN, R. Gold Nanocluster-Catalyzed Semihydrogenation: A Unique Activation Pathway for Terminal Alkynes. **Journal of the American Chemical Society**, v. 136, n. 32, p. 11347–11354, 13 ago. 2014.

LI, G.; ZENG, C.; JIN, R. Thermally Robust Au₉₉(SPh)₄₂ Nanoclusters for Chemoselective Hydrogenation of Nitrobenzaldehyde Derivatives in Water. **Journal of the American Chemical Society**, v. 136, n. 9, p. 3673–3679, 5 mar. 2014.

LIANG, S. et al. Supported Gold Nanoparticle-Catalyzed Hydration of Alkynes under Basic Conditions. **Organic Letters**, v. 17, n. 1, p. 162–165, 2 jan. 2015.

LIU, X. et al. Supported Gold Catalysis: From Small Molecule Activation to Green Chemical Synthesis. **Accounts of Chemical Research**, v. 47, n. 3, p. 793–804, 18 mar. 2014.

LU, G. et al. Gold catalyzed hydrogenations of small imines and nitriles: enhanced reactivity of Au surface toward H₂ via collaboration with a Lewis base. **Chem. Sci.**, v. 5, n. 3, p. 1082–1090, 2014.

MA, Y. et al. Semi-solid and solid frustrated Lewis pair catalysts. **Chemical Society Reviews**, v. 47, n. 15, p. 5541–5553, 2018.

MALLAT, T.; BAIKER, A. Selectivity enhancement in heterogeneous catalysis induced by reaction modifiers. **Applied Catalysis A: General**, v. 200, n. 1–2, p. 3–22, ago. 2000.

MCCUE, A. J.; ANDERSON, J. A. Recent advances in selective acetylene hydrogenation using palladium containing catalysts. **Frontiers of Chemical Science and Engineering**, v. 9, n. 2, p. 142–153, 22 jun. 2015.

MITSUDOME, T.; KANEDA, K. Gold nanoparticle catalysts for selective hydrogenations. **Green Chemistry**, v. 15, n. 10, p. 2636, 2013.

MOLNÁR, Á.; SÁRKÁNY, A.; VARGA, M. Hydrogenation of carbon-carbon multiple bonds: Chemo-, regio- and stereo-selectivity. **Journal of Molecular Catalysis A: Chemical**, v. 173, n. 2001, p. 185–221, 2001.

PAN, M. et al. Model studies of heterogeneous catalytic hydrogenation reactions with gold. **Chemical Society Reviews**, v. 42, n. 12, p. 5002–5013, 2013.

REN, D. et al. An Unusual Chemoselective Hydrogenation of Quinoline Compounds Using Supported Gold Catalysts. **Journal of the American Chemical Society**, v. 134, n. 42, p. 17592–17598, 24 out. 2012.

SHELDON, R. A.; BEKKUM, H. VAN. **Fine Chemicals through Heterogeneous Catalysis**. [s.l.: s.n.].

STEPHAN, D. W. Frustrated Lewis pairs: From concept to catalysis. **Accounts of Chemical Research**, v. 48, n. 2, p. 306–316, 2015.

STEPHAN, D. W. The broadening reach of frustrated Lewis pair chemistry. **Science**, v. 354, n. 6317, p. aaf7229-aaf7229, 9 dez. 2016.

TROTUŞ, I.-T.; ZIMMERMANN, T.; SCHÜTH, F. Catalytic Reactions of Acetylene: A Feedstock for the Chemical Industry Revisited. **Chemical Reviews**, v. 114, n. 3, p. 1761–1782, 12 fev. 2014.

WELCH, G. C. et al. Reversible, Metal-Free Hydrogen Activation. **Science**, v. 314, n. 5802, p. 1124–1126, 17 nov. 2006.

WHITTAKER, T. et al. H₂ Oxidation over Supported Au Nanoparticle Catalysts: Evidence for Heterolytic H₂ Activation at the Metal–Support Interface. **Journal of the American Chemical Society**, p. jacs.8b04991, 19 nov. 2018.

ZHANG, Y. et al. Nano-gold catalysis in fine chemical synthesis. **Chemical Reviews**, v. 112, n. 4, p. 2467–2505, 2012.

2. OBJECTIVES

2.1. GENERAL OBJECTIVE

The main goal of this Thesis is the development of gold-based catalytic systems that combine high activity and preserve the high selectivity of gold for hydrogenation process. Gold-based catalysts still suffer from the lack of activity for hydrogenations, mainly due to limited capacity to dissociate molecular hydrogen (H_2). Hence, strategies to engineer the catalytic activity and surpassing the H_2 activation barrier, while preserving high selectivity of gold under mild conditions, constitutes a major challenge. Besides, in this Thesis, we will study activation and deactivation processes involving the adsorption of ligands on gold metal surface. Ligands can be used as stabilizers or purposely added to the reaction medium or support to stimulate new reactivity and selectivity. Very little has been studied so far on the role of organic ligands adsorbed on metal nanoparticles for applications in catalysis.

2.2. SPECIFIC OBJECTIVES

Considering the general objective, the following specific objectives have been proposed:

- To prepare gold nanoparticles with controllable size by simple and reproducible methodologies;
- To study the effect of the addition of external ligands in the catalytic activity of Au NPs in hydrogenation reactions.

- To analyze the effect of capping ligand nanoparticles in the formation of FLP surface;
- To develop a “full heterogeneous” and recyclable gold-based catalyst for hydrogenation reactions;
- To characterize the catalyst using techniques such as Flame Atomic Absorption Spectroscopy (FAAS), Transmission Electron Microscopy (TEM), X-ray diffraction (XRD) and X-ray photoelectron spectroscopy (XPS);
- To study the stability of catalysts against leaching process;
- To apply the established catalytic systems in scope studies;
- To rationalize the effect of the ligands on the formation of FLP surface.

3. CHAPTER 1

Gold-catalyzed selective hydrogenation of alkynes into cis-alkenes via H₂ heterolytic activation by frustrated Lewis pairs

“Accepted version of article reproduced with permission from [Fiorio, J. L.; López, N.; Rossi, L. M. Gold–Ligand-Catalyzed Selective Hydrogenation of Alkynes into cis-Alkenes via H₂ Heterolytic Activation by Frustrated Lewis Pairs. **ACS Catalysis**, 2017, 7, 2973–2980.] Copyright [2017] American Chemical Society.” The written permission from the editor is given in Appendices A1. The published version of this article can be accessed in the link: DOI: [10.1021/acscatal.6b03441](https://doi.org/10.1021/acscatal.6b03441) ([ACS Articles on Request](#)).

Abstract

The selective hydrogenation of alkynes to alkenes is an important synthetic process in the chemical industry. It is commonly accomplished using palladium catalysts that contain surface modifiers, such as lead or silver. Here we report that the adsorption of nitrogen-containing bases on gold nanoparticles results in a frustrated Lewis pair interface that activates H₂ heterolytically allowing an unexpected high hydrogenation activity. The so-formed tight-ion pair can be selectively transferred to an alkyne in a cis configuration controlled by electrostatic interactions. Activity correlates with H₂ dissociation energy, which depends on the basicity of the ligand and on the reorganization energy of the

ligand on the surface required to activate hydrogen. High surface occupation and strong Au atom-ligand interactions might affect the accessibility and stability of the active site making the activity prediction a multiparameter function. The remarkable promotional effect found for nitrogen-containing bases with two heteroatoms was mechanistically described as a strategy to boost gold activity.

3.1.MOTIVATION

Catalytic hydrogenation is a key process technology in petrochemical industry and has evolved into an important transformation for the manufacture of pharmaceutical and fine chemicals, replacing stoichiometric chemical reduction methods that generate large amounts of toxic waste. Catalytic hydrogenations are usually accomplished by the activation of molecular hydrogen via homolytic H₂ dissociation on metal surfaces, such as Rh, Pt, Pd, Ni.(KYRIAKOU et al., 2012) Selective hydrogenations with discrimination between reducible functional groups, such as carbon-carbon triple and double bonds, are very challenging. Palladium remains the catalyst of choice for many hydrogenations, but the selective conversion of alkynes into cis-alkenes requires the used of a palladium catalyst partially poisoned with lead (Lindlar catalysts).(VILÉ et al., 2015) Auxiliary ligands containing -N, -S, and -O groups have been combined with Lindlar catalysts to improve selectivity. The presence of toxic lead and deactivation are driving forces for the search of lead-free Lindlar catalyst replacements for alkyne to cis-alkene hydrogenations. More active and selective palladium catalysts have appeared, but there is still room

for the development of catalyst systems based on more available metals.(JAGADEESH et al., 2013; WESTERHAUS et al., 2013)

Gold nanoparticles (Au NPs) have attracted a significant amount of interest as catalysts due to their exceptional selectivity and surprisingly high activity, which is not replicated by other metals, for some reactions, such as CO oxidation.(CIRIMINNA et al., 2016; HASHMI; HUTCHINGS, 2006; STRATAKIS; GARCIA, 2012; WITTSTOCK; BÄUMER, 2014) However, gold was considered only a modest hydrogenation catalyst.(BOND, 2008; BOND; SERMON, 1973) Comparatively to the number of studies with gold in oxidations, there are fewer studies on Au NPs as hydrogenation catalysts.(HASHMI; HUTCHINGS, 2006) Ultrafine gold particles supported on alumina were regarded as a unique metal for the selective hydrogenation of acetylene into ethylene, and gold received attention as a selective catalyst for this gas-phase reaction.(JIA et al., 2000; SEGURA; LÓPEZ; PÉREZ-RAMÍREZ, 2007) More recently, a new interest emerged for selective hydrogenation of carbonyl or nitro groups by Au NPs.(CLAUS et al., 2000; CORMA; SERNA, 2006; CORMA; SERNA; GARCÍA, 2007; GRIRRANE; CORMA; GARCÍA, 2008) The main virtue was gold's unique chemoselectivity, which is controlled by thermodynamics of the adsorption of the organic reactants and products.(SEGURA; LÓPEZ; PÉREZ-RAMÍREZ, 2007; VILÉ et al., 2016) In general, the low activity associated to gold is a consequence of poor H₂ dissociation on gold surfaces,(FUJITANI et al., 2009; HAMMER; NORSKOV, 1995) though nanostructuring can improve H₂ dissociation at structural defects on nanoparticles or nanoporous materials, improving activity.(SEGURA; LÓPEZ; PÉREZ-RAMÍREZ, 2007)

The use of molecular modifiers or auxiliary ligands is a well-known strategy to enhance selectivity in heterogeneous catalysis, mainly as a result of ensemble control,(MALLAT; BAIKER, 2000; SCHOENBAUM; SCHWARTZ; MEDLIN, 2014) and similarly capping ligands (e.g. nitrogen-containing bases) were found to influence the catalytic properties of metal nanoparticles.(CHEN et al., 2016a; KAHSAR; SCHWARTZ; MEDLIN, 2014; KWON et al., 2012; MARSHALL et al., 2010; MORENO et al., 2011; SCHRADER et al., 2015; WU et al., 2012) Quinoline is the most frequently used modifier, either alone or with lead, for the selective hydrogenation of alkynes performed on Pd Lindlar and Pt catalysts.(CHINCHILLA; NÁJERA, 2014; GARCÍA-MOTA et al., 2011) Nitrogen-containing bases have also been explored as promoters for hydrogenation reactions by gold via H₂ activation (quinoline(REN et al., 2012) and pyridine(LI; JIN, 2014)) and using other hydrogen sources, such as PhMe₂SiH(YAN et al., 2012) and HCOOH,(LI et al., 2016) in combination with reaction modifiers. The use of H₂ as the hydrogen source is highly desired as it avoids the production of residues, but the channels for activation of H₂ on gold are not yet fully understood.

Herein, we report the unique promotion effect of nitrogen-containing bases on the catalytic activity of gold nanoparticles. The starting inactive naked gold nanoparticles supported on silica become highly active for the selective hydrogenation of alkyne into *cis*-alkenes. The hydrogenation can proceed smoothly and fully alkene selective using H₂ as the hydrogen source and under relatively mild conditions (80 °C, 6 bar H₂). According to density functional theory calculations, molecular hydrogen dissociation occurs at the ligand-gold

interface generating a tight-ion pair that can be selectively transferred to the adsorbed alkyne in a *cis* configuration controlled by electrostatic interactions.

3.2. RESULTS AND DISCUSSION

The synthesis of gold nanoparticles supported on amino-functionalized silica (Au/SiO₂-NH₂) followed a previously highly reproducibly reported method.(LIU et al., 2009) The functionalization of the support surface with amino-groups has been reported as an effective way to strengthen the metal-support interaction,(OLIVEIRA et al., 2011) and when associated to an appropriate reducing agent for rapid nucleation of the metal species, lead to uniform composition and size distribution. This method allows for obtaining metal nanoparticles in a well-controlled manner.(WANG et al., 2013) Characterizations with transmission electron microscopy (TEM) revealed that the Au NPs were highly dispersed on the silica support with an average diameter of 2.3 ± 0.6 nm, according to the size distribution histogram obtained by analyzing more than 200 particles (Fig. 2a, b). The HRTEM image shown in the inset of Figure 1a corroborates the presence of Au NPs since an interplanar distance of 2.21 Å, corresponding to the {111} Bragg plane of cubic Au(0), was obtained. The formation of the Au NPs could also be evidenced by the appearance of an SPR (surface plasma resonance) band at 525 nm observed in the UV-Vis spectrum (Fig. 2c). The XRD pattern (Fig. 2d) of the Au/SiO₂-NH₂ showed diffraction peaks at $2\theta = 38.21^\circ$, 44.61° , 64.71° and 77.51° , which can

be ascribed to Au {111}, {200}, {220} and {311}, respectively.(PEI et al., 2014);(WEI et al., 2015)

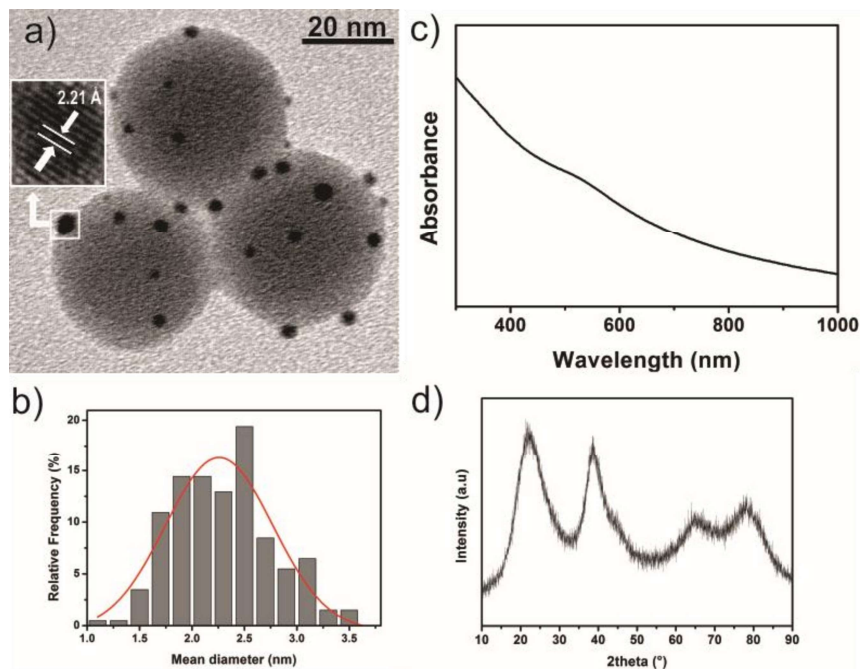


Figure 3. (a) TEM image, (b) size distribution histogram and (c) UV-vis spectrum and (d) XRD pattern of Au/SiO₂

Screening of a series of N-containing bases (**B1-B19**) (Figure 3) with a broad range of pK_a values and chemical structures (primary, secondary and tertiary amines, and also heteroaromatic and cycloaliphatic amines) for the hydrogenation of phenylacetylene **1a** over Au NPs. Au/SiO₂ itself performed poorly (conversion < 1%), but it is highly selective and provides exclusively the alkene **1b**. The Au/SiO₂ catalyst becomes active in the presence of some of the N-containing bases studied, but there was no correlation with the amine pK_a values.

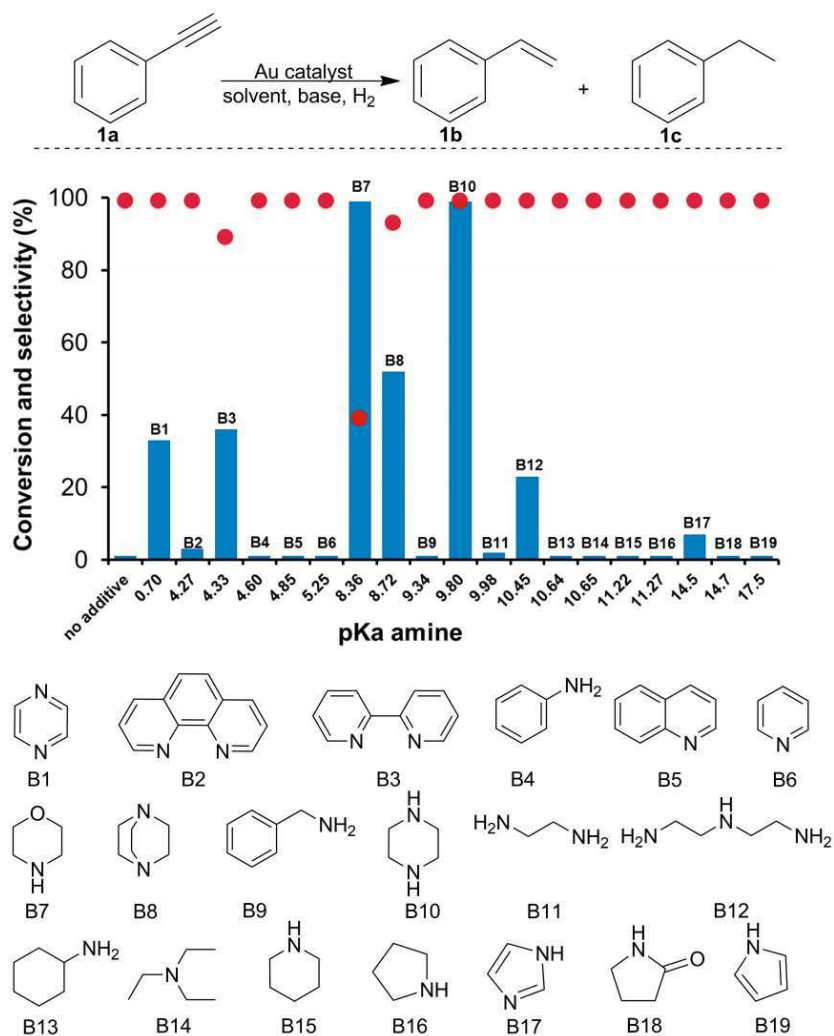


Figure 4. Screening of nitrogen-containing bases for phenylacetylene **1a** hydrogenation with Au/SiO₂ catalyst. Reaction conditions: 1 mmol **1a**, 0.01 mmol Au (50 mg Au/SiO₂), 1 mmol amine, 2 mL of ethanol, 100 °C, 6 bar H₂, 24 h.

Nitrogen-containing bases with two heteroatoms (pyrazine **B1**, 2,2'-bipyridine **B3**, morpholine **B7**, 1,4-diazabicyclo[2.2.2]octane (DABCO) **B8**, piperazine **B10**) exhibited a higher promotion effect in the hydrogenation of **1a** by gold. Morpholine **B7** was able to give full conversion of **1a**, but the competing hydroamination process(LI; JIN, 2014) occurred and the ketone product was formed in the crude products (selectivity for acetophenone **1d**: 60%). Piperazine **B10** provided full conversion of **1a** and selectivity to the

alkene **1b**. Piperazine **B10** gave the best catalytic result among the amines tested and was used for further studies. It is worth to mention that a blank experiment with **B10** and without the catalyst or with the support without Au NPs showed no conversion of **1a** (Table S2). Another experiment carried out in the presence of catalyst but in the absence of H₂ (reaction performed under nitrogen atmosphere) showed no conversion of **1a** (Table S2). The catalyst was active for five successive reactions using fresh portions of **1a**, piperazine **B10**, and solvent. No appreciable loss of catalytic activity and selectivity was observed after five cycles (Figure 5). ICP OES analysis of the products isolated showed negligible amounts of gold (detection limit: 0.10 ppm). A filtration test revealed that the obtained activity is not related to leaching of the catalytically active metal (no remaining activity in the supernatant), which suggests that gold surfaces containing adsorbed auxiliary ligands catalyze the hydrogenation reaction.

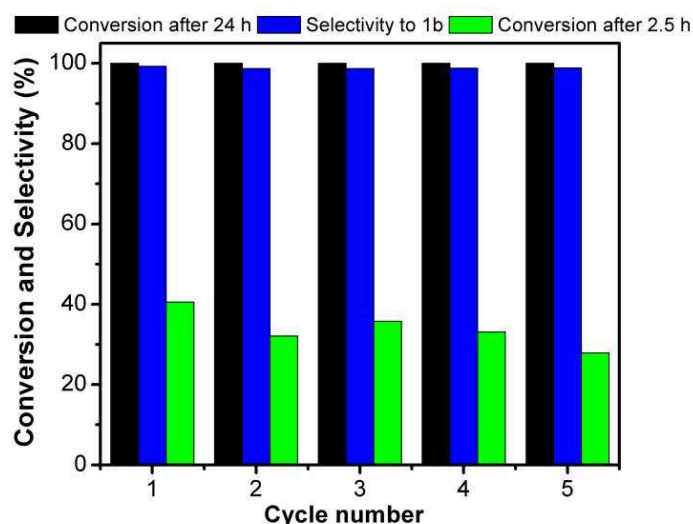


Figure 5. Catalyst recycling of the hydrogenation of phenylacetylene catalyzed by Au/Fe₃O₄@SiO₂ catalyst. Reaction conditions: 1 mmol phenylacetylene, 0.01 mmol Au (Au/Fe₃O₄@SiO₂), 1 mmol piperazine, 2 mL of ethanol, 80°C, 6 bar H₂.

The Au/SiO₂ catalyst was further tested in the hydrogenation of **1a** using different solvents and temperatures. The “green” and protic solvent ethanol gave the best catalytic results (full conversion), while the aprotic solvents such as toluene and DMF were slightly less efficient (Table 1). Decreasing the reaction temperature to 80 °C did not affect conversion and selectivity, while further reducing the temperature to 60 °C caused a decreased in conversion to 53% (Table 1). On the basis of the above experiments, we chose ethanol as solvent, piperazine **B10** as the auxiliary ligand and temperature of 80 °C as the optimized conditions for the semi-hydrogenation reaction. We further examined Au NPs immobilized on different supports, such as Au/Al₂O₃, Au/TiO₂, and Au/CeO₂, under the aforementioned conditions (Table 1). TiO₂ provided the same activity and selectivity as for SiO₂, but the CeO₂ support was detrimental to activity while the Al₂O₃ support was detrimental to selectivity.

Table 1. Phenylacetylene hydrogenation by Au catalysts promoted by piperazine^a

Entry	Catalyst	Temperature (°C)	Solvent	Conversion (%) ^b	Selectivity to 1b (%) ^b
1	No catalyst			0	0
2	SiO ₂ ^c			0	0
3 ^d	Au/SiO ₂	100	EtOH	0	0
4	Au/Fe ₃ O ₄ @SiO ₂			>99	>99
5	Au/SiO ₂		Toluene	97	>99
6	Au/SiO ₂		DMF	90	>99
7	Au/SiO ₂	60		53	>99
8	Au/SiO ₂			>99	>99
9	Au/TiO ₂	80	EtOH	>99	>99
10	Au/CeO ₂			63	97
11	Au/Al ₂ O ₃			>99	75

^aReaction conditions: 1 mmol phenylacetylene, 0.01 mmol Au, 1 mmol piperazine, 2 mL of solvent, 6 bar H₂, 24 h. ^bDetermined by GC using internal standard technique. ^c Amino modified silica. ^dReaction under nitrogen.

Next, we turned our attention to analyze the effect of adding different amounts of piperazine **B10** (Figure 5). Low conversion of **1a** (13%) was obtained using **1a**:ligand: Au 100:1:1 (Figure 5a), but full conversion was achieved with any other concentration of **B10** studied (Figure 5b, c, d). The hydrogenation of styrene **1b** to ethylbenzene **1c** was completely suppressed when a large excess of **B10** was used (**1a**:ligand: Au 100:100:1). It is worth to

note that the reaction rate enhances with the increase in the concentration of the piperazine (reaction rate = 0.87, 9.0, 15.7, 15.4 mmol g_{cat}⁻¹ h⁻¹, for 1, 10, 50 and 100 equivalents of **B10**, respectively) suggesting that piperazine plays a very important role for the activation of Au NPs as hydrogenation catalysts (activity enhancement effect), but it also works as a selectivity enhancer to avoid the subsequent hydrogenation of the alkene into alkane. Particularly, in a large excess of piperazine (**1a**:ligand: Au 100:100:1), which would correspond to about 240 ligands per surface Au atom (estimated surface atoms = 42%), the alkene desorbs without being converted into the alkane.

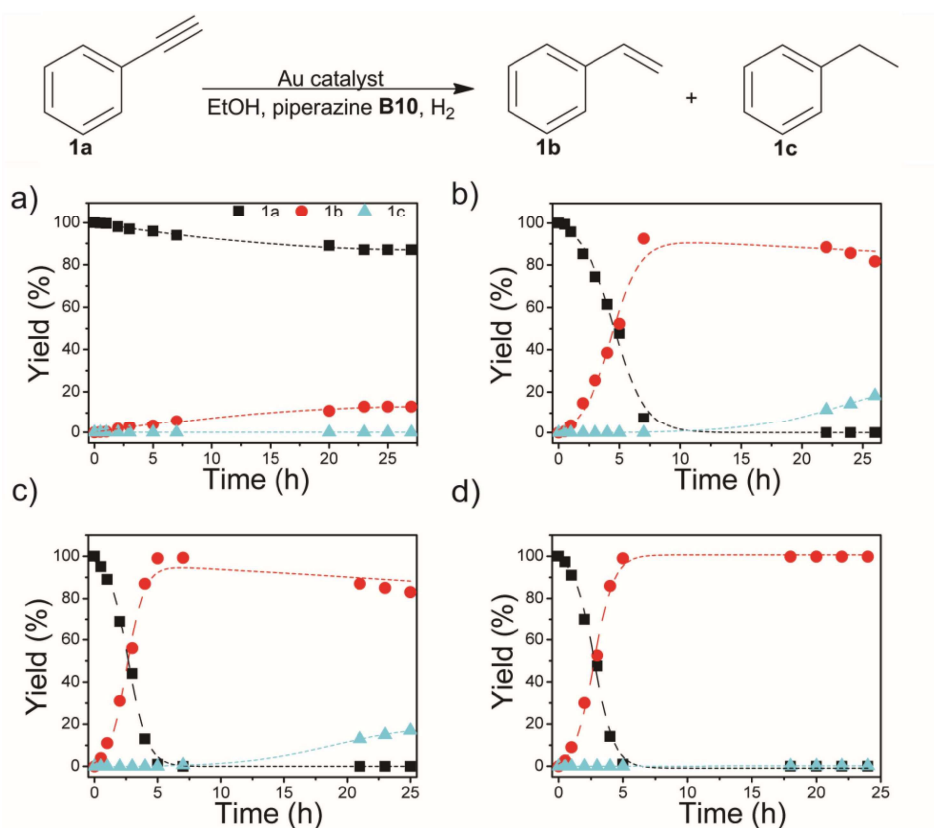
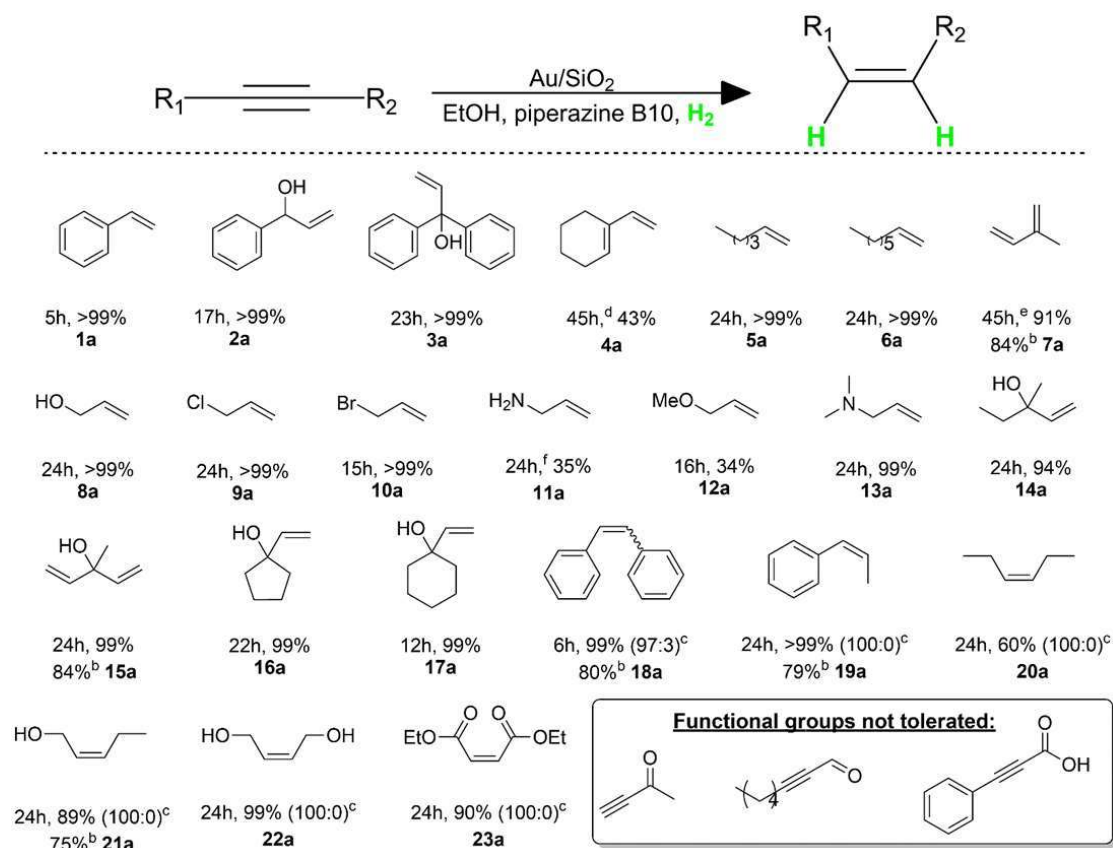


Figure 6. Time course of hydrogenation of phenylacetylene catalyzed by Au/SiO₂ with increasing amounts of piperazine: a) 0.04 mmol; b) 0.4 mmol; c) 2 mmol and d) 4 mmol. Reaction conditions: 4 mmol phenylacetylene, 0.04 mmol Au, 0.04 – 4 mmol of amine, 8 mL of ethanol, 80 °C, 6 bar H₂.

The developed catalytic system was tested in a competition hydrogenation starting from a mixture of phenylacetylene **1a** and styrene **1b**. This kind of experiment is relevant to evaluate the application of our gold catalyst system for purification of styrene, which is an important monomer and usually contains small quantities of acetylene compounds, which poison olefin polymerization catalysts and must be removed via selective hydrogenation before polymerization. (SHAO et al., 2014) Under competitive conditions, our gold catalyst converted preferentially the alkyne **1a** to alkene **1b** and less than 1% of ethylbenzene **1c** was formed. A variety of terminal and internal alkynes were readily hydrogenated to the desired alkene and *cis*-alkene with moderate to excellent yield and, importantly, hardly any over-reduction to alkane (Table 2). Moreover, both electron-deficient substituents, such as esters, and electron-rich groups, for example amino and methoxy, were tolerated well. Clearly, the most-challenging substrates are those alkynes with an alkene moiety. We were pleased that our Au NP catalyst system was able to reduce only the alkyne unit without any detectable concurrent reduction of the alkene moieties both in the parent and product molecules. The results depicted in Table 2 confirmed that a broad range of sensitive and reducible functional groups, including halide, ether and ester substituents, were tolerated in the alkyne hydrogenation process. The prominent isoprene, which is an essential building block in the polymer industry, was obtained via hydrogenation of 2-methylbut-1-en-3-yne **9a** in 84% isolated yield. (*Z*)-alkenes were mostly formed from internal alkynes. Notably, the semi-hydrogenation of non-polar internal alkynes such as diphenylacetylene **18a** and 1-phenyl-1-propyne **19a** proceed quite smoothly under mild conditions.

Table 2. Scope of semi-hydrogenation of alkynes to alkenes using Au/SiO₂ and piperazine **B10**.^a

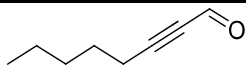
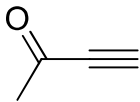
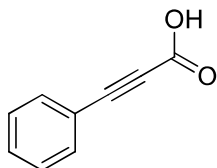


^aReaction conditions: 1 mmol alkyne, 0.01 mmol Au, 1 mmol piperazine **B10**, in 2 mL of ethanol at 80 °C, 6 bar H₂. ^bDetermined by GC using internal standard technique (>99% means no other product detected); numbers in parenthesis refer to isolated yield. ^cZ/E ratio was determined by ¹H NMR spectroscopy. ^d1% of alkane detected by GC. ^e0.02 mmol Au and toluene as solvent (2 mL). ^f0.02 mmol Au. ^gtoluene as solvent (2 mL).

The only functional groups that do not tolerate the reaction conditions are aldehydes, ketones or carboxylic acids (Table 3), which are known to couple with amines. The catalyst system was also applicable for scaled-up

conditions, **1a** (50 mmol; 5.1 g) and **18a** (50 mmol, 8.9 g) were successfully converted into the alkenes **1b** (4.6 g, 88%) and **19b** (7.1 g, 79%), respectively. Considering full conversion, the turnover number (TON) of 5000 was reached, with excellent productivity of approximately 200 mol.mol⁻¹.h⁻¹. These TON and productivity values (not optimized) are remarkably higher than those reported for other heterogeneous Au catalyst systems for semi-hydrogenation of alkynes employing molecular hydrogen or any other hydrogen source.(LI; JIN, 2014; LI et al., 2014b; LIANG; HAMMOND; XU, 2016; MITSUDOME et al., 2015; VASILIKOGIANNAKI et al., 2015)

Table 3. Hydrogenation of various alkynes using Au/SiO₂ and piperazine^a

Entry	Substrate	t (h)	Conversion (%) ^b	Selectivity (%) ^b
1		24	>99	0
2		24	>99	0
3		24	>99	0

^a Reaction conditions: 1 mmol alkyne, 0.01 mmol Au, 1 mmol piperazine, in 2 mL of ethanol at 80 °C, 6 bar H₂. ^bDetermined by GC using internal standard technique.

Based on the above-mentioned facts and bearing in mind that primary and secondary amines are used as ligands in homogeneous catalysis to promote heterolytic cleavage of H₂ to give metal-hydride species,(REN et al.,

2012);(SCHRADER et al., 2015) we suggest that the key role of piperazine **B10** is to facilitate the crucial heterolytic H₂ activation at the Au NPs. Namely, the nitrogen atom of **B10** can serve as a basic ligand to promote the heterolytic H₂ cleavage, providing a favorable situation for hydrogen activation under very mild conditions. The reaction network and the configurations are presented in Figure 6. Piperazine **B10** is adsorbed on the gold surface through one of the N-centers, due to the configuration in a boat site the second N is higher on the surface. The adsorption energy is sufficiently low (-0.27 eV) to ensure that no leaching of gold occurs.(JOVER; GARCÍA-RATÉS; LÓPEZ, 2016) Upon adsorption, the H₂ molecule can split between the ligand forming a quaternary N center and a second H that goes to the surface. Such kind of heterolytic splitting has been proposed for phosphine ligands,(CANO et al., 2014, 2015; LIU et al., 2016a; LÓPEZ-SERRANO; DUCKETT; LLEDÓS, 2006) nitrogen-ligands on metals,(CHEN et al., 2016d) and single atom catalyst(LIU et al., 2016b; VILÉ et al., 2015) while the active participation of the reactant in the activation of H₂ was also found for Ag catalysts in hydrogenation.(VILÉ et al., 2013) The metal-ligand system can be understood as a tight ion-pair induced by the frustrated Lewis pair (FLP) formed by the ligand and the surface.(CHERNICHENKO et al., 2013; WELCH et al., 2006) H₂ dissociation occurs on the Au(111) surface through an energy barrier of 1.45 eV, the reaction is endothermic by 0.69 eV. Instead, if the surface is decorated with piperazine **B10** the dissociation shows a barrier of 0.32 eV (therefore close to zero if zero point vibrational energies, ZPVE, are taken into account) and the final state is thermoneutral when compared to reactants (H₂ and the FLP). Then the alkyne can be adsorbed on the Au(111). Alkynes are weakly adsorbed on Au but due to the van der Waals

contributions, the adsorption energy is -0.28 eV for 1-phenyl-1-propyne **19a**. From the coadsorbed state, the hydride can be transferred to the alkyne. The reaction is slightly endothermic by 0.28 eV the barrier being 0.74 eV from the coadsorbed state. Upon the first hydrogenation the moiety is negatively charged and interacts by electrostatic forces with the protonated piperazine **B10**, this is shown in the inset of Figure 6. From this pair, proton transfer occurs, with barriers 0.13 eV and the total process is exothermic by -2.39 eV. The alkene requires 0.53 eV for desorption.

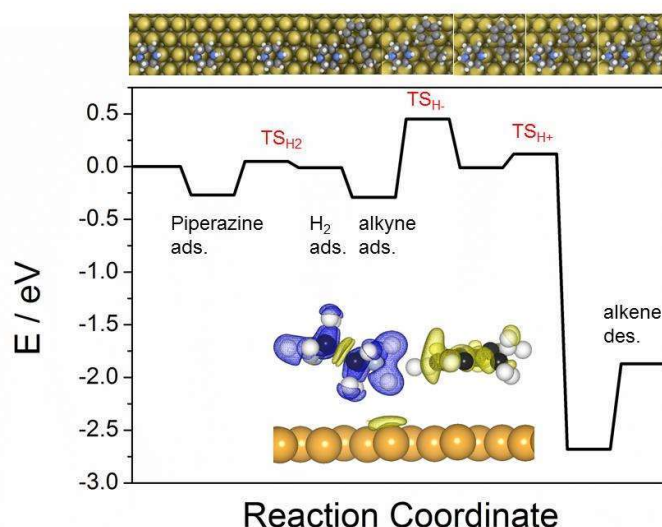


Figure 7. Reaction energy profiles with the corresponding configurations for the hydrogenation of 1-phenyl-1-propyne **19a**. The inset corresponds to the charge distribution with respect to the neutral fragments after the first hydrogenation step. The separation between the yellow-blue colors indicates the electrostatic interactions. Yellow spheres represent Au, blue N, black C, and white H.

The particular structures for the transition states are shown in Figure 7. Notice, that even if H₂ is barrierless according to the potential energy surface the introduction of entropies in the gas-phase molecules implies that there is an

entropic barrier ongoing from the gas to the adsorbed phase.(CHORKENDORFF; NIEMANTSVERDRIET, 2003) Finally, an alternative path considering first the transfer of the H⁺ and then the hydride was calculated, however, the intermediate is more than 1.5 eV higher in energy than that of the H⁻, H⁺ transfer and thus was discarded.

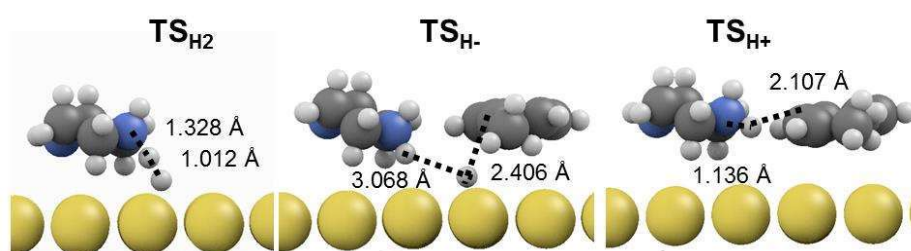


Figure 8. Transition state geometries for the hydrogenation of 1-phenyl-1-propyne **19a**. Yellow spheres represent Au, blue N, black C, and white H.

Calculations also highlight the limited basicity window for the N-containing bases able to provide the aforementioned promotion effect for hydrogenation on gold surfaces. Piperazine **B10** is unique because it is not strongly bound to the surface, and thus cannot extract the metal, for instance when compared to pyridine **B6**. The binding energies for the linear complexes from the atomic reference are exothermic for pyridine **B6** (-0.1 eV) and very endothermic for piperazine **B10** (> 5 eV). When comparing the N-containing bases (Figure 8), the activity (reaction rates were obtained from the kinetic curves given in Figure S3) is found to correlate with the energy barrier for H₂ dissociation at the ligand/Au(111) interface for piperazine, DABCO, pyrazine, imidazole, ethyleneamine and diethylenetriamine (Table 4).

Table 4. Reaction, ΔE , and activation energies, E_a , for heterolytic H_2 dissociation at the N-ligand/Au(111) interface and the imaginary frequencies for the transition states, ν_i in cm^{-1} . All energies in eV. On the clean Au(111) surface dissociation is homolytic in nature.

System	ΔE	E_a	ν_i
Au	0.78	1.55	970
Pyrazine (B1)/Au	0.37	0.67	938
Quinoline (B5)/Au	0.43	0.95	374
DABCO (B8)/Au	0.41	0.54	129
Piperazine (B10)/Au	0.27	0.37	683
Ethyleneamine (B11)/Au	0.28	0.76	280
Diethylenetriamine (B12) /Au	0.41	0.75	280
Piperidine (B15)/Au	0.24	0.43	214
Imidazole (B17)/Au	0.43	0.72	1035
2,2'-Bipyridine (B3)/Au	0.18	0.34	525
Morpholine (B7)/Au	0.27	0.39	559

The barrier is the lowest for **B10** thus an indicative of the unique catalytic activity of the piperazine-gold interface. The barrier for the activation is formed by different terms. One stems for the formation of a proton-hydride pair, this is a constant going from (H_2 to a $H^+...H^-$ pair separated by a average distance of 2 Å). The second appears as a consequence of the intrinsic basicity of the N-containing bases. A third term appears since at the transition state some of the N-containing bases need to rearrange in order to be an active part in the transition state, this is the case for quinolone **B5** that presents a much larger H_2 splitting barrier than would correspond to its thermodynamic (ΔE)

value. The fourth term depends on the adsorption of H^- to the metal, which is in this case invariant. Notice, that **B5** due to its large size can also block too many adsorption sites. Finally, the structures with two basic N-heteroatoms seem to be more active for hydrogenation purposes. There are two reasons for that, the first is that two molecules can be dissociated for each ligand, thus being double active. This is clear with imidazole **B17**, as only one of the N atoms seems capable of trap H_2 (notice that diethylenetriamine **B12** converts 23 % while imidazole **B17** about 7% even if the barrier is comparable). The second reason is that having only one N-heteroatom does not ensure adsorption to the surface for systems, like piperidine **B15** that contains one N only. Piperidine **B15**, thus easily leaves the surface as in the transition state structure there is no element binding it to the surface making the configuration unstable.

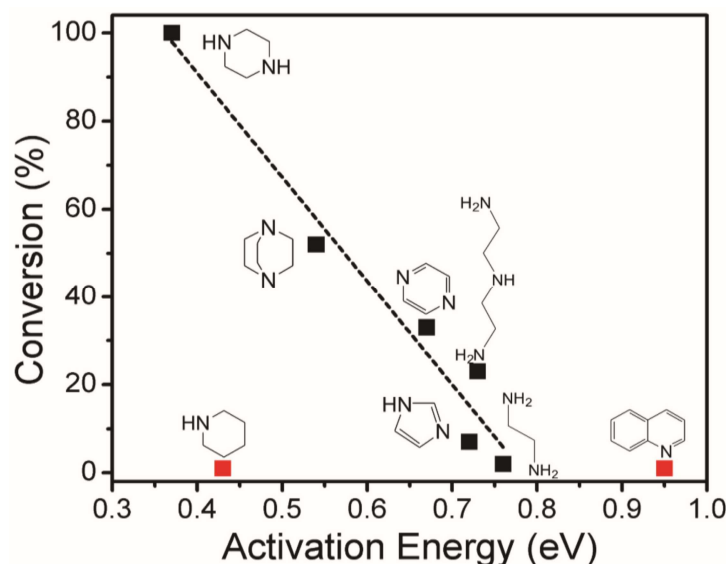


Figure 9. Activation energies for heterolytic H_2 dissociation at the N-ligand/Au(111) interface.

Finally, to gain a better understanding of the H₂ activation process, we conducted H₂-D₂ exchange experiments (Au catalyst, toluene, H₂:D₂ 1:1, 6 bar, 80 °C, 24 h). The H₂-D₂ exchange, attested by the formation of HD in the gas phase (detected by mass spectrometry m/z=3), was much higher over the Au/**B10** systems than with pure Au catalyst. These results suggest that H₂ and D₂ molecules dissociate and recombine to produce HD, and this process is significantly enhanced by piperazine. Upon switching H₂ for D₂ in the hydrogenation reaction under similar conditions, it is noteworthy that a primary isotope effect ($k_H/k_D \approx 2.7$, Figure 9) was observed, suggesting hydrogen is involved in the rate-determining step.(CAREY; SUNDBERG, 2007)

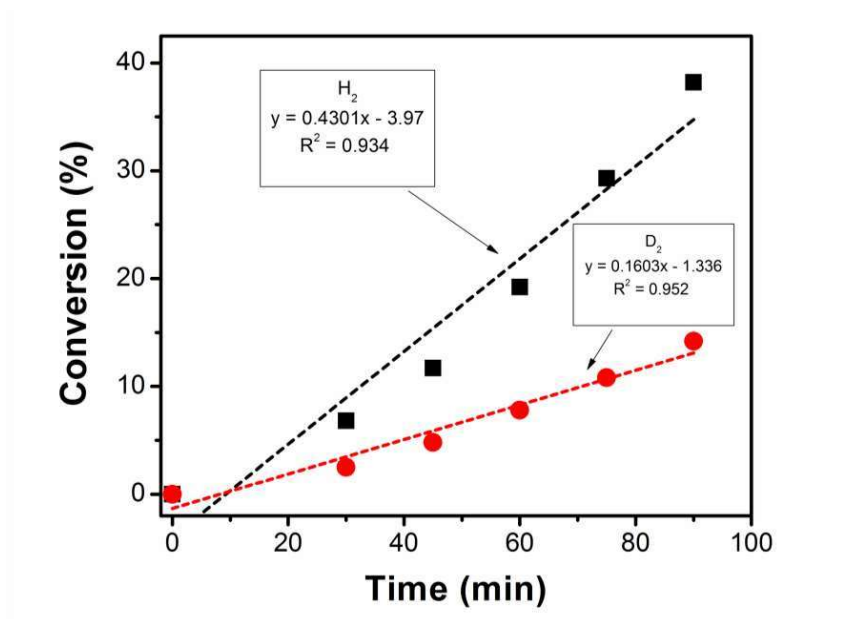


Figure 10. Plot of the conversion of phenylacetylene determined using Au NPs and piperazine with H₂ (squares) and D₂ (circles). Reaction conditions: 4 mmol phenylacetylene, 0.04 mmol Au, 4 mmol of amine, 8 mL of ethanol, 100 °C, 6 bar H₂ or D₂.

To obtain quantitative information about H₂ dissociation, different amounts of **1a** were hydrogenated under limited H₂ conditions (H₂ was pre adsorbed on Au catalysts and **B10**/Au catalysts system and the reaction was conducted under inert atmosphere, see details in supporting information and Table 5). Within the limits of experimental error, while increasing **1a** from 0.01 to 0.05 mmol, a similar amount of **1b** (~0.008 mmol) was obtained, allowing us to estimate that H₂ was the limiting reagent (~0.008 mmol of H₂ activated by **B10**/Au catalyst). For pure Au catalyst, a low yield of **1b** (~0.0001-0.00045 mmol) was obtained, confirming the very unfavorable hydrogen dissociation by Au in the absence of **B10**.

Table 5. Hydrogenation of phenylacetylene **1a** under a limited hydrogen amount.^a

Entry	Catalyst system	Yield of styrene 1b (mmol)		
		(a)	(b)	(c)
1	Au/SiO ₂ + 1 mmol of B10	0.0075	0.00875	0.00800
2	Au/SiO ₂	0.0001	0.0002	0.00045

^aReaction conditions: (a) 0.01, (b) 0.025 and (c) 0.05 mmol **1a**, 0.01 mmol Au (previously treated with H₂ at 6 bar for 24 h in the presence of solvent), 2 mL of toluene, 80 °C, 24 h. The excess of H₂ was removed and the reaction was performed under inert atmosphere.

3.3. CONCLUSIONS

In summary, we have described that high conversion of a range of alkynes with excellent selectivity for *cis* alkenes was achieved by combining

supported Au NPs, N-containing bases and H₂ as hydrogen source. We emphasize the role of the nitrogen-containing ligand as a means for substantial enhancement of catalytic activity and selectivity since the auxiliary ligands play a key role by opening a new channel for the heterolytic dissociation of molecular hydrogen on the frustrated Lewis pair. This ability to switch on the catalytic activity of Au NPs provides a promising new method for controlling a reactive system with ligands. The control is such that stereochemistry of the addition is also achieved due to electrostatic forces. A delicate balance between (i) the basicity of the ligand, (ii) the reorganization energy of the ligand to activate H₂, (iii) the possibility of site blocking by large ligands and (iv) the metal leaching induced by some ligands; is the responsible for the activity-selectivity-stability controls in the catalyst system. We believe this remarkable promotional effect by N-containing ligands may have implications for gold catalysis while stimulating more applications in the field of selective hydrogenations not envisaged before. The versatile concept presented can be transferrable to other metal nanoparticle catalysts.

3.4. EXPERIMENTAL SECTION

3.4.1. Materials and Methods

All the reagents used for the support and catalyst preparation were of analytical grade, purchased from Sigma-Aldrich and used as received. Tetrachloroauric(III) acid was purchased as a 30 wt% aqueous solution in dilute HCl (Sigma-Aldrich). Alkynes, alkenes, amines and standards for GC analysis

were purchased from Sigma-Aldrich having the highest grade available and used as received. Liquid amines used as additives were purified by standard methods just before use. Ethanol (99.5%) and DMF (99%) was purchased from Synth (Brazil) and used as received. Toluene was purchased from Synth (Brazil) and dried before use. The glass reactor was thoroughly cleaned with aqua regia (HCl:HNO₃ = 3:1 v/v), rinsed with copious pure water, and then dried in an oven prior to use. Gold content in the catalyst was measured by FAAS analysis, on a Shimadzu AA-6300 spectrophotometer using an Au hollow cathode lamp (Photron). Metal leaching into the supernatant solution was measured by ICP-AES, performed on a Spectro Arcos ICP AES. UV-Vis spectra were recorded on a Shimadzu UV-1700. TEM analyses were performed with a JEOL 2100. X-ray diffraction (XRD) of the samples was recorded using a Rigaku miniflex diffractometer with Cu K α radiation ($\lambda = 1.54 \text{ \AA}$) at a 2θ range from 20 to 90° with a 0.02° step size and measuring time of 5 s per step. GC analyses were carried out with a Shimadzu GC-2010 equipped with a RTX-Wax column (30 m x 0.25 mm x 0.25 mm) and a FID detector. Method: T_i = 40 °C, T_f = 200 °C, 25 min, T FID and SPLIT = 200 °C. Internal standard: biphenyl. The conversion and selectivity were determined from the total amount of detected products and reactant.(SCANLON; WILLIS, 1985)

3.4.2. Preparation of Au/SiO₂ and Au/Fe₃O₄@SiO₂

Silica nanospheres (SiO₂) and silica-coated magnetite nanoparticles (Fe₃O₄@SiO₂) were obtained by means of a reverse microemulsion process and functionalized with (3-aminopropyl)triethoxysilane, as reported

elsewhere.(JACINTO et al., 2008) Gold nanoparticles were prepared by the impregnation-reduction method, as reported in literature.(LIU et al., 2009) Typically, 1.0 g of the amino-modified support was added to 20 mL of HAuCl₄ aqueous solution (1.3×10^{-2} mol L⁻¹) under continuous stirring. After 30 min, the mixture was filtered and the solid thoroughly washed with deionized water. The recovered material was dispersed in 10 mL of water and an aqueous NaBH₄ solution (10 mL, 0.2 mol L⁻¹) was added dropwise under vigorous stirring. After further stirring for 20 min, the solid was recovered by filtration and thoroughly washed with water and dried in vacuum. Both Au/SiO₂ and Au/Fe₃O₄@SiO₂ catalysts contain 3.4 wt% of gold as determined by FAAS.

3.4.3. Preparation of Au/Support (TiO₂; CeO₂ and Al₂O₃)

Au NPs supported on TiO₂, CeO₂ and Al₂O₃ were prepared by DP method, as reported in literature.(DEKKERS; LIPPITS; NIEUWENHUYS, 1998)(ZANELLA et al., 2002) Typically, 1.0 g of oxide support was added to 100 mL of an aqueous solution of HAuCl₄ (2.1×10^{-3} mol L⁻¹) and urea (0.42 mol L⁻¹). The mixture was heated to 80 °C under vigorous stirring for 4 h, centrifuged, washed and dispersed in 10 mL of water. Then, an aqueous NaBH₄ solution (10 mL, 0.2 mol L⁻¹) was added dropwise under vigorous stirring. After further stirring for 20 min, the solid was recovered by filtration and thoroughly washed with water and dried in vacuum. The Au loadings were: Au/TiO₂ 3.4 wt%; Au/CeO₂ 3.5 wt%, Au/Al₂O₃ 2 wt%.

3.4.4. General procedure for catalytic hydrogenation of alkynes

A typical procedure for the semihydrogenation of alkynes is as follows: alkyne (1 mmol), N-containing base (1 mmol), Au/SiO₂ (1 mol%) and 2 mL of solvent were added to a modified Fischer–Porter 100 mL glass reactor. The reactor was purged five times with H₂, leaving the vessel at 6 bar. The resulting mixture was vigorously stirred using Teflon-coated magnetic stir and the temperature was maintained with an oil bath on a hot stirring plate connected to a digital controller (ETS-D5 IKA). After the desired time, the catalyst was removed by centrifugation and the products were analyzed by GC with an internal standard to determine the conversion of alkyne and the selectivity for alkene. For kinetic studies, the reaction was performed using 4 times the amount of each component given above and aliquots were collected and analyzed by GC at different reaction time intervals. To determine the isolated yield of the obtained products, after the reaction was complete, the crude reaction mixture was transferred to a funnel extraction, and treated with HCl (20 mL, 10% v/v). The aqueous phase was extracted three times with 5 mL of dichloromethane. The organic layers were dried with anhydrous MgSO₄ and the solvent was removed under reduced pressure, to give the corresponding desired alkene. ¹H NMR confirmed the purity of the isolated products.

3.4.5. Recycling experiment

For the recycle experiments, a magnetic catalyst ($\text{Au/Fe}_3\text{O}_4@\text{SiO}_2$) was used to avoid any catalyst loss during the catalytic cycles. After each catalytic experiment under the above typical reaction conditions, the catalyst was recovered by magnetically by placing a magnet in the reactor wall. The used catalyst was tested again under identical reaction conditions just by adding to the reactor a new amount of substrate and amine. The product obtained after centrifugation was analyzed by GC with an internal standard to determine the conversion and selectivity.

3.4.6. Scale-up hydrogenation of alkynes

Alkyne (50 mmol), Au/SiO_2 (0.01 mmol Au), piperazine (1 mmol), and 10 mL of ethanol were added to a glass-lined stainless steel reactor (Parr Instrument Company, 75 mL capacity, Series 5000 Multiple Reactor System). After sealing the reactor and degassed internal air, H_2 was introduced until 30 bar. Then, the mixture was extensively stirred (1200 rpm) at 100 °C for 24 h. The crude reaction mixture was transferred to a funnel extraction and treated with HCl (100 mL, 10% v/v). The aqueous phase was extracted three times with 50 mL of dichloromethane. The organic layers were dried with anhydrous MgSO_4 and the solvent was removed under reduced pressure. ^1H NMR confirmed the purity of the isolated product.

3.4.7. Catalytic hydrogenation using limited amount of H₂

The reactions were performed following a procedure reported elsewhere with modifications. (GARCÍA-ANTÓN et al., 2008) In the first step, 50 mg of catalysts and 2 mL of toluene were added to a modified Fischer–Porter 100 mL glass reactor, which was then pressurized with 6 bar of H₂. After 24 hours under stirring, H₂ was evacuated and N₂ was bubbled. Five cycles of 1 minute vacuum/1 minute bubbling of N₂ were performed in order to eliminate any H₂ dissolved into the solvent. In the second step, different amounts of phenylacetylene (from 0.01 to 0.05 mmol) were added to the reactor under inert atmosphere. The reaction was maintained under inert atmosphere and stirring at 80 °C. After 24 h, the catalyst was removed by centrifugation and the products were analyzed by GC with an internal standard to determine the conversion of alkyne and the selectivity for alkene.

3.4.8. Isotope H₂–D₂ Exchange Reaction

The H₂–D₂ exchange reaction was carried out in a Fischer–Porter 100 mL glass reactor at 80 °C. To the glass reactor, 200 mg of catalyst and 2 mL of toluene were added, and then the reactor was pressurized with 6 bar of a gas mixture of H₂/D₂ (1:1). After 24 h, the reaction products in the gas phase (H₂, HD and D₂) were analyzed with an online mass spectrometer (QIC-20 MS module, Hiden Analytical, UK). Trace amounts of HD formed in the experimental setup without catalyst and the product concentrations were corrected accordingly.

3.4.9. Determination of the isotopic effect

A typical procedure for the semihydrogenation of phenylacetylene was performed in H₂ and D₂, under similar conditions, as follows: alkyne (4 mmol), nitrogen-containing base (4 mmol), Au/SiO₂ (1 mol%) and 8 mL of ethanol were added to a modified Fischer–Porter 100 mL glass reactor. The reactor was purged five times with H₂ (or D₂) leaving the vessel at 6 bar. The resulting mixture was vigorously stirred using Teflon-coated magnetic stir and the temperature was maintained at 100 °C with an oil bath on a hot stirring plate connected to a digital controller (ETS-D5 IKA). After the desired time, the reactor was cooled down to room temperature and aliquots of the reaction mixture were collected. The catalyst was removed by centrifugation and the products were analyzed by GC with an internal standard to determine the conversion of alkyne and the selectivity for alkene at different reaction times. k_H and k_D were determined from the hydrogenation curves.

3.4.10. Computational Details

Density functional theory calculations were performed by Prof. Núria Lopez (ICIQ-Spain). The calculations were conducted on slabs representing the gold surface with the VASP code.(KRESSE; HAFNER, 1993)(KRESSE; FURTHMÜLLER, 1996) The RPBE was the functional of choice(HAMMER; HANSEN; NØRSKOV, 1999) and due to the large size of the molecules dispersion terms were introduced through our modified version of the D2

formulation(ALMORA-BARRIOS et al., 2014a) for the metal. The inner electrons were replaced by PAW(KRESSE; JOUBERT, 1999) and the valence electrons were expanded in plane waves with a kinetic cutoff energy of 450 eV. The Au(111) surface was represented by a p(4x4) supercell and four metal layers (>12 Å vacuum) for the adsorption and reaction. The k-point sampling was 3x3x1 in the Monkhorst-Pack scheme.(MONKHORST; PACK, 1976) Transition states were located through the Climbing Image Nudged Elastic Band (ci-NEB) method,(HENKELMAN; UBERUAGA; JÓNSSON, 2000) the nature of the structures was assessed through the vibrational analysis with a 0.02 Å.

3.5. REFERENCES

ALMORA-BARRIOS, N. et al. Costless Derivation of Dispersion Coefficients for Metal Surfaces. *Journal of Chemical Theory and Computation*, v. 10, n. 11, p. 5002–5009, 11 nov. 2014.

BOND, G. The early history of catalysis by gold. *Gold Bulletin*, v. 41, n. 3, p. 235–241, set. 2008.

BOND, G. C.; SERMON, P. A. Hydrogenation over Supported Gold Catalysts. *Journal of the Chemical Society, Chemical Communications*, n. 13, p. 444–445, 1973.

CANO, I. et al. Air-Stable Gold Nanoparticles Ligated by Secondary Phosphine Oxides for the Chemoselective Hydrogenation of Aldehydes: Crucial Role of the Ligand. *Journal of the American Chemical Society*, v. 136, n. 6, p. 2520–2528, 12 fev. 2014.

CANO, I. et al. Air-Stable Gold Nanoparticles Ligated by Secondary Phosphine

Oxides as Catalyst for the Chemoselective Hydrogenation of Substituted Aldehydes: a Remarkable Ligand Effect. *Journal of the American Chemical Society*, v. 137, n. 24, p. 7718–7727, 24 jun. 2015.

CÁRDENAS-LIZANA, F.; KEANE, M. A. The development of gold catalysts for use in hydrogenation reactions. *Journal of Materials Science*, v. 48, n. 2, p. 543–564, 10 jan. 2013.

CAREY, F. A.; SUNDBERG, R. J. *Advanced Organic Chemistry Part A: Structure and Mechanisms*. Boston, MA: Springer US, 2007.

CHEN, F. et al. Selective Semihydrogenation of Alkynes with N-Graphitic-Modified Cobalt Nanoparticles Supported on Silica. *ACS Catalysis*, v. 7, p. 1526–1532, 30 jan. 2017.

CHEN, G. et al. Interfacial electronic effects control the reaction selectivity of platinum catalysts. *Nature Materials*, v. 15, n. 5, p. 564–569, 25 jan. 2016a.

CHEN, Z. et al. Merging Single-Atom-Dispersed Silver and Carbon Nitride to a Joint Electronic System via Copolymerization with Silver Tricyanomethanide. *ACS Nano*, v. 10, n. 2, p. 3166–3175, 2016b.

CHERNICHENKO, K. et al. A frustrated-Lewis-pair approach to catalytic reduction of alkynes to cis-alkenes. *Nature chemistry*, v. 5, n. 8, p. 718–23, 2013.

CHINCHILLA, R.; NÁJERA, C. Chemicals from alkynes with palladium catalysts. *Chemical Reviews*, v. 114, n. 3, p. 1783–1826, 2014.

CHORKENDORFF, I.; NIEMANTSVERDIET, J. W. *Concepts of Modern Catalysis and Kinetics*. Weinheim, FRG: Wiley-VCH Verlag GmbH & Co. KGaA, 2003.

CIRIMINNA, R. et al. Industrial Applications of Gold Catalysis. *Angewandte Chemie International Edition*, v. 55, n. 46, p. 14210 –14217, 2016.

CLAUS, P. et al. Supported Gold Nanoparticles from Quantum Dot to

Mesoscopic Size Scale: Effect of Electronic and Structural Properties on Catalytic Hydrogenation of Conjugated Functional Groups. *Journal of the American Chemical Society*, v. 122, n. 46, p. 11430–11439, nov. 2000.

CORMA, A.; SERNA, P. Chemoselective Hydrogenation of Nitro Compounds with Supported Gold Catalysts. *Science (New York, N.Y.)*, v. 313, p. 332–334, 2006.

CORMA, A.; SERNA, P.; GARCÍA, H. Gold catalysts open a new general chemoselective route to synthesize oximes by hydrogenation of α,β -unsaturated nitrocompounds with H₂. *Journal of the American Chemical Society*, v. 129, n. 20, p. 6358–6359, 2007.

DEKKERS, M. A. P.; LIPPITS, M. J.; NIEUWENHUYS, B. E. CO adsorption and oxidation on Au/TiO₂. *Catalysis Letters*, v. 56, n. 4, p. 195–197, 1998.

FUJITANI, T. et al. Hydrogen Dissociation by Gold Clusters. *Angewandte Chemie International Edition*, v. 48, n. 50, p. 9515–9518, 7 dez. 2009.

GARCÍA-ANTÓN, J. et al. Reactions of Olefins with Ruthenium Hydride Nanoparticles: NMR Characterization, Hydride Titration, and Room-Temperature C-C Bond Activation. *Angewandte Chemie International Edition*, v. 47, n. 11, p. 2074–2078, 28 fev. 2008.

GARCÍA-MOTA, M. et al. Selective Homogeneous and Heterogeneous Gold Catalysis with Alkynes and Alkenes: Similar Behavior, Different Origin. *ChemPhysChem*, v. 9, n. 11, p. 1624–1629, 4 ago. 2008.

GARCÍA-MOTA, M. et al. A density functional theory study of the 'mythic' Lindlar hydrogenation catalyst. *Theoretical Chemistry Accounts*, v. 128, n. 4–6, p. 663–673, 7 mar. 2011.

GIESBRECHT, P. K.; HERBERT, D. E. Electrochemical Reduction of Carbon Dioxide to Methanol in the Presence of Benzannulated Dihydropyridine Additives. *ACS Energy Letters*, v. 2, p. 549–555, 6 fev. 2017.

- GRIRRANE, A.; CORMA, A.; GARCÍA, H. Gold-Catalyzed Synthesis of Aromatic Azo Compounds from Anilines and Nitroaromatics. *Science (New York, N.Y.)*, v. 322, p. 1661–1664, 2008.
- HAMMER, B.; HANSEN, L.; NØRSKOV, J. Improved adsorption energetics within density-functional theory using revised Perdew-Burke-Ernzerhof functionals. *Physical Review B*, v. 59, n. 11, p. 7413–7421, 1999.
- HAMMER, B.; NORSKOV, J. K. Why gold is the noblest of all the metals. *Nature*, v. 376, n. 6537, p. 238–240, jul. 1995.
- HASHMI, A. S. K.; HUTCHINGS, G. J. Gold Catalysis. *Angewandte Chemie International Edition*, v. 45, n. 47, p. 7896–7936, 2006.
- HENKELMAN, G.; UBERUAGA, B. P.; JÓNSSON, H. A climbing image nudged elastic band method for finding saddle points and minimum energy paths. *The Journal of Chemical Physics*, v. 113, n. 22, p. 9901, 2000.
- JACINTO, M. J. et al. Recoverable rhodium nanoparticles: Synthesis, characterization and catalytic performance in hydrogenation reactions. *Applied Catalysis A: General*, v. 338, n. 1–2, p. 52–57, 2008.
- JAGADEESH, R. V. et al. Nanoscale Fe₂O₃-Based Catalysts for Selective Hydrogenation of Nitroarenes to Anilines. *Science*, v. 342, n. 6162, p. 1073–1076, 29 nov. 2013.
- JIA, J. et al. Selective Hydrogenation of Acetylene over Au/Al₂O₃ Catalyst. *The Journal of Physical Chemistry B*, v. 104, n. 47, p. 11153–11156, nov. 2000.
- JOVER, J.; GARCÍA-RATÉS, M.; LÓPEZ, N. The Interplay between Homogeneous and Heterogeneous Phases of PdAu Catalysts for the Oxidation of Alcohols. *ACS Catalysis*, v. 6, n. 7, p. 4135–4143, jul. 2016.
- KAHSAR, K. R.; SCHWARTZ, D. K.; MEDLIN, J. W. Control of Metal Catalyst Selectivity through Specific Noncovalent Molecular Interactions. *Journal of the American Chemical Society*, v. 136, n. 1, p. 520–526, 8 jan. 2014.

- KRESSE, G.; FURTHMÜLLER, J. Efficiency of ab-initio total energy calculations for metals and semiconductors using a plane-wave basis set. *Computational Materials Science*, v. 6, n. 1, p. 15–50, jul. 1996.
- KRESSE, G.; HAFNER, J. Ab initio molecular dynamics for liquid metals. *Physical Review B*, v. 47, n. 1, p. 558–561, 1 jan. 1993.
- KRESSE, G.; JOUBERT, D. From ultrasoft pseudopotentials to the projector augmented-wave method. *Physical Review B*, v. 59, n. 3, p. 1758–1775, 15 jan. 1999.
- KWON, S. G. et al. Capping Ligands as Selectivity Switchers in Hydrogenation Reactions. *Nano Letters*, v. 12, n. 10, p. 5382–5388, 10 out. 2012.
- KYRIAKOU, G. et al. Isolated Metal Atom Geometries as a Strategy for Selective Heterogeneous Hydrogenations. *Science*, v. 335, n. 6073, p. 1209–1212, 9 mar. 2012.
- LI, G.; JIN, R. Gold Nanocluster-Catalyzed Semihydrogenation: A Unique Activation Pathway for Terminal Alkynes. *Journal of the American Chemical Society*, v. 136, n. 32, p. 11347–11354, 13 ago. 2014.
- LI, S.-S. et al. Efficient and exceptionally selective semireduction of alkynes using a supported gold catalyst under a CO atmosphere. *Chemical Communications*, v. 50, n. 42, p. 5626–5628, 2014.
- LI, S.-S. et al. Heterogeneous Gold-Catalyzed Selective Semireduction of Alkynes using Formic Acid as Hydrogen Source. *Advanced Synthesis & Catalysis*, v. 358, n. 9, p. 1410–1416, 28 abr. 2016.
- LIANG, S.; HAMMOND, G. B.; XU, B. Supported gold nanoparticles catalyzed cis-selective semihydrogenation of alkynes using ammonium formate as the reductant. *Chem. Commun.*, v. 52, n. 35, p. 6013–6016, 2016.
- LIU, C. et al. One-Pot Synthesis of Au₁₁(PPh₂)₇Br₃ for the Highly Chemoselective Hydrogenation of Nitrobenzaldehyde. *ACS Catalysis*, v. 6, n. 1,

p. 92–99, 4 jan. 2016a.

LIU, P. et al. Photochemical route for synthesizing atomically dispersed palladium catalysts. *Science*, v. 352, n. 6287, p. 797–800, 13 maio 2016b.

LIU, X. et al. Synthesis of thermally stable and highly active bimetallic Au-Ag nanoparticles on inert supports. *Chemistry of Materials*, v. 21, n. 2, p. 410–418, 2009.

LÓPEZ-SERRANO, J.; DUCKETT, S. B.; LLEDÓS, A. Palladium-catalyzed hydrogenation: Detection of palladium hydrides. A joint study using para-hydrogen-enhanced NMR spectroscopy and density functional theory. *Journal of the American Chemical Society*, v. 128, n. 30, p. 9596–9597, 2006.

MALLAT, T.; BAIKER, A. Selectivity enhancement in heterogeneous catalysis induced by reaction modifiers. *Applied Catalysis A: General*, v. 200, n. 1–2, p. 3–22, ago. 2000.

MARSHALL, S. T. et al. Controlled selectivity for palladium catalysts using self-assembled monolayers. *Nature Materials*, v. 9, n. 10, p. 853–858, 12 out. 2010.

MITSDOME, T. et al. One-step Synthesis of Core-Gold/Shell-Ceria Nanomaterial and Its Catalysis for Highly Selective Semihydrogenation of Alkynes. *Journal of the American Chemical Society*, v. 137, n. 42, p. 13452–13455, 28 out. 2015.

MONKHORST, H. J.; PACK, J. D. Special points for Brillouin-zone integrations. *Physical Review B*, v. 13, n. 12, p. 5188–5192, 15 jun. 1976.

MORENO, M. et al. Hydrogen reactivity of palladium nanoparticles coated with mixed monolayers of alkyl thiols and alkyl amines for sensing and catalysis applications. *Journal of the American Chemical Society*, v. 133, n. 12, p. 4389–4397, 2011.

OLIVEIRA, R. L. et al. On the stabilization of gold nanoparticles over silica-based magnetic supports modified with organosilanes. *Chemistry - A European*

Journal, v. 17, n. 16, p. 4626–4631, 2011.

PEI, G. X. et al. Promotional effect of Pd single atoms on Au nanoparticles supported on silica for the selective hydrogenation of acetylene in excess ethylene. *New Journal of Chemistry*, v. 38, n. 5, p. 2043, 2014.

REN, D. et al. An Unusual Chemoselective Hydrogenation of Quinoline Compounds Using Supported Gold Catalysts. *Journal of the American Chemical Society*, v. 134, n. 42, p. 17592–17598, 24 out. 2012.

SCANLON, J. T.; WILLIS, D. E. Calculation of flame ionization detector relative response factors using the effective carbon number concept. *Journal of Chromatographic Science*, v. 23, p. 333–340, 1985.

SCHOENBAUM, C. A.; SCHWARTZ, D. K.; MEDLIN, J. W. Controlling the Surface Environment of Heterogeneous Catalysts Using Self-Assembled Monolayers. *Accounts of Chemical Research*, v. 47, n. 4, p. 1438–1445, 15 abr. 2014.

SCHRADER, I. et al. Functionalization of Platinum Nanoparticles with α -Proline: Simultaneous Enhancements of Catalytic Activity and Selectivity. *Journal of the American Chemical Society*, v. 137, n. 2, p. 905–912, 21 jan. 2015.

SEGURA, Y.; LÓPEZ, N.; PÉREZ-RAMÍREZ, J. Origin of the superior hydrogenation selectivity of gold nanoparticles in alkyne + alkene mixtures: Triple- versus double-bond activation. *Journal of Catalysis*, v. 247, n. 2, p. 383–386, 2007.

SHAO, L. et al. Gold supported on graphene oxide: An active and selective catalyst for phenylacetylene hydrogenations at low temperatures. *ACS Catalysis*, v. 4, n. 7, p. 2369–2373, 2014.

STRATAKIS, M.; GARCIA, H. Catalysis by Supported Gold Nanoparticles: Beyond Aerobic Oxidative Processes. *Chemical Reviews*, v. 112, n. 8, p. 4469–4506, 8 ago. 2012.

- VASILIKOGIANNAKI, E. et al. cis-Semihydrogenation of alkynes with amine borane complexes catalyzed by gold nanoparticles under mild conditions. *Chemical Communications*, v. 51, n. 12, p. 2384–2387, 2015.
- VILÉ, G. et al. Silver Nanoparticles for Olefin Production: New Insights into the Mechanistic Description of Propyne Hydrogenation. *ChemCatChem*, v. 5, n. 12, p. 3750–3759, dez. 2013.
- VILÉ, G. et al. A Stable Single-Site Palladium Catalyst for Hydrogenations. *Angewandte Chemie International Edition*, v. 54, n. 38, p. 11265–11269, 14 set. 2015.
- VILÉ, G. et al. Advances in the Design of Nanostructured Catalysts for Selective Hydrogenation. *ChemCatChem*, v. 8, p. 21–33, 2016.
- WANG, A. et al. Understanding the synergistic effects of gold bimetallic catalysts. *Journal of Catalysis*, v. 308, p. 258–271, 2013.
- WANG, X.; CÁRDENAS-LIZANA, F.; KEANE, M. A. Toward Sustainable Chemoselective Nitroarene Hydrogenation Using Supported Gold as Catalyst. *ACS Sustainable Chemistry & Engineering*, v. 2, n. 12, p. 2781–2789, dez. 2014.
- WEI, H. et al. Supported Au-Ni nano-alloy catalysts for the chemoselective hydrogenation of nitroarenes. *Chinese Journal of Catalysis*, v. 36, n. 2, p. 160–167, 2015.
- WELCH, G. C. et al. Reversible, Metal-Free Hydrogen Activation. *Science*, v. 314, n. 5802, p. 1124–1126, 17 nov. 2006.
- WESTERHAUS, F. A. et al. Heterogenized cobalt oxide catalysts for nitroarene reduction by pyrolysis of molecularly defined complexes. *Nature Chemistry*, v. 5, n. 6, p. 537–543, 12 maio 2013.
- WITTSTOCK, A.; BÄUMER, M. Catalysis by unsupported skeletal gold catalysts. *Accounts of chemical research*, v. 47, n. 3, p. 731–9, 18 mar. 2014.

WU, B. et al. Selective Hydrogenation of α,β -Unsaturated Aldehydes Catalyzed by Amine-Capped Platinum-Cobalt Nanocrystals. *Angewandte Chemie International Edition*, v. 51, n. 14, p. 3440–3443, 2 abr. 2012.

YAN, M. et al. Nanoporous gold catalyst for highly selective semihydrogenation of alkynes: remarkable effect of amine additives. *Journal of the American Chemical Society*, v. 134, n. 42, p. 17536–17542, 2012.

ZANELLA, R. et al. Alternative Methods for the Preparation of Gold Nanoparticles Supported on TiO₂. *The Journal of Physical Chemistry B*, v. 106, n. 31, p. 7634–7642, 2002.

ZHANG, Y. et al. Nano-gold catalysis in fine chemical synthesis. *Chemical Reviews*, v. 112, n. 4, p. 2467–2505, 2012.

4. CHAPTER 2

Influence of capping ligands on the formation of surface-frustrated Lewis pairs at gold-ligand interfaces

"Pre-print of article reproduced with permission from [Fiorio, J. L.; Barbosa, E. C. M.; Kikuchi, D. K.; Camargo, P. H. C.; Rossi, L. M. Influence of capping ligands on the formation of surface-frustrated Lewis pairs at gold-ligand interfaces. *Catal. Sci. Technol.*, 2020, x, xxxx.] Copyright [2020] The Royal Society of Chemistry." The written permission from the editor is given in the Appendices A1. The published version of this article can be accessed in the link: <https://doi.org/10.1039/C9CY02016K>.

Abstract

The concept of frustrated Lewis pairs (FLPs) has been expanded to surface-FLP analogous formed by combining gold nanoparticles (NPs) and Lewis bases, such as amines or phosphines, creating a new channel for the heterolytic cleavage of H₂, and thereby performing selective hydrogenation reactions with gold. Since gold nanoparticles can be prepared by many different methodologies and using different capping ligands, in this study, we investigated the influence of the capping ligands, adsorbed on gold surfaces, on the formation of the FLPs interface. The catalytic activity in the hydrogenation of alkynes is low in the presence of citrate (Citr), poly(vinyl alcohol) (PVA),

polyvinylpyrrolidone (PVP), and oleylamine (Oley), but is greatly enhanced after removing the capping ligands from the gold surface. This demonstrates that the capping ligand blocks the sites to adsorption of the Lewis base. Moreover, once the ligands were removed by calcination, the FLPs can be formed and the catalytic system enables the highly selective semihydrogenation of various alkynes under mild reaction conditions.

4.1.MOTIVATION

Colloidal metal nanoparticles (NPs) are often prepared by colloidal synthesis methods and stabilized in solution by the interaction of specific capping ligands molecules with the surface, which ensures the nanoparticles does not coalesce.(THANH; MACLEAN; MAHIDDINE, 2014)(XIA et al., 2009) This type of methodology has received attention for the preparation of supported catalysts, allowing the preparation of metal catalysts with high control on particles' size, shape, and surface composition.(SONSTRÖM; BÄUMER, 2011)(JIA; SCHÜTH, 2011)(OTT; FINKE, 2007) The major concern of using colloidal synthetic methods is the influence of capping ligands adsorbed on the metallic surface both on the immobilization efficiency and on the catalyst performance, due to their binding affinity to the metallic surface.(VILLA et al., 2013)(ZHONG et al., 2014)(MUNNIK; DE JONGH; DE JONG, 2015) Overall, the presence of capping ligands can also decrease the accessibility of substrates to the metal surface, causing a low catalytic activity, since reactants cannot bind to surface atoms and undergo chemical transformations into the

desired products.(ROSSI et al., 2018)(CAMPISI et al., 2016)(WANG et al., 2018b)

Based on the assumption that the catalytic activity is diminished if the surface of metal nanoparticles is partly covered by capping ligands, until very recently, ligands were often removed either by extraction or pyrolysis prior to catalytic applications.(LOPEZ-SANCHEZ et al., 2011)(NIU; LI, 2014) However, it has been discussed that the capping ligands could be a dynamic component of the active catalyst which improves selectivity and activity.(ZHANG et al., 2018)(MAKOSCH et al., 2012)(CHEN et al., 2016)(HAO et al., 2016)(KWON et al., 2012)(WU et al., 2012)(KAEFFER et al., 2018) In this context, we recently demonstrated an enhancement in the catalytic activity of gold nanocatalysts when amine-ligands are added to the reaction medium. The heterolytic activation of molecular hydrogen occurs via a frustrated Lewis pair (FLP) interface, triggered by the combination of the added amine ligand (Lewis base) and the gold surface (Lewis acid), allowing an unexpectedly high activity in the hydrogenation reaction.(FIORIO; LÓPEZ; ROSSI, 2017) This behavior was demonstrated with gold catalysts prepared by an impregnation-reduction method, therefore free of capping ligands; however, since capping ligands are generally present when colloidally synthesized nanoparticles are used in catalysis, a systematic study analyzing the effect of capping ligands in the formation of FLP surface is missing.

Herein, we investigate how capping ligands adsorbed on the surface of Au NPs can obscure the formation of FLP interface needed to activate H₂ in hydrogenation reactions. Our studies reveal that the presence of capping ligands blocks the adsorption of the amine to the gold surface, avoiding the

FLPs interface and thereby leading to low catalytic activity. When the capping ligands were removed from the catalyst surface and an amine ligand was added, the FLPs interface is recovered and an enhanced catalytic activity was observed.

4.2. RESULTS AND DISCUSSION

Colloidal Au NPs with various capping ligands but similar sizes were prepared by different methodologies to evaluate the effect of each capping ligand in the catalytic activity while avoiding a possible size-dependent effects. The colloidal Au NPs with different capping ligands were immobilized on carbon and the TEM analyses of the supported Au/C catalysts confirmed the uniform dispersion over the support and the control over the NPs size (Figure 11a-d).

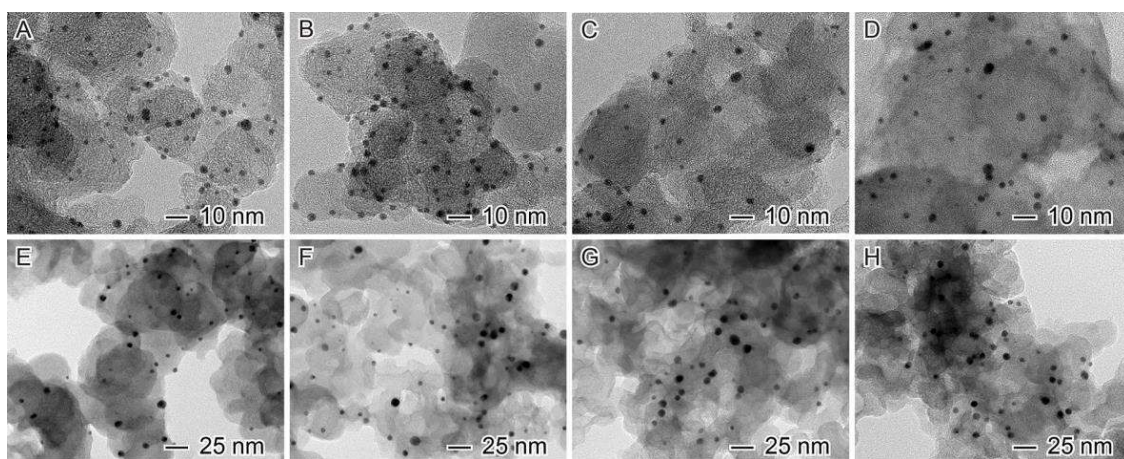


Figure 11. TEM images of nanoparticles before and after thermal treatment (a, e) $\text{Au}_{\text{PVA}}/\text{C}$, (b, f) $\text{Au}_{\text{PVP}}/\text{C}$, (c, g) $\text{Au}_{\text{Oley}}/\text{C}$, (d, h) $\text{Au}_{\text{Citr}}/\text{C}$.

The corresponding particle size distributions (Figure 12) indicate that the mean particle size on each sample is around 3 nm. In order to remove the

ligand from the catalyst surface and compare the adsorption of the amine-ligand in a clean surface and other with capping ligands, we conducted a thermal treatment in a portion of the as-prepared catalyst. An obvious increase in size was observed for all catalyst (Figure 12e-h), and the mean diameter after thermal treatment was 8 nm.

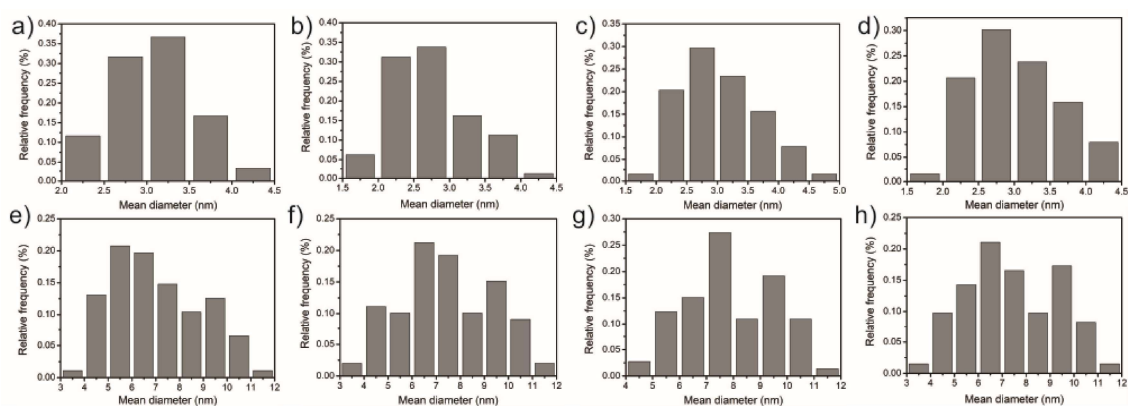


Figure 12. Size distribution of Au NPs before and after thermal (a, e) Au_{PVA}/C, (b, f) Au_{PVP}/C, (c, g) Au_{oleyl}/C, (d, h) Au_{citrate}/C.

Different UV-vis spectrum profiles for the catalysts were noticed (Figure 13), suggesting that the electronic structure of the Au NPs can be disturbed by the surrounding organic ligands or it might be related with differences in size distribution, both these factors may cause a shift in the surface plasmon resonance dipole mode of the Au NPs.(WAN et al., 2017)(KELLY et al., 2003)(ZHONG et al., 2013)

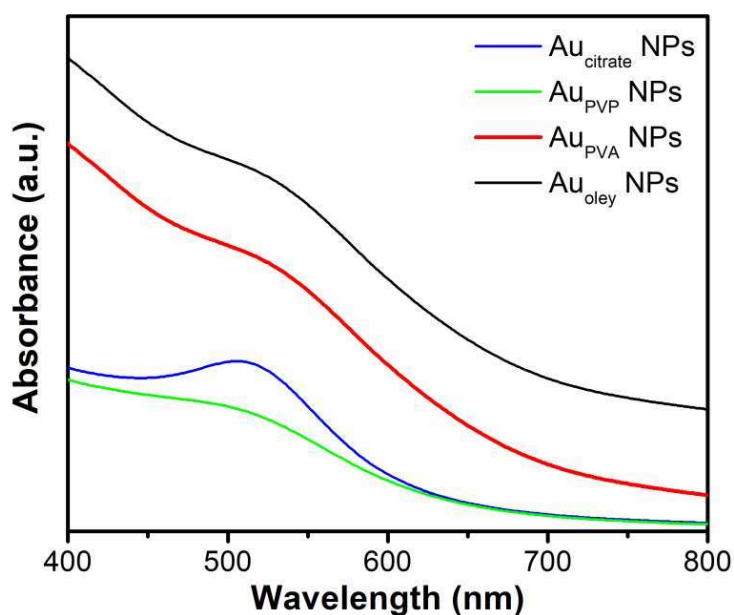


Figure 13. UV-vis spectra of Au NPs according to the different stabilizers.

Characteristic absorption peaks related to the corresponding protective agents were observed in the FTIR spectra of the samples (Figure 14 a–d). The catalyst prepared using citrate as stabilizer showed absorptions in the region of 1500 cm^{-1} corresponding to C=O stretching and an absorption band around $3000\text{--}3600\text{ cm}^{-1}$ assigned to the O-H stretch, a peak around 1300 cm^{-1} arises from the symmetric --COO-- vibration, and a weak absorption in the region of $3000\text{--}2800\text{ cm}^{-1}$ corresponding to the C-H stretching. When PVP was used as stabilizer, absorptions in the region of $3000\text{--}2800\text{ cm}^{-1}$ were characteristic of CH_2 stretching vibrations from the hydrocarbon backbone and the pyrrolidone rings of PVP while the ones in $1500\text{--}1400\text{ cm}^{-1}$ were characteristic of C-N stretching and C-H scissoring vibrations. The strong absorption at 1600 cm^{-1} was superimposed on the background absorption from the H-O-H bending vibration of adsorbed water molecules. The presence of PVA in the catalyst was characterized by CH_2 stretching modes at 2900 and 2800 cm^{-1} , CH_2 scissoring

at ca. 1400 cm^{-1} (broad), C–O–H in-plane bending at 1385 cm^{-1} , and the stretching vibration of the polar C–O bond at 1050 cm^{-1} .(ZHONG et al., 2013);(ZHONG et al., 2014) The FTIR of oleylamine capped Au NPs showed a strong C–N stretching mode at 1384 cm^{-1} , an N–H bending mode at 1635 cm^{-1} , and a weak band for N–H stretch at 3425 cm^{-1} , indicating the presence of oleylamine on the particle surface. The C–N stretch was blue shifted from that of free amines ($1000\text{--}1350\text{ cm}^{-1}$), probably due to the interaction between N and Au through coordination. Moreover, typical absorption bands for hydrocarbon groups assigned to CH_2 and CH_3 symmetric and asymmetric stretching vibrations in the range of $2840\text{--}2950\text{ cm}^{-1}$ and CH_2 bending vibration at 1460 cm^{-1} were observed.(LU et al., 2007)

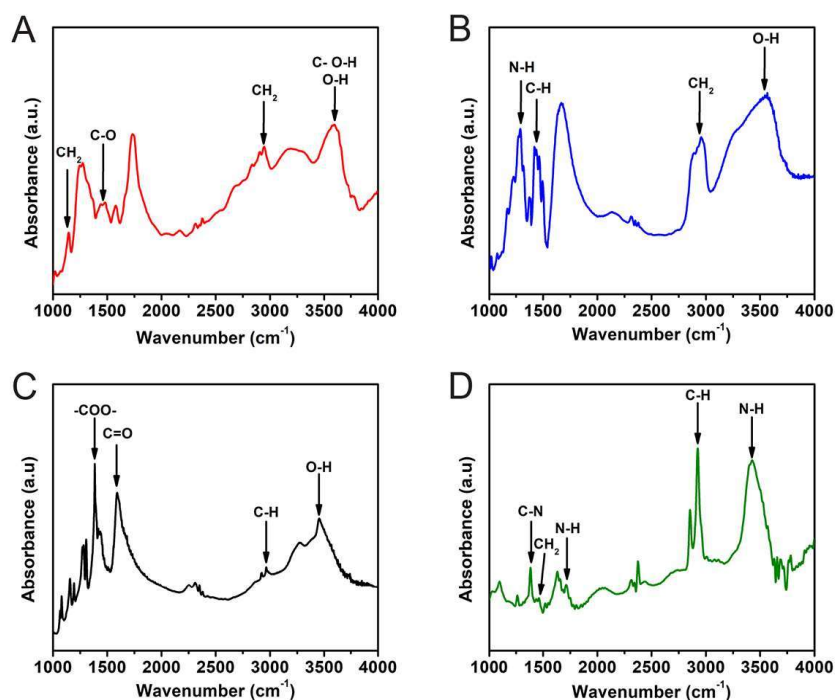
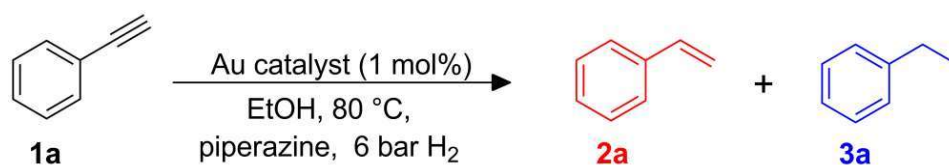


Figure 14. FTIR spectra of the (a) $\text{Au}_{\text{PVA}}/\text{C}$, (b) $\text{Au}_{\text{PVP}}/\text{C}$, (c) $\text{Au}_{\text{Cit}}/\text{C}$, (d) $\text{Au}_{\text{Oley}}/\text{C}$ catalysts.

It is anticipated that capping ligands on the surface of the Au NPs might affect the adsorption of amine-ligands, possibly blocking the formation of a surface-FLP metal-ligand interface.(WANG et al., 2018a)(MA et al., 2018) In order to probe this hypothesis, we examined the hydrogenation of phenylacetylene as a model transformation under conditions optimized elsewhere (6 bar of H₂, piperazine as ligand and 80 °C)(FIORIO; LÓPEZ; ROSSI, 2017) using the as-prepared supported Au NP catalysts with different capping ligands (PVA, citrate, oleylamine and PVP) and their thermal treated counterparts. All catalysts were inactive in the absence of piperazine (Table 6, entries 1, 3, 5, 7, 9, 11, 13 and 15). Clearly, the as-prepared Au catalysts, which contain capping ligands, were less active than the thermally treated Au catalysts (Table 6, entries 4, 8, 12 and 16). This trend suggests that the capping ligands act as a physical barrier to restrict the free access of reactants to the catalytically active sites on the Au NP surface and/or prevents the adsorption of piperazine, which is crucial to lower the energy barrier for H₂ dissociation. Once these capping ligands are removed from the Au NP surface, a favorable activation barrier to the H₂ splitting was reached when piperazine is added to the reaction medium. The loss of selectivity in some cases (Table 6, entries 8 and 12) may be due to the presence of large (> 7 nm) Au NPs.(NOUJIMA et al., 2011)

Table 6. Catalytic activity of Au catalysts in the hydrogenation of phenylacetylene **1a**.^a

Entry	Catalyst	Calcined	Amine	Conversion (%)	Selectivity to 2a (%)
1	Au _{PVA} /C	No	No	6	>99
2	Au _{PVA} /C	No	Yes	3	>99
3	Au _{PVA} /C	Yes	No	8	>99
4	Au _{PVA} /C	Yes	Yes	>99	>99
5	Au _{Citr} /C	No	No	5	>99
6	Au _{Citr} /C	No	Yes	3	>99
7	Au _{Citr} /C	Yes	No	2	>99
8	Au _{Citr} /C	Yes	Yes	70	94
9	Au _{Oley} /C	No	No	2	>99
10	Au _{Oley} /C	No	Yes	3	>99
11	Au _{Oley} /C	Yes	No	4	>99
12	Au _{Oley} /C	Yes	Yes	68	85
13	Au _{PVP} /C	No	No	3	>99
14	Au _{PVP} /C	No	Yes	6	>99
15	Au _{PVP} /C	Yes	No	8	>99
16	Au _{PVP} /C	Yes	Yes	82	>99

^aReaction conditions: 1 mmol of alkyne, 0.5 mol% of Au, 1 mmol of piperazine, 2 mL of EtOH, 80 °C, 6 bar of H₂, 24 h. Conversion and selectivity were determined by GC using the internal standard technique.

Kinetic studies were carried out with the four most active catalytic systems (Figure 15). Notably, the thermal treated Au_{PVA}/C in the presence of piperazine is the most active catalytic system. According to the reaction rate, calculated at lower than 30% of conversion, the Au catalysts could be ranked in the order PVA > PVP > citrate > oleylamine. The lower activity of the catalyst stabilized with citrate and oleylamine might be due to carbonaceous residue formation during the thermal treatment, which may affect some catalytic sites of the Au NPs, indicating that the nature of the organic residues influences the catalytic properties of Au NPs, (ZHONG et al., 2014) since no significant size change was noticed in comparison with the two others capping ligand.

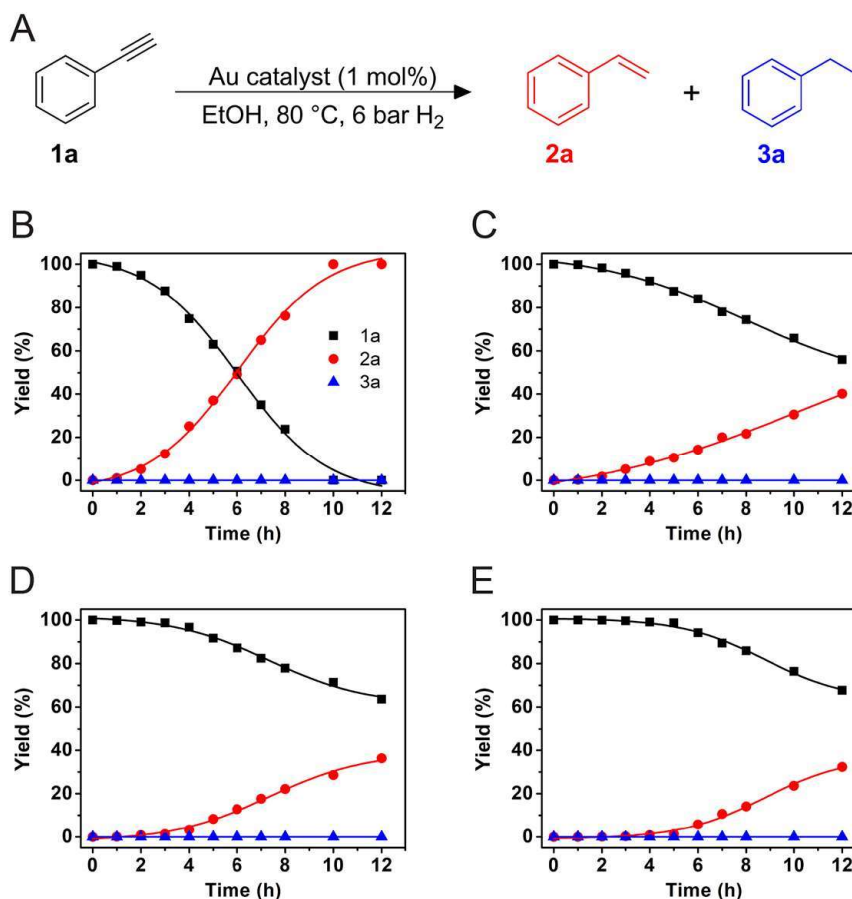


Figure 15. a) Time course studies comparing the reaction profile of the calcined catalysts with addition of piperazine b) Au_{PVA}/C; c) Au_{PVP}/C; d) Au_{Citr}/C; e) Au_{Oley}/C; Reaction conditions: 4 mmol of alkyne, 0.5 mol% of Au, 4 mmol of piperazine, 8 mL of EtOH, 80 °C, 6 bar of H₂.

At this point, we studied the influence of the calcination temperature in the reaction rate, using Au_{PVA}/C catalyst as model. As shown in Figure 16, the calcination temperature and catalytic activity exhibit a volcano-type relationship. The reaction rate increases alongside with the calcination temperature (ranging from 200 to 400 °C), reaching its maximum, and abruptly decreasing at higher temperatures. Probably, the drop in reaction rate at higher temperatures is due to nanoparticle sintering. (LOPEZ-SANCHEZ et al., 2011) The low catalytic

activity at lower calcination temperatures may happen due to the presence of capping ligands blocking adsorption of the amine ligand.

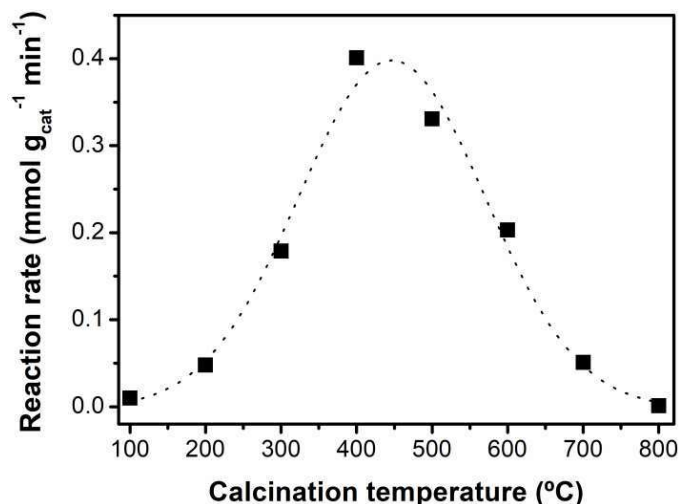
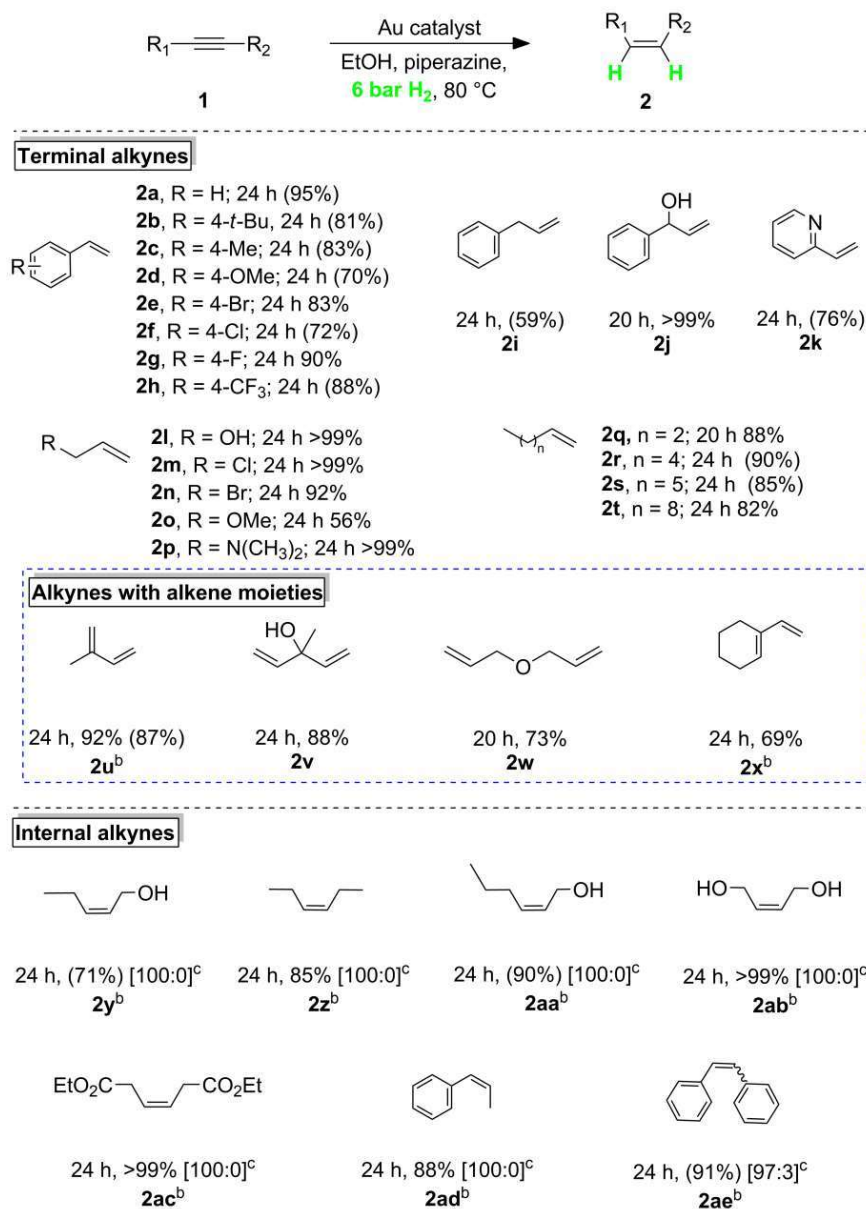


Figure 16. Reaction rates performance of the Au_{PVA}/C catalyst thermal treated in different temperatures.

The catalytic potential of Au_{PVA}/C thermally treated at 400 °C, which exhibited the best performance, was investigated using various alkynes. Ethynylbenzenes bearing electron-donating and electron-withdrawing groups were selectively hydrogenated to the corresponding terminal alkenes with excellent selectivity and reducible functional groups, such as halogen, hydroxyl moieties were compatible in the reaction (Table 7, entries 2a-2t). Various aliphatic terminal alkynes were also efficiently converted into the terminal alkenes without isomerization into internal alkenes (Table 7, entries 2u-2x). Importantly, alkynes with an alkene moiety were smoothly hydrogenated, whereas alkene moieties in the parent and product molecules were completely intact (Table 7, entries 2q-2t). Moreover, a series of internal alkynes were

smoothly hydrogenated to the Z-alkenes with excellent selectivity (Table 7, entries 2y-2ae).

Table 7. Semihydrogenation of various alkynes to alkenes.^a



^aReaction conditions: 1 mmol of alkyne, 0.5 mol% of Au, 1 mmol of piperazine, 2 mL of EtOH, 80 °C, 6 bar of H₂. Conversion and selectivity were determined by GC using the internal standard technique. In all cases, the selectivity was >99%. Isolated yields in parenthesis. ^b 1 mol% of Au. ^c Determined by ¹H NMR.

After the reaction, the catalyst was easily separated from the reaction mixture by filtration (Figure 17a). Inductively coupled plasma atomic emission spectrometry (ICP AES) analysis revealed that no leaching of Au species into the reaction mixture occurred (detection limit: 0.1 ppm). Overall, the catalyst was reusable and a significant decrease in the catalytic activity was noticed after the second recycle, though keeping the selectivity towards the alkene (Figure 17b) through all recycles.

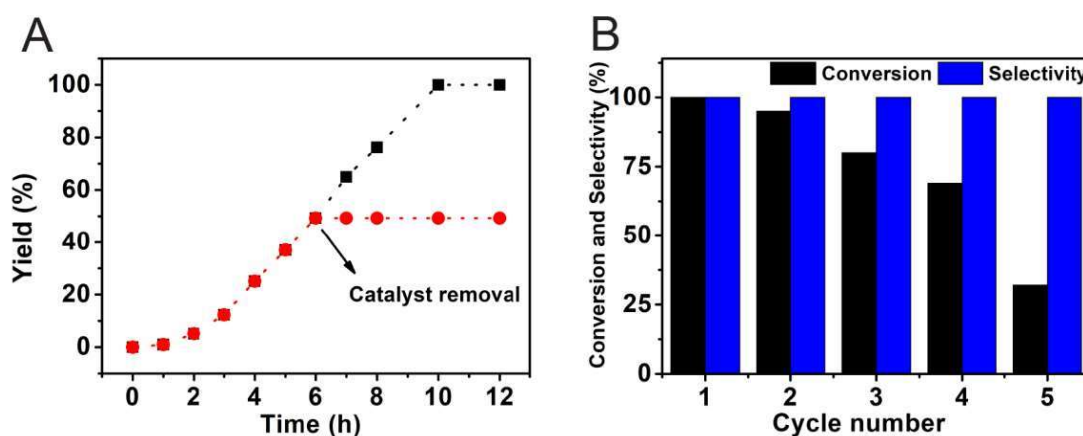


Figure 17. a) Hot filtration test and b) Recycling experiments

The TEM analysis of the recycled catalyst (Figure 18) revealed that the decrease in the catalytic activity is associated with a significant increase in the mean diameter size of the Au NPs to ~20 nm. Therefore, as previously described, the capping ligand might play an important role in preventing the agglomeration of the nanoparticles and increasing the lifetime of the catalyst. However, once the capping ligand is completely removed, a drop in activity is observed over the recycling process. (VILLA et al., 2013)

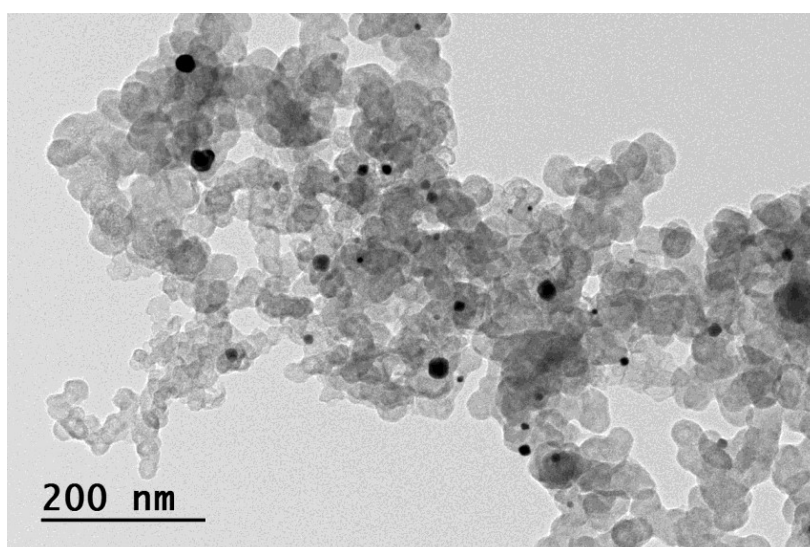


Figure 18. TEM image of Au_{PVA}/C thermal treated after fifth-run reactions

Altogether, the above catalytic results imply that, as previously described, the amine ligand, piperazine, once adsorbed on the gold surface facilitates the heterolytic H₂ activation at the Au NPs. (FIORIO; LÓPEZ; ROSSI, 2017);(REN et al., 2012);(GHUMAN et al., 2016a);(MA et al., 2018);(STEPHAN, 2016);(LU et al., 2014b) However, the presence of capping ligands on the surface of Au NPs compromises the adsorption of the amine ligand, avoiding the formation of the FLPs interface (Figure 19), providing an unfavorable situation for hydrogen activation. Effective removal of the capping ligand by thermal treatment exposes the nanoparticles' surfaces and thus enhances the catalytic activity, as a result of the successful formation of the Au-piperazine FLPs-like system, which increases the molecular hydrogen splitting, the rate-determining step of the reaction.

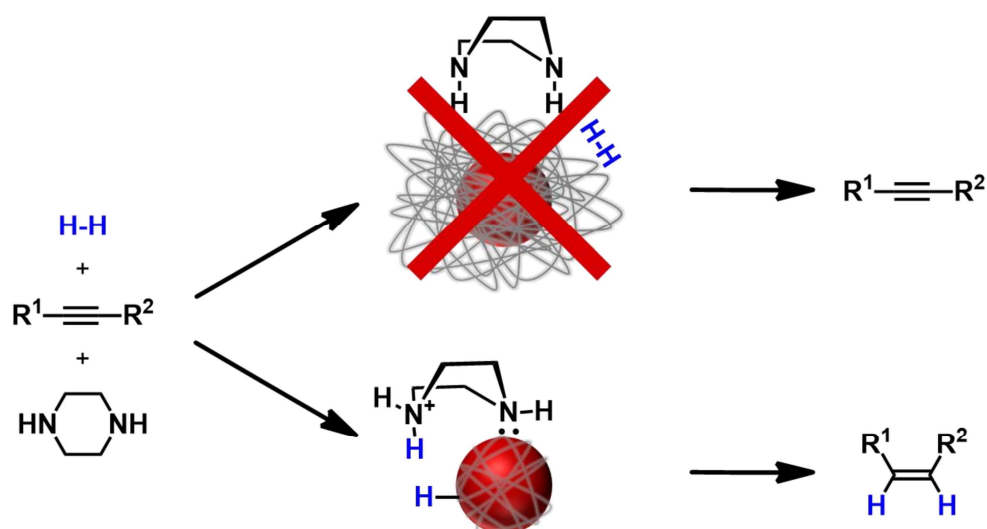


Figure 19. Scheme showing the differences in the activity of Au NPs with and without capping ligand.

To gain insight into the nature of the catalytic active species, NMR investigations were carried out using the Au_{PVA} NPs and piperazine, before tests the colloid was thoroughly washed in order to remove the excess of capping ligand. Figure 5 shows the proton NMR spectra of piperazine solutions in D_2O at $80\text{ }^\circ\text{C}$. As observed in the Figure 1c, when the system was pressurized with H_2 in the presence of the amine and Au NPs resulted in a new peaked around 3.1 ppm, while either the free ligand or the ligand in the presence of Au NPs exhibit peaks around 2.7 and 4.8 ppm. A similar shift is also observed when in the reaction medium was acidified, favoring the formation of the iminium species. Our results indicated that the presence of the ligand is critical to the observed reactivity in the activation of H_2 , and we speculate that this is related to the ligand to metal cooperative effect that can be comprehended as a surface frustrated Lewis pairs (FLPs) created by combining the gold surface (Lewis acid) and the amine ligand (Lewis base).

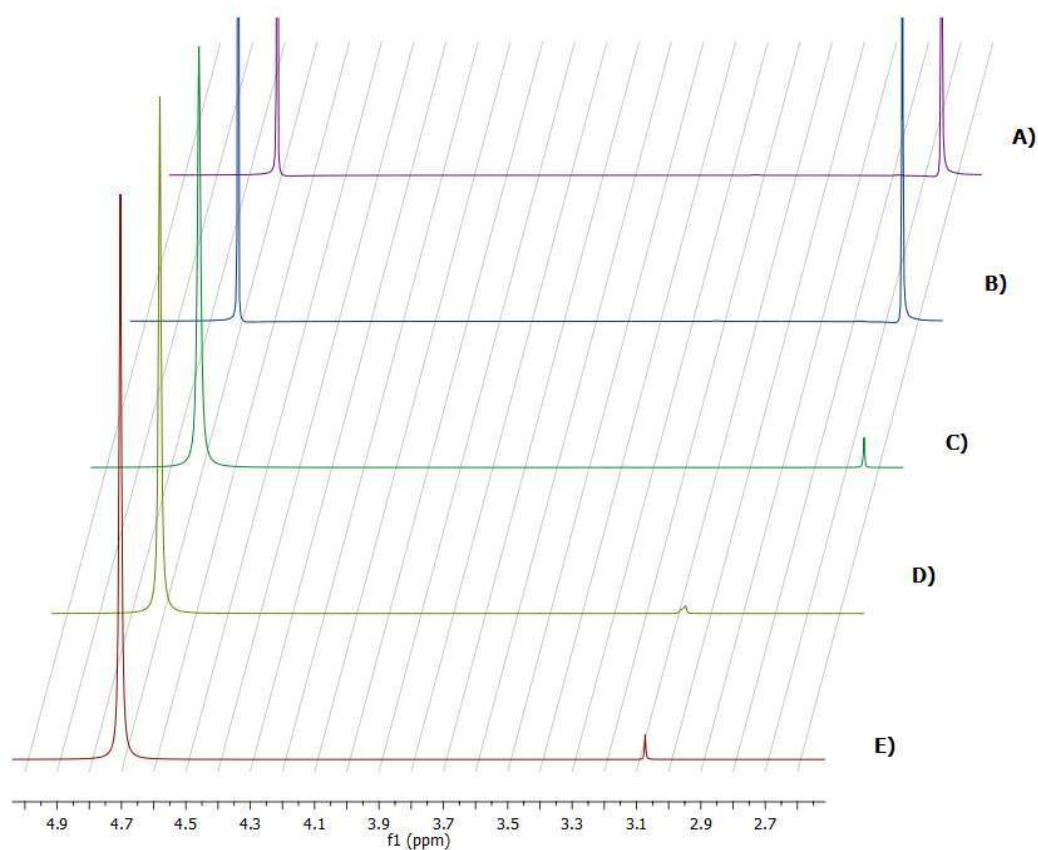


Figure 5. Overlay of ^1H NMR spectra of (a) piperazine; (b) piperazine/ H_2 ; (c) piperazine/Au colloid; (d) piperazine/Au colloid/ H_2 and (e) piperazine/Au colloid/ H^+ .

4.3. CONCLUSIONS

In conclusion, we have studied the limitations of using Au NPs with different capping ligands in the preparation of FLP gold-ligand interface necessary to boost gold activity towards hydrogenation reactions. The presence of capping agents blocks the adsorption of the Lewis base (amine-ligand), avoiding the formation of the FLP interface, leading to low catalytic activity. The removal of the stabilizing agents by thermal treatment leads to an increase in the catalytic activity most probably due to the exposition of the metal surface,

which allows the successful adsorption of the amine-ligand to generate FLPs-like surfaces. Moreover, the catalytic system enables the highly selective semihydrogenation of various alkynes under mild reaction conditions, with excellent selectivity for alkenes. This work represents a clear demonstration of the ligand–metal cooperative effect in the activation of H₂ via FLPs surface, where the nature of the capping ligand plays a crucial role and can obscure the catalytic activity.

4.4. EXPERIMENTAL SECTION

4.4.1. Materials and Methods

All the reagents used for the support and catalyst preparations were of analytical grade, purchased from Sigma-Aldrich and used as received. Tetrachloroauric(III) acid was purchased as a 30 wt% aqueous solution in dilute HCl (Sigma-Aldrich). Commercial reagents were purchased from Sigma Aldrich, and used as received. The glass reactors were thoroughly cleaned with aqua regia (HCl:HNO₃ = 3:1 v/v), rinsed with copious pure water, and then dried in an oven prior to use.

UV-Vis spectra were recorded on a Shimadzu UV-1700. Gold content in the catalyst was measured by FAAS analysis, on a Shimadzu AA-6300 spectrophotometer using an Au hollow cathode lamp (Photron). Metal leaching into the supernatant solution was measured by inductively coupled plasma atomic emission spectroscopy measurements, performed on a Spectro Arcos ICP-OES. TEM analyses were performed with a JEOL 2100. Catalyst samples

for TEM were prepared by sonicating the catalyst powder in propan-2-ol. A drop of the resulting dispersion was placed on a carbon-coated copper grid (Ted Pella, Inc.). The histogram of nanoparticle size distribution was obtained from the measurement of about 200 particles. NMR spectras were recorded on Bruker 500 or 300 MHz spectrometers at ambient temperature. Chemicals shifts (δ) are reported in ppm downfield of tetramethylsilane. ^1H NMR spectra were referenced to the residual solvent signals (δ_{H} 7.26 ppm for CDCl_3).

4.4.2. Catalysts preparation

Preparation of $\text{Au}_{\text{PVA}}/\text{C}$

The gold catalyst stabilized with PVA (average molecular weight $\text{MW} = 9000 - 10\,000 \text{ g mol}^{-1}$, 80% hydrolyzed) was prepared as previously described in literature (PORTA et al., 2000) (LOPEZ-SANCHEZ et al., 2011) as followed: to an aqueous HAuCl_4 solution ($5.08 \times 10^{-4} \text{ M}$), the required amount of a PVA solution (1 wt %) was added ($\text{PVA}/(\text{Au}) (\text{w/w}) = 1.2$); a freshly prepared solution of NaBH_4 (0.1 M, $\text{NaBH}_4/(\text{Au}) (\text{mol/mol}) = 5$) was then added to form a dark-brown sol. After 30 min of sol generation, 1 g of the carbon support (Vulcan XC 72R) was added to the colloid, and the mixture was vigorous stirred overnight to immobilize the Au NPs in the support. The slurry was filtered, and the catalyst was washed three times with acetone and dried under vacuum. The final metal loading was 0.7 wt% as determined by FAAS.

Preparation of $\text{Au}_{\text{PVP}}/\text{C}$

The gold nanoparticles stabilized with PVP were prepared according to a procedure reported elsewhere.(AGARWAL et al., 2017):(ABIS et al., 2017) In a typical synthesis of 1 g of Au_{PVP}/C, an aqueous solution of HAuCl₄·3H₂O (0.8 mL, 25 mg HAuCl₄·3H₂O/mL Sigma Aldrich, ≥49.0%) was added to 400 mL of deionized water under vigorous stirring conditions, followed by the addition of a 1 wt% aqueous solution of PVP (Sigma Aldrich, average molecular weight MW = 10 000 g mol⁻¹). Next, a 0.1 M freshly prepared solution of NaBH₄ was added (mol NaBH₄/ mol Au = 5) to form a red sol. After 30 min of sol generation, the colloid was immobilized by adding 1 g of carbon support (Vulcan XC 72R). The mixture was stirred overnight. After, the slurry was filtered, the catalyst washed three times with acetone and dried under vacuum. The metal loading was 0.5 wt% as determined by FAAS.

Preparation of Au_{Oleylamine}/C

In a typical synthesis as described elsewhere,(PENG et al., 2008) 10 mL of tetralin, 10 mL of oleylamine and 278.4 mg of HAuCl₄ were added to three-neck round-bottom flask and the mixture was magnetically stirred under N₂ flow for 10 min, at 35 °C. After, a reducing solution containing 0.5 mmol of TBAB, tetralin (1 mL), and oleylamine (1 mL) was prepared by sonication and injected all at once into the precursor solution. The reduction was instantaneously initiated, and the solution changed to a deep purple color. The mixture was allowed to react at 35 °C for 1 h before 1 g of carbon support was added and vigorously stirred overnight. The slurry was filtrated, washed three times with acetone and dried under vacuum. The metal content was 0.5 wt% as determined by FAAS.

Preparation of Au_{Citrate}/C

To prepare the gold catalyst stabilized by citrate, we adopted a previous described method in literature.(PIELLA; BASTÚS; PUNTES, 2016) A typical procedure is as followed: to a three-necked round-bottom flask was added a freshly prepared aqueous solution of sodium citrate (150 mL, 2.2 mM), tannic acid (0.1 mL, 2.5 mM) and K₂CO₃ (1 mL, 150 mM), and the resulting solution was heated in a heating mantle to 70°C. Once the temperature reached 70 °C, 1 mL of HAuCl₄ (25 mM) was injected. The solution was kept at 70 °C for 5 min more to ensure complete reaction of the gold precursor. After, 1 g of the carbon support was added, and the mixture was stirred overnight to immobilize the Au NPs. The catalyst was collected by centrifugation, washed three times with acetone and dried under vacuum. The metal content was 0.4 wt% as determined by FAAS.

4.4.3. Thermal treatment to remove the ligand

Typically, to remove the ligand from the catalyst surface a certain amount of the as-prepared catalyst was placed in a crucible and the solid was thermally treated in an oven at a rate of 10 °C per minute and held at the desired temperature for 2 h in N₂ atmosphere.

4.4.4. Catalytic Investigations

Catalytic hydrogenation reactions

In a modified Fischer–Porter 100 mL glass reactor substrate (1 mmol), piperazine (100 eq.) and gold catalyst (1 mol%) were mixed with 2 mL of ethanol. The reactor was closed and purged five times with H₂, leaving the vessel at 6 bar of H₂. All the reactions were performed at 80 °C, the temperature was maintained with an oil bath on a hot stirring. After the completion of the reaction, the catalyst was removed by centrifugation and the products were analyzed by GC with an internal standard to determine the conversion of substrate and the selectivity for the product.

Recycling experiment

In a typical recycling experiment, substrate (1 mmol), piperazine (100 eq.) and gold catalyst (1 mol%) were added to a Fischer–Porter 100 mL glass reactor equipped with a magnetic stirring bar, the reactor was then closed, purged five times with H₂, leaving the vessel at 6 bar of H₂, and the resulting reaction mixture was heated at 80 °C for 24 h. After the reaction was complete, the reactor was cooled to room temperature and the hydrogen was released. An internal standard (biphenyl) was added to the solution to determine the conversion and selectivity by GC analysis of the mixture. The catalyst separated by centrifugation was washed with ethanol for three times, then dried under vacuum, and reused for the next reaction.

Product Analysis of Catalytic Experiments

All the products were determined by GC analyses carried out with a Shimadzu GC-2010 equipped with a RTx-5 column (30 m x 0.25 mm x 0.25 mm) and a FID detector (all GC yields are average values from at least 2 runs).

Method: $T_i = 40\text{ }^\circ\text{C}$, $T_f = 200\text{ }^\circ\text{C}$, 17 min. Internal standard: biphenyl. The conversion and selectivity were determined from the total amount of detected products and reactant.

4.5. REFERENCES

ABIS, L. et al. Highly Active Gold and Gold-Palladium Catalysts Prepared by Colloidal Methods in the Absence of Polymer Stabilizers. **ChemCatChem**, v. 9, n. 15, p. 2914–2918, 9 ago. 2017.

AGARWAL, N. et al. Aqueous Au-Pd colloids catalyze selective CH₄ oxidation to CH₃OH with O₂ under mild conditions. **Science**, v. 358, n. 6360, p. 223–227, 13 out. 2017.

CAMPISI, S. et al. Untangling the Role of the Capping Agent in Nanocatalysis: Recent Advances and Perspectives. **Catalysts**, v. 6, n. 12, p. 185, 27 nov. 2016.

CHEN, G. et al. Interfacial electronic effects control the reaction selectivity of platinum catalysts. **Nature Materials**, v. 15, n. January, p. 564, 2016.

FIORIO, J. L.; LÓPEZ, N.; ROSSI, L. M. Gold–Ligand-Catalyzed Selective Hydrogenation of Alkynes into cis -Alkenes via H₂ Heterolytic Activation by Frustrated Lewis Pairs. **ACS Catalysis**, v. 7, n. 4, p. 2973–2980, 7 abr. 2017.

GHUMAN, K. K. et al. Surface Analogues of Molecular Frustrated Lewis Pairs in Heterogeneous CO₂ Hydrogenation Catalysis. **ACS Catalysis**, v. 6, n. 9, p. 5764–5770, 2016.

HAO, P. et al. Application of thiolate self-assembled monolayers in selective alcohol oxidation for suppression of Pd catalyst deactivation. **Journal of Catalysis**, v. 344, p. 722–728, dez. 2016.

JIA, C.-J.; SCHÜTH, F. Colloidal metal nanoparticles as a component of

designed catalyst. **Physical Chemistry Chemical Physics**, v. 13, n. 7, p. 2457–2487, 2011.

KAEFFER, N. et al. An N-heterocyclic carbene ligand promotes highly selective alkyne semihydrogenation with copper nanoparticles supported on passivated silica. **Chemical Science**, v. 9, n. 24, p. 5366–5371, 2018.

KELLY, K. L. et al. The Optical Properties of Metal Nanoparticles: The Influence of Size, Shape, and Dielectric Environment. **The Journal of Physical Chemistry B**, v. 107, n. 3, p. 668–677, jan. 2003.

KWON, S. G. et al. Capping Ligands as Selectivity Switchers in Hydrogenation Reactions. **Nano Letters**, v. 12, n. 10, p. 5382–5388, 10 out. 2012.

LOPEZ-SANCHEZ, J. A. et al. Facile removal of stabilizer-ligands from supported gold nanoparticles. **Nature Chemistry**, v. 3, n. 7, p. 551–556, 5 jun. 2011.

LU, G. et al. Gold catalyzed hydrogenations of small imines and nitriles: enhanced reactivity of Au surface toward H₂ via collaboration with a Lewis base. **Chem. Sci.**, v. 5, n. 3, p. 1082–1090, 2014.

LU, X. et al. Mechanistic studies on the galvanic replacement reaction between multiply twinned particles of Ag and H₂AuCl₄ in an organic medium. **Journal of the American Chemical Society**, v. 129, n. 6, p. 1733–1742, 2007.

MA, Y. et al. Semi-solid and solid frustrated Lewis pair catalysts. **Chemical Society Reviews**, v. 47, n. 15, p. 5541–5553, 2018.

MAKOSCH, M. et al. Organic Thiol Modified Pt/TiO₂ Catalysts to Control Chemoselective Hydrogenation of Substituted Nitroarenes. **ACS Catalysis**, v. 2, n. 10, p. 2079–2081, 5 out. 2012.

MUNNIK, P.; DE JONGH, P. E.; DE JONG, K. P. Recent Developments in the Synthesis of Supported Catalysts. **Chemical Reviews**, v. 115, n. 14, p. 6687–6718, 22 jul. 2015.

- NIU, Z.; LI, Y. Removal and utilization of capping agents in nanocatalysis. **Chemistry of Materials**, v. 26, n. 1, p. 72–83, 2014.
- NOUJIMA, A. et al. Selective Deoxygenation of Epoxides to Alkenes with Molecular Hydrogen Using a Hydrotalcite-Supported Gold Catalyst: A Concerted Effect between Gold Nanoparticles and Basic Sites on a Support. **Angewandte Chemie International Edition**, v. 50, n. 13, p. 2986–2989, 21 mar. 2011.
- OTT, L. S.; FINKE, R. G. Transition-metal nanocluster stabilization for catalysis: A critical review of ranking methods and putative stabilizers. **Coordination Chemistry Reviews**, v. 251, n. 9–10, p. 1075–1100, maio 2007.
- PENG, S. et al. A facile synthesis of monodisperse Au nanoparticles and their catalysis of CO oxidation. **Nano Research**, v. 1, n. 3, p. 229–234, 2008.
- PIELLA, J.; BASTÚS, N. G.; PUNTES, V. Size-Controlled Synthesis of Sub-10-nanometer Citrate-Stabilized Gold Nanoparticles and Related Optical Properties. **Chemistry of Materials**, v. 28, n. 4, p. 1066–1075, 23 fev. 2016.
- PORTA, F. et al. Metal sols as a useful tool for heterogeneous gold catalyst preparation: Reinvestigation of a liquid phase oxidation. **Catalysis Today**, v. 61, n. 1, p. 165–172, 2000.
- REN, D. et al. An Unusual Chemoselective Hydrogenation of Quinoline Compounds Using Supported Gold Catalysts. **Journal of the American Chemical Society**, v. 134, n. 42, p. 17592–17598, 24 out. 2012.
- ROSSI, L. M. et al. The role and fate of capping ligands in colloiddally prepared metal nanoparticle catalysts. **Dalton Transactions**, v. 47, n. 17, p. 5889–5915, 2018.
- SONSTRÖM, P.; BÄUMER, M. Supported colloidal nanoparticles in heterogeneous gas phase catalysis: on the way to tailored catalysts. **Physical Chemistry Chemical Physics**, v. 13, n. 43, p. 19270–19284, 2011.

- STEPHAN, D. W. The broadening reach of frustrated Lewis pair chemistry. **Science**, v. 354, n. 6317, p. aaf7229–aaf7229, 9 dez. 2016.
- THANH, N. T. K.; MACLEAN, N.; MAHIDDINE, S. Mechanisms of Nucleation and Growth of Nanoparticles in Solution. **Chemical Reviews**, v. 114, n. 15, p. 7610–7630, 13 ago. 2014.
- VILLA, A. et al. Sol immobilization technique: a delicate balance between activity, selectivity and stability of gold catalysts. **Catalysis Science & Technology**, v. 3, n. 11, p. 3036, 2013.
- WAN, X.-K. et al. Ligand effects in catalysis by atomically precise gold nanoclusters. **Science Advances**, v. 3, n. 10, p. e1701823, 6 out. 2017.
- WANG, L. et al. Solid state frustrated Lewis pair chemistry. **Chemical Science**, v. 9, n. 21, p. 4859–4865, 2018a.
- WANG, Q. et al. Scalable Solid-State Synthesis of Highly Dispersed Uncapped Metal (Rh, Ru, Ir) Nanoparticles for Efficient Hydrogen Evolution. **Advanced Energy Materials**, v. 1801698, p. 1801698, 19 set. 2018b.
- WU, B. et al. Selective Hydrogenation of α,β -Unsaturated Aldehydes Catalyzed by Amine-Capped Platinum-Cobalt Nanocrystals. **Angewandte Chemie International Edition**, v. 51, n. 14, p. 3440–3443, 2 abr. 2012.
- XIA, Y. et al. Shape-Controlled Synthesis of Metal Nanocrystals: Simple Chemistry Meets Complex Physics? **Angewandte Chemie International Edition**, v. 48, n. 1, p. 60–103, 2009.
- ZHANG, J. et al. Control of interfacial acid–metal catalysis with organic monolayers. **Nature Catalysis**, v. 1, n. 2, p. 148–155, 15 fev. 2018.
- ZHONG, R.-Y. et al. Stabilizer substitution and its effect on the hydrogenation catalysis by Au nanoparticles from colloidal synthesis. **Catalysis Science & Technology**, v. 3, n. 11, p. 3013, 2013.
- ZHONG, R. Y. et al. Impacts of organic stabilizers on catalysis of Au

nanoparticles from colloidal preparation. **ACS Catalysis**, v. 4, n. 11, p. 3982–3993, 2014.

5. CHAPTER 3

Catalysis at gold-organophosphorus ligands interfaces: a frustrated Lewis pair mechanism for selective reduction reactions

Abstract

The cooperative action of ligands on heterogeneous catalysts leading to the activation of small molecules, such as the H₂ heterolytic splitting across the Au–ligand interface, has expanded the range of transformations achievable using gold catalysis. Here, we disclose the utilization of commercially available organophosphorus ligands that enable the Au-catalyzed selective reduction of epoxides, N-oxides, sulfoxides and alkynes using molecular hydrogen. The Au NP catalyst combined with alkyl-phosphines or alkyl-phosphites is remarkably more reactive than solely Au NPs. However, aryl phosphines, aryl-phosphites, phosphine oxides and organophosphates did not boost gold's activity. Although the mechanistic aspects remain somewhat speculative at this time, the method is not only a complementary Au-catalyzed reductive reaction under mild conditions, but also a niche procedure for selective reductions of wide range of valuable molecules that would be either synthetically inconvenient or even intractable to access by alternative synthetic protocols or by using classical transition metal catalysts.

5.1. MOTIVATION

Although common in enzymatic reactions and also present in homogeneous catalysts,(LIU; HU, 2002)·(NOYORI, 2002) the cooperative action of ligands has been less investigated in heterogeneous catalysis. When properly applied, catalysis at metal-ligand interfaces can lead to very significant increases in activity and selectivity.(MARSHALL et al., 2010)·(TESCHNER et al., 2008)·(CHEN et al., 2016c)·(XIAO et al., 2015) Organic modifiers (ligands) adsorbed on metal surfaces of heterogeneous catalysts have been used to control parameters such as reactive intermediates and the electronic nature of the surface of the heterogeneous catalyst and, in some cases, enhancing selectivity and catalytic activity.(SCHOENBAUM; SCHWARTZ; MEDLIN, 2014) A number of recent studies have demonstrated the tunability in the catalytic activity when amines,(CHEN et al., 2016c)·(LI; JIN, 2014) thiols,(SCHOENBAUM; SCHWARTZ; MEDLIN, 2014)·(MAKOSCH et al., 2012) phosphorous-based,(FEDOROV et al., 2016)·(LARI et al., 2017)·(ALMORA-BARRIOS et al., 2017)·(CANO et al., 2014)·(CANO et al., 2015)·(LIU et al., 2016a) and *N*-heterocyclic carbenes(ERNST et al., 2017)·(ERNST et al., 2016)·(YE et al., 2018) are combined with the metallic catalyst.

In this respect, combining gold nanoparticles (Au NPs) with ligands allowed the discovery of new reactivity of gold catalysts leading to highly selective hydrogenation reactions. Gold has a very limited capacity for molecular hydrogen activation; the energy barrier for H₂ dissociation on the Au surface is very high,(ALMORA-BARRIOS et al., 2017)·(ZHANG et al., 2012)·(STRATAKIS; GARCIA, 2012)·(HAMMER; NORSKOV, 1995) affording

low catalytic activity in hydrogenation reaction using H₂ as reductant. Nevertheless, gold's low activity is largely compensated by its intrinsic selectivity, especially in hydrogenation of triple bonds to double bonds, due to the preferential adsorption of alkyne in comparison to alkene, thermodynamic selectivity.(SEGURA; LÓPEZ; PÉREZ-RAMÍREZ, 2007) When applied in the hydrogenation of multifunctional molecules, gold catalysts are able to preserve the carbon-carbon double bond intact after reduction of -C≡C-,(MITSUDOME et al., 2015)(LI et al., 2016)(VASILIKOGIANNAKI et al., 2015)(LIANG; HAMMOND; XU, 2016)(YAN et al., 2012) -C=O,(CANO et al., 2014)(LI et al., 2015)(TAKALE et al., 2014b) -NO₂,(LIU et al., 2014c)(YU et al., 2015)(LIU et al., 2014a) epoxides,(URAYAMA et al., 2016)(NOUJIMA et al., 2011) imines,(TAKALE et al., 2014a) and quinoline.(REN et al., 2012)(TAO et al., 2015)

Some nitrogen and phosphorous-based ligands adsorbed on the gold surface are able to promote a favorable interface to activate H₂ heterolytically, which was understood as a frustrated Lewis pair (FLP) surface, improving gold's activity.(ALMORA-BARRIOS et al., 2017)(FIORIO; LÓPEZ; ROSSI, 2017) Our research group, while screening the use of amine ligands, found a correlation between the catalytic activity for the selective semihydrogenation of alkynes and the computed activation energies for heterolytic H₂ dissociation at the N ligand–Au(111) interface for structurally different amines. Piperazine–gold interface showed a unique catalytic activity, attributed to the favorable dissociation of H₂, and was successfully used for the hydrogenation of a variety of terminal and internal alkynes. A broad range of sensitive and reducible functional groups were tolerated, but the amine-gold system was incompatible

with aldehydes, ketones, and carboxylic acids, which are known to couple with amines. The group of van Leeuwen demonstrated hydrogenation of aldehydes when using secondary phosphine oxides adsorbed on Au NPs.(CANO et al., 2014)(CANO et al., 2015) The nanoparticles prepared using aryl secondary phosphine oxides as stabilizer were highly selective for aldehyde hydrogenation, a crucial ligand effect was noticed in the heterolytic hydrogenation mechanism. The need for a systematic study of the effect of other phosphorous-based ligands, with focus on those commercially available and air stable, in Au NPs for the application in the hydrogenation of other functional groups still remains.

Herein, we demonstrate the successful use of simple organophosphorus ligands to boost the catalytic activity of Au NPs for a range of important reduction reactions, namely, epoxides, N-oxides, sulfoxides, and alkynes. We reached excellent catalytic activity for a broad scope of substrates while keeping high selectivity; e.g., intact carbon-carbon double bonds. Furthermore, the choice of phosphorus-containing ligands resulted in a decrease in the amount necessary to reach high conversion and selectivity in comparison with our previous study with N-containing ligands. The ligand-to-metal ratio decreased from 100 (amine/Au) to 1 (phosphite/Au).

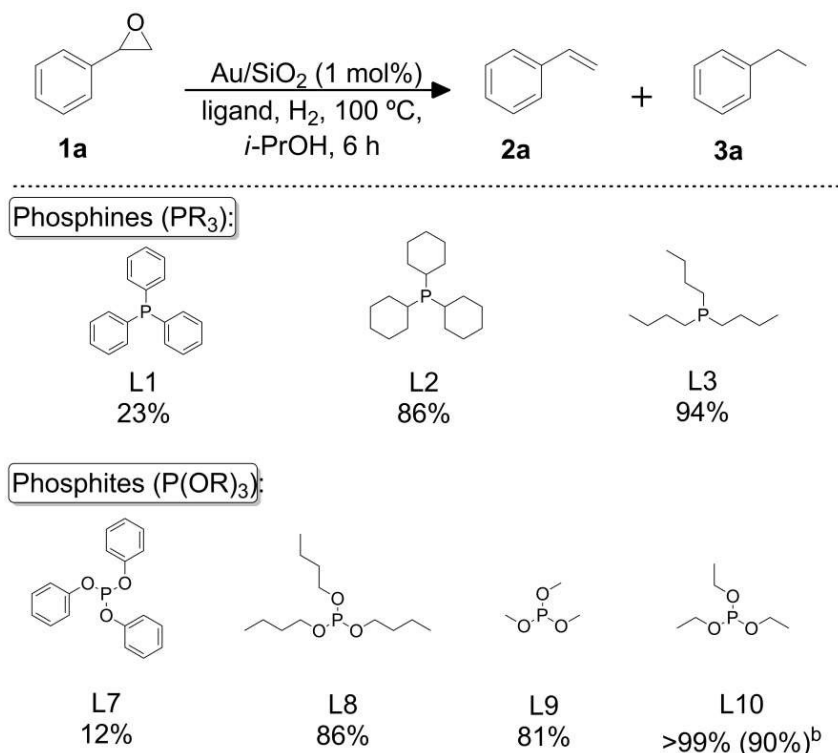
5.2. RESULTS AND DISCUSSION

The selective deoxygenation of styrene epoxide **1a** was chosen as benchmark reaction to investigate the effect of organophosphorus ligands on

the catalytic activity of gold nanoparticles supported on silica (Table 8). The Au/SiO₂ catalyst without ligand reached 23% of conversion after 6 hours of reaction (1 mmol of epoxide, 1 mol% of Au, 2 mL of *i*-PrOH, 100 °C, 6 bar of H₂). However, the catalytic activity of the Au/SiO₂ catalyst varied significantly depending on the identity of the organophosphorus ligand added to the reaction mixture. Alkyl-phosphine ligands such as PCy₃ L2 and P*n*Bu₃ L3 have significantly improved the catalytic activity of gold to catalyze the deoxygenation of **1a**. In contrast, the aryl-phosphine PPh₃ L1 did not affect the catalytic activity of gold. These results suggest that the strong adsorption energy of the aromatic ring to the metallic surface may have hindered the interaction of the P atom with the NP surface in a way necessary to form the FLP interface; alkyl groups usually do not interact with the surface allowing a more effective adsorption of the ligand on the surface through P atoms.(LOU; JIANG, 2018);(GONZÁLEZ-GÁLVEZ et al., 2012) Additionally, phosphites were also tested as ligand, since the oxygen atom insulates the phosphorus (and therefore the metal to which it is attached) from steric and electronic effects arising from substituent modification.(COONEY et al., 2003) While the triphenylphosphite (L7) was detrimental to reactivity, the alkyl phosphites (L8-L10) afforded an improved reactivity of the gold catalyst. The highest activity among the studied ligands was achieved using triethylphosphite (P(OEt)₃) (L10), a commercially available, cheap and quite stable to air-phosphite, which delivered the desired deoxygenate product in 90% isolated yield. In contrast, tertiary phosphine oxides or organophosphates ligands did not show the same activating effect of the parent ligands. Although the mechanistic aspects remain somewhat speculative at this time, we envisioned a catalytic cycle initiated by the H₂

activation occurring via a FLP's interface between gold NP surface and the adsorbed ligand. Parameters such as electronic and steric effects of the substituents attached to phosphorus atoms as well as the ligand basicity may play a key role in the FLP's interface formation. Another class of phosphorous ligands, namely secondary phosphine oxides (SPO), $R_2P(O)H$, have already been reported to be able to increase the activity of gold NPs via a FLP mechanism.(ALMORA-BARRIOS et al., 2017) According to DFT studies, H_2 molecule dissociates heterolytically at the AuNP-SPO interface, entailing the formation of a hydride on the metal surface ($Au-H^-$) and a proton which bonds to the carbonyl oxygen of SPO (R_2PO-H^+). In the case of ligands used in the present study, PR_3 and $P(OR)_3$, the formation of $P-H^+$ bonds are necessary to support a FLP mechanism, which also occurs in main-group phosphine-borane FLPs. Nonetheless, the potential for catalysis resides in the proton and hydride transfer from the phosphonium borate (main-group FLP) or phosphonium-hydride pair (at the gold surface) to a substrate, sustaining the catalytic cycle.

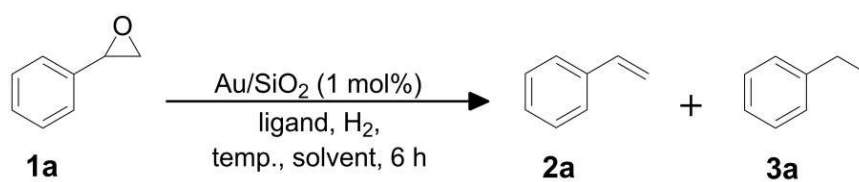
Table 8. Influence of organophosphorus ligands on the conversion of styrene epoxide 1a into styrene 2a catalyzed by Au/SiO₂.^a



^aReaction conditions: 1 mmol of epoxide, 1 mol% of Au, 2 mol% of ligand, 2 mL of *i*-PrOH, 100 °C, 6 bar of H₂, 6 h. Conversion values are shown, selectivity was >99% as determined by GC analysis using biphenyl as an internal standard. ^b Isolated yield.

A systematic survey of parameters such as the effect of the amount of added ligand, solvent, temperature and H₂ pressure led to the optimized reaction conditions (Table 9). Lowering the amount of added phosphite from 2 to 1 mol% molar equivalent did not decrease de catalytic activity (>99% conversion) and selectivity to the corresponding alkene, but a decrease in the reaction conversion to 75% was noticed after further reducing the amount of ligand to 0.5 mol% (Table 9). A series of blank experiments indicate that the ligand is not acting as a reductant as previously reported for rhenium, (NAKAGIRI; MURAI; TAKAI, 2015) and molybdenum catalyst. (ASAKO et al.,

2016) Even when performing the reaction using a stoichiometric amount of L10 (1 mmol of L10 and 1 mmol of epoxide), no conversion was detected after 24 h of reaction. A homogeneous gold catalyst, such as Au(PPh₃)Cl, was tested under similar conditions and was not able to catalyze the hydrogenation either. In summary, the reaction can be conducted with 1 mol% of L10, *i*-PrOH at 100 °C and 6 bar of H₂. In principle, the hydrogenation reaction can be conducted at lower temperature and H₂ pressure but lead to decreased reaction conversions.

Table 9. Screening of reaction conditions.^a

Entry	Amount of ligand (mol%)	Reaction temperature (°C)	H ₂ pressure (bar)	Solvent	Conversion of 1a (%)	Yield of 2a (%)
1	2				>99	>99
2	1	100			>99	>99
3	0.5		6		75	>99
4		80		<i>i</i> -PrOH	86	>99
5		60			43	>99
6			4		88	>99
7			2		40	>99
8				EtOH	>99	93
9				Toluene	96	>99
10	1			DMF	65	>99
11		100		THF	42	>99
12			6	Hexane	32	>99
13				1,4-dioxane	61	>99
15				MeCN	38	>99

^aReaction conditions: 1 mmol of epoxide, 1 mol% of Au, ligand, 2 mL of *i*-PrOH, temperature, 6 bar of H₂, 6 h. Determined by GC using internal standard technique.

Furthermore, timepoint studies illustrate that the catalyst system with triethylphosphite L10 (Figure 20a) affords superior reaction rates when compared to the reaction without ligand (Figure 1a). Moreover, the Au/SiO₂ solid catalyst was easily separated from the reaction mixture, washed and reused after adding new portions of substrate and L10. By running kinetic curves, no loss of catalytic efficiency was noticed in five successive reactions (Figure 20a). To gain insight into the catalytic active species, a hot filtration test was performed (Figure 20b). No conversion took place after the Au/SiO₂ catalyst was filtered off, indicating that the catalysis was heterogeneous in nature, and the catalytic activity and selectivity is not related to homogeneous species formation. To corroborate with this, no gold content was detected by ICP-AES analysis of the reaction product. Comparing the morphology and size of as-prepared catalyst (Figure 20c) with the recycled catalyst (Figure 1d) by TEM images revealed only a slight increase of the mean diameter size from 2.3 ± 0.6 nm to 3.2 ± 1 nm after five recycles.

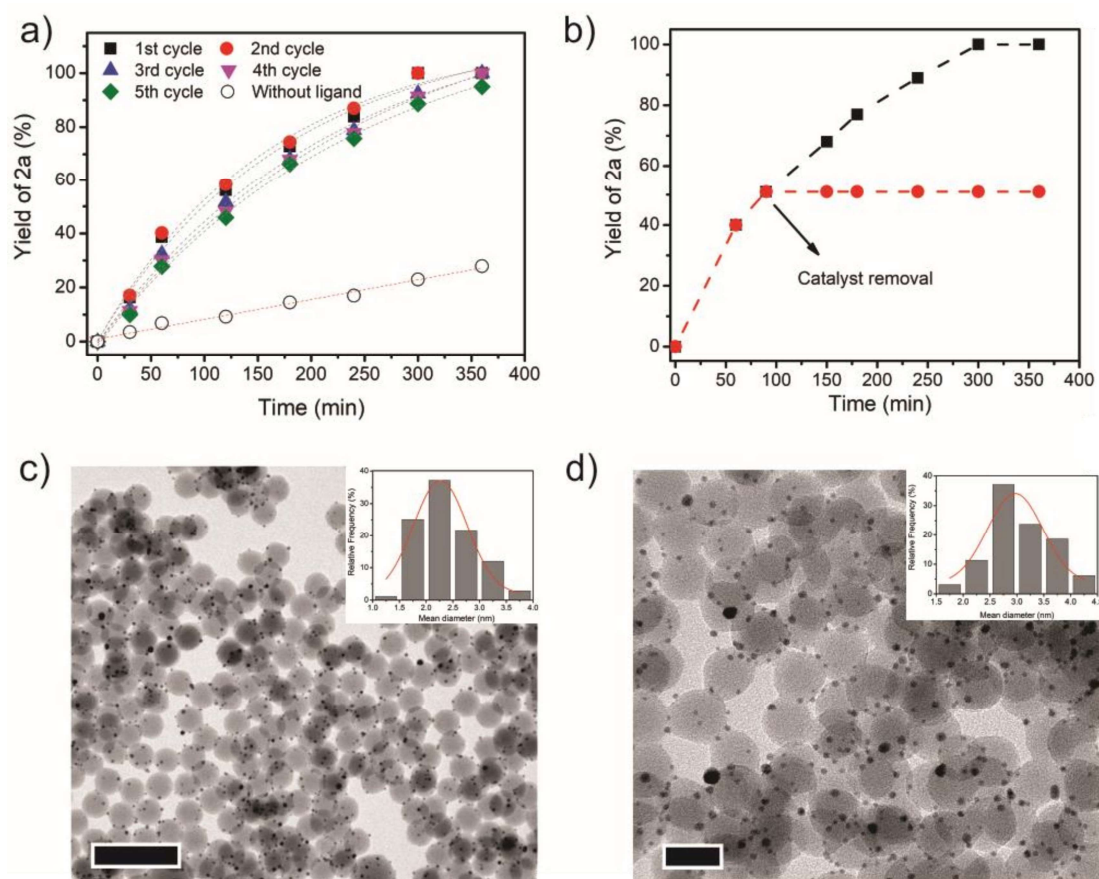
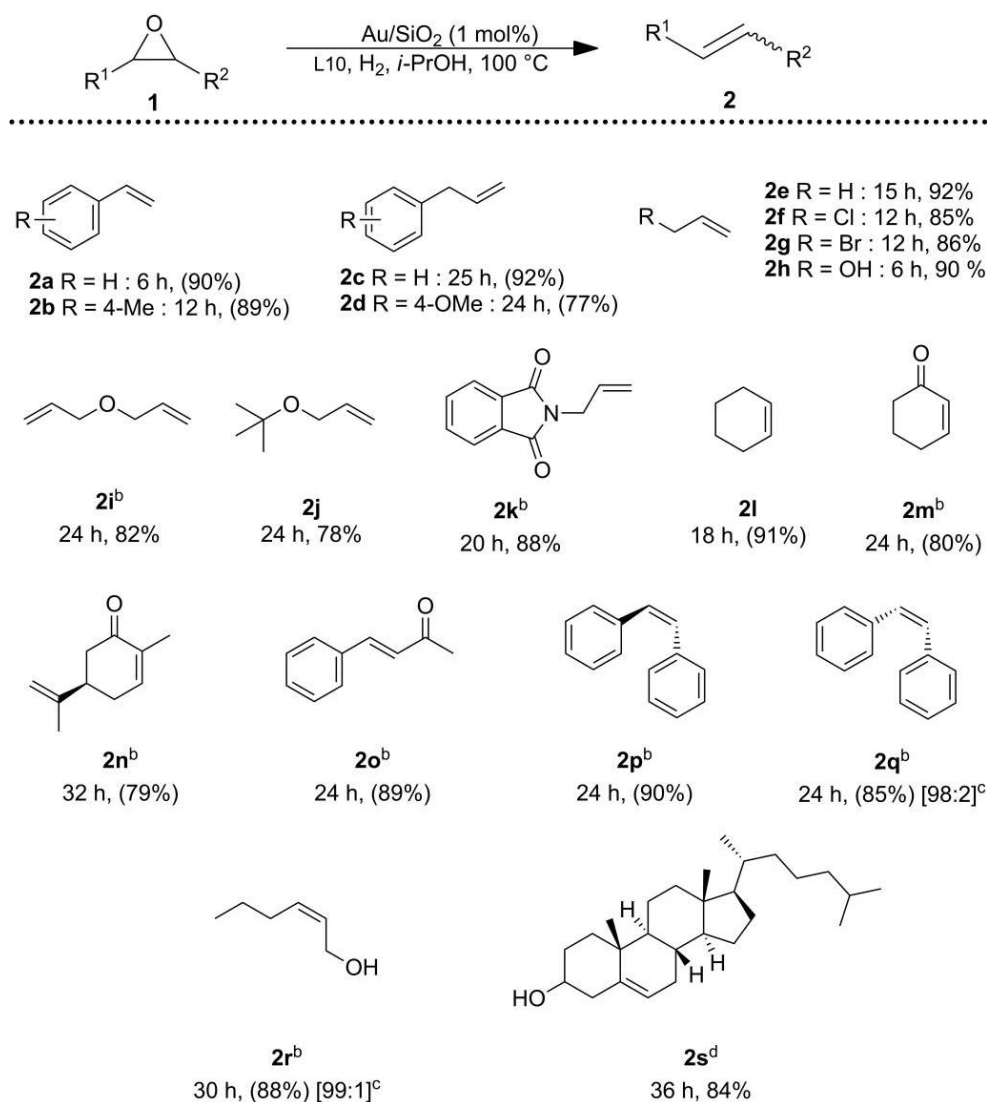


Figure 20. a) Timepoint study and recycles of Au/SiO₂ catalysts using with and without triethylphosphite L10 as ligand for the hydrogenation of styrene epoxide; b) Hot filtration test; c) TEM image and size distribution of fresh Au/SiO₂ catalyst (Scale bar, 100 nm) and d) after the fifth reuse (Scale bar, 25 nm). Reaction conditions: 1 mmol of epoxide, 1 mol% of Au, 1 mol% of L10, 2 mL of *i*-PrOH, 100 °C, 6 bar of H₂, 6 h.

The catalytic system (L10 + AuNPs) was able to catalyze the deoxygenation of a wide range of epoxides (Table 10), affording the corresponding alkenes in good to excellent yields, while hydrogenation of the alkene products did not occur. Styrene oxide substituted with methoxy group **2b** was completely converted into the desired alkene. Benzylic epoxides could also be deoxygenated with a yield over 75% of alkene (**2c** and **2d**). Aliphatic epoxides were converted into the corresponding alkenes in high yields (**2e-2j**). Importantly, halides, hydroxy, ketone and alkene moieties remained intact

during the deoxygenation of epoxides (**2f-h**, **2m**, **2n**, and **2i**). Deoxygenation of α,β -epoxy carbonyl compounds occurred smoothly to the unsaturated α,β -carbonyl compound **2o**. The deoxygenation proceeded in a stereospecific fashion: trans-stilbene oxide to trans-stilbene (**2p**) and cis-epoxides to cis-alkenes (**2q** and **2r**). Moreover, 25-hydroxy-4,5-epoxy-cholestan-3-one, undergo the reaction in good yield, furnishing to 25-hydroxycholestenone (**2s**), the biologically active compound responsible for the regulation of calcium and phosphate ion concentration in cells.

Table 10. Chemoselective reduction of epoxides to alkenes catalyzed by Au/SiO₂ and triethylphosphite L10.^a



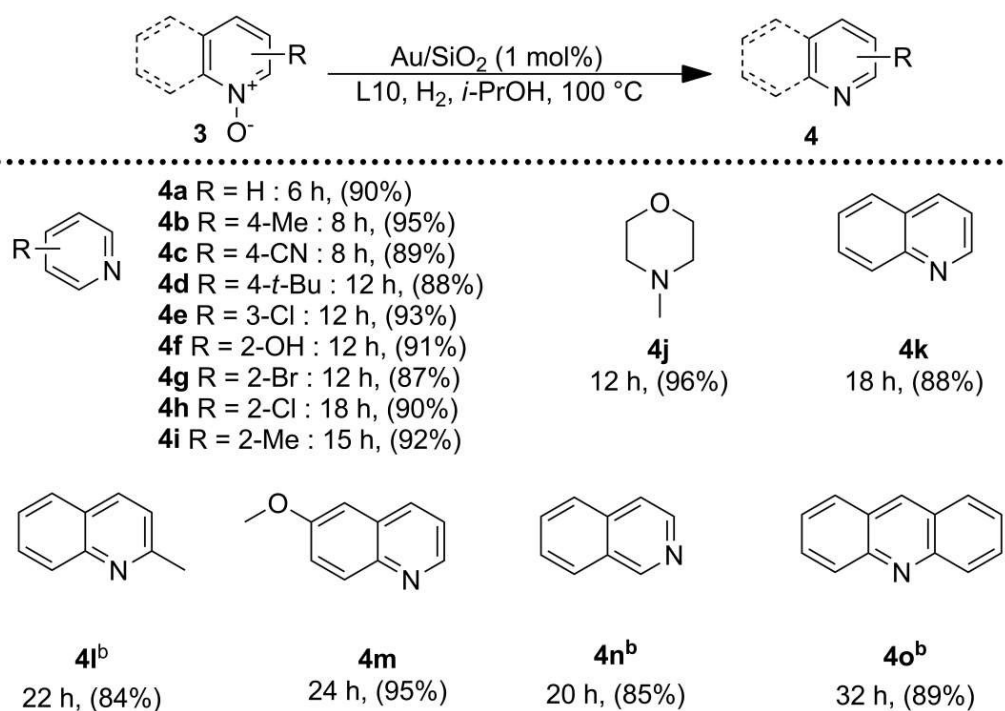
^aReaction conditions: 1 mmol of epoxide, 1 mol% of Au, 1 mol% of L10, 2 mL of *i*-PrOH, 100 °C, 6 bar of H₂. Conversion and selectivity were determined by GC (selectivity was >99%). Isolated yields in parenthesis.^b 8 bar.^c Determined by ¹H NMR ^d 2 mol% of Au, 10 bar of H₂.

Encouraged by these results, we became interested in the deoxygenation of a series of heterocyclic *N*-oxides to *N*-heteroarenes, an important class of heterocycles key structures in a wide range of

pharmacologically and biologically relevant natural products. (HAN et al., 2017)

Deoxygenation of a representative selection of heterocyclic *N*-oxides using H₂ as reductant revealed to be compatible with the catalytic system affording the corresponding reduced products in good to excellent yields. Notably, substrates possessing reducible functionalities such as halides, cyano, and hydroxyl were also chemoselectively reduced to the corresponding *N*-heterocycles (Table 11).

Table 11. Selective deoxygenation of pyridine *N*-oxides catalyzed by Au/SiO₂ and triethylphosphite L10.^a

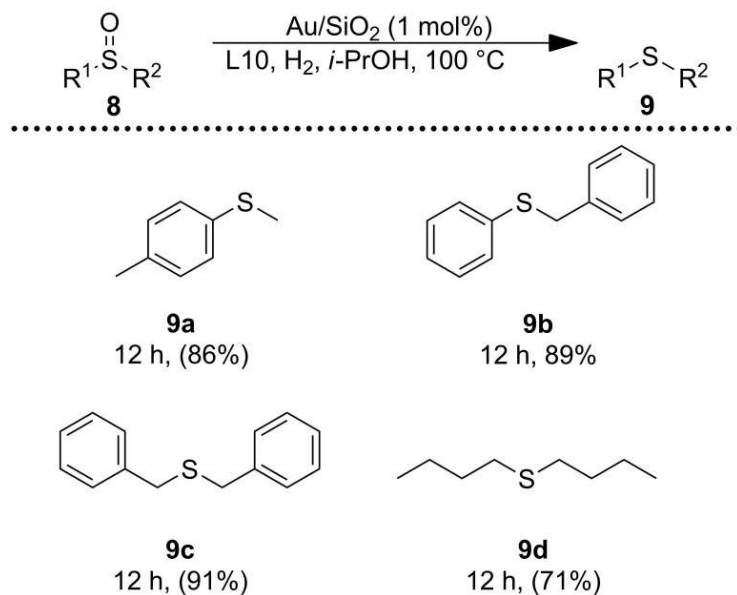


^aReaction conditions: 1 mmol of epoxide, 1 mol% of Au, 1 mol% of L10, 2 mL of *i*-PrOH, 100 °C, 6 bar of H₂. Conversion and selectivity were determined by GC (selectivity was >99%). Isolated yields in parenthesis.^b 8 bar.

Furthermore, to investigate the scope of the deoxygenation ability of the present catalytic system, we next applied this system to deoxygenation of

sulfoxides (Table 12). Phenyl, benzylic, and aliphatic sulfoxides were converted into the corresponding sulfides in yields over 70%.

Table 12. Hydrogenation of sulfoxides.^a

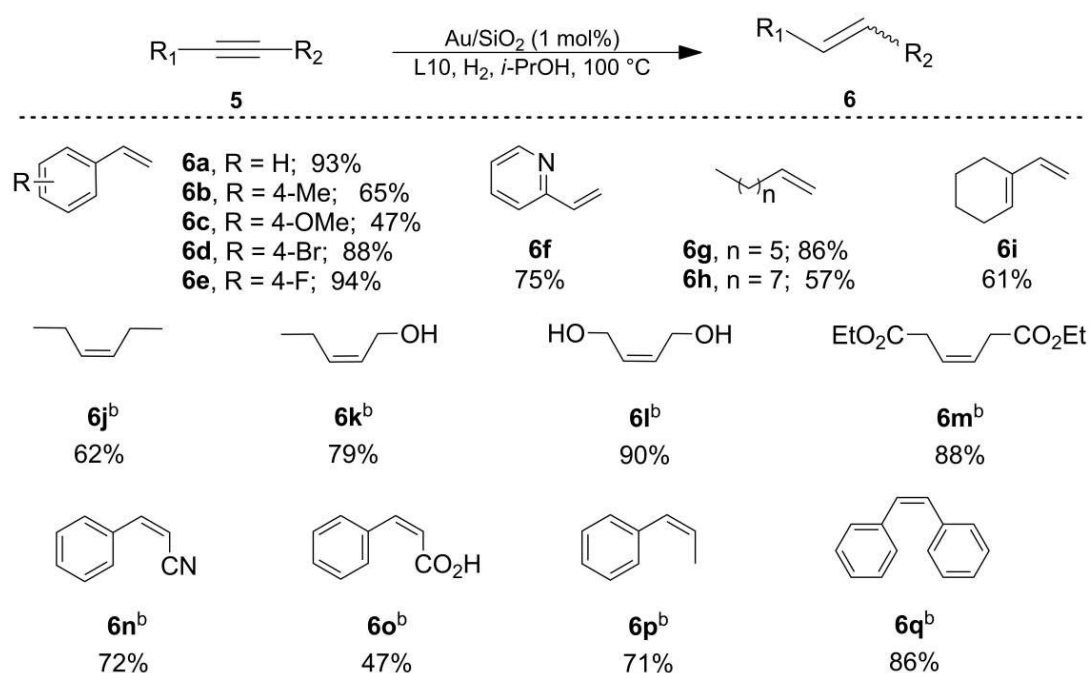


^aReaction conditions: 1 mmol of sulfoxide, 0.01 mmol of Au, 1 mol% of L10, 2 mL of *i*-PrOH, 100 °C, 10 bar of H₂.

Apart from deoxygenation of epoxides, N-oxides, and sulfoxides, the new Au-phosphite catalysts system was investigated in the selective hydrogenation of alkynes to the corresponding alkenes (Table 13). It is worth to note that only 1 equivalent of the phosphorus-containing ligand, triethylphosphite L10, was used here (phosphite/Au=1), while 100 equivalents of ligand were necessary to reach full conversion and selectivity with the best N-containing ligand used previously, piperazine (same Au catalyst and reaction conditions),(FIORIO; LÓPEZ; ROSSI, 2017) leading to a more economical and sustainable process. The general applicability and limitations of the

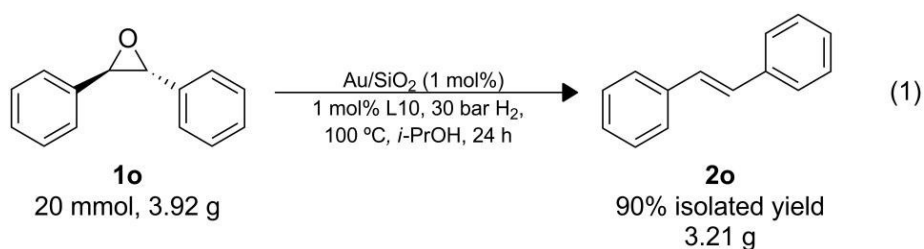
methodology were evaluated through the hydrogenation of alkynes using 100:1:1 alkyne: Au:L10. A variety of terminal aryl alkynes (Table 13, entries 6a-6f) and terminal aliphatic alkynes (entries 6g, h) were readily hydrogenated to the desired alkene. Internal alkynes also gave moderate to high yields of cis-alkenes (entries 6j-6q). It is noteworthy that the present catalytic system was adaptable to the semihydrogenation of alkyne moieties in substrates bearing hydroxy, cyano, carboxylic acid, ester, and halogen groups, without any detectable concurrent reduction of the alkene moieties.

Table 13. Catalytic hydrogenation of alkynes.^a



^aReaction conditions: 1 mmol of epoxide, 1 mol% of Au, 1 mol% of L10, 2 mL of *i*-PrOH, 100 °C, 6 bar of H₂. GC yields are shown, conversion and selectivity were determined by GC (selectivity was >99%) using internal standard technique.^b 10 bar of H₂.

The utility of this protocol was also demonstrated under scaled-up conditions (eq. 1); **1n** (20 mmol; 3.92 g) was successfully converted to the alkene, **2n** (90% isolated yield; 3.21 g). A turnover number (TON) of 1800 was reached with a productivity of approximately 75 mol.mol⁻¹.h⁻¹, and the catalyst can be recycled as demonstrated above.



Considering our previous studies on the activation of gold with N-containing ligands, (FIORIO; LÓPEZ; ROSSI, 2017) and the studies by van Leeuwen(CANO et al., 2014)(CANO et al., 2015)(ALMORA-BARRIOS et al., 2017) on the activation of gold with secondary phosphine oxides, the most likely hypothesis to explain the enhancement of the hydrogenation activity of Au NPs in the presence of alkyl-phosphine and phosphite ligands might involve a cooperative effect of the Au NPs and ligand interface leading to the heterolytic cleavage of H₂, which could be understood as a surface frustrated Lewis pair (FLP).(LU et al., 2014a)(GHUMAN et al., 2016b)(GHUMAN et al., 2015)(DONG et al., 2018)(STEPHAN, 2016)(FIORIO et al., 2018)(WANG et al., 2018a) The heterolytic dissociation of H₂ produces a hydride (delivered to a metal) and the proton is incorporated into the ligand (e.g., amine protonation, RR'N⁺-H).(LIU et al., 2016a)(FIORIO; LÓPEZ; ROSSI, 2017)(LU et al., 2014a)(LI et al., 2015) When associating secondary phosphine oxide ligands

with Au NPs, the RR'P-OH intermediate was suggested during the activation of H₂. In main-group FLP systems, the activation of H₂ when reacting with sterically demanding phosphines and boranes leads to phosphonium borates.(WELCH et al., 2006)(WELCH; STEPHAN, 2007)(GREB et al., 2012)(WANG et al., 2018a)(WANG et al., 2017) Mechanistic investigation demonstrated that the activation of H₂ occurs via interaction of the Lewis acidic B center followed by intramolecular proton migration to P.(WELCH; STEPHAN, 2007) According to the aforementioned literature data and the experimental results obtained, we propose a concerted effect between P(OEt)₃ molecules and the surface of the Au NPs, improving the rate-determining step of H₂ activation via a heterolytic pathway. In this regard, the formation of Au...P interactions(BARANOV et al., 2015)(ORTUÑO; LÓPEZ, 2018) and further protonation of the P atom is suggested, followed by proton transfer to the organic moiety. To further support our hypothesis, we conducted a Hammett study with *para*-substituted alkynes to get insights into the mechanism and to analyze the electronic influence of the substituents in the reaction rates. A linear plot of $[\log(k_X/k_H)]$ vs neutral ρ value was obtained (Figure 21) with a good correlation ($R^2 = 0.967$). The positive reaction constant ($\rho = +1.05$) indicates that negative charge is built up during the catalytic cycle in the transition state during the rate-determining step, which is better stabilized by the electron-withdrawing groups. The magnitude of +1.05 indicated a moderately anionic nature of the transition state, which might be due to a heterolytic H₂ dissociation mechanism since the rate-limiting step of catalytic hydrogenation reactions using gold is the activation of molecular hydrogen.(HAMMER; NORSKOV, 1995)(BUS; MILLER; VAN BOKHOVEN, 2005)(BARRIO et al., 2006)

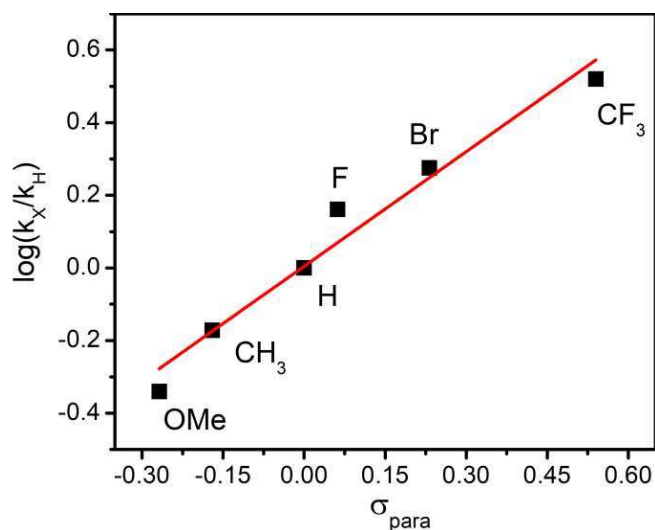


Figure 21. Hammett plot for hydrogenation of substituted alkynes catalyzed by Au/SiO₂ and L10.

Although the mechanistic aspects of our gold catalyzed hydrogenation reactions remain somewhat speculative at this time, we have greatly improved the practical applicability of gold catalysts possibly via a heterolytic H₂ cleavage-driven reaction at mild conditions.

5.3. CONCLUSIONS

In summary, a general approach to selective deoxygenation of epoxides, *N*-oxides, and sulfoxides was developed by the cooperative effect of Au NPs and P-containing ligands, through a novel surface frustrated Lewis pair interface. Notably, the deoxygenation reactions furnished the desired products in high yields for a broad scope of substrates, with excellent functional-group tolerance providing access to an array of diversely functionalized alkenes, sulfides and *N*-heteroarenes compounds, which are valuable building blocks in

organic synthesis. Experimental results give us insights that Au NPs react with alkyl-phosphine/phosphite to form a reactive FLP, which provoke the heterolytic cleavage of H₂ at mild conditions. We believe that the current work will be of broad synthetic and mechanistic interest for chemists, disclosing a promising and efficient way to improve the catalytic activity of Au NPs in hydrogenation reaction while showing new applications for the well-known phosphine chemistry in homogeneous catalysis. Further efforts on the application of this novel frustrated Lewis pair are currently underway.

5.4. EXPERIMENTAL SECTION

5.4.1. Materials and Methods

All the reagents used for the support and catalyst preparation were of analytical grade, purchased from Sigma-Aldrich and used as received. Tetrachloroauric(III) acid was purchased as a 30 wt% aqueous solution in dilute HCl (Sigma-Aldrich). Commercial reagents were purchased from Sigma Aldrich, and used as received with the following exceptions. The glass reactor was thoroughly cleaned with aqua regia (HCl:HNO₃ = 3:1 v/v), rinsed with copious pure water, and then dried in an oven prior to use.

The gold content in the catalyst was measured by FAAS analysis, on a Shimadzu AA-6300 spectrophotometer using an Au hollow cathode lamp (Photron). Metal leaching into the supernatant solution was measured by inductively coupled plasma measurements, performed on a Spectro Arcos ICP-OES. TEM analyses were performed with a JEOL 2100. Catalyst samples for

TEM were prepared by sonicating the catalyst powder in propan-2-ol. A drop of the resulting dispersion was placed on a carbon-coated copper grid (Ted Pella, Inc.). The histogram of nanoparticle size distribution was obtained from the measurement of about 200 particles.

5.4.2. Catalyst preparation

Preparation of Au/SiO₂

Gold nanoparticles were prepared by the deposition-reduction method reported elsewhere. (LIU et al., 2009); (FIORIO; LÓPEZ; ROSSI, 2017) Briefly, in a typical method 1.0 g of the amino-modified silica was added to aqueous solution of HAuCl₄ (20 mL, 1.3×10^{-2} mol L⁻¹) under continuous stirring. After 30 min, the mixture was centrifugated and the recovered solid was dispersed in 10 mL of water. Subsequently, under vigorous stirring an as-prepared cold aqueous NaBH₄ solution (10 mL, 0.2 mol L⁻¹) was added dropwise. After further stirring for 20 min, the solid was recovered by filtration and thoroughly washed twice with hot water (60 °C), acetone and dried in vacuum. The Au/SiO₂ contains 3.5 wt% of gold as determined by FAAS and the mean diameter was 2.3 ± 0.6 nm (See Chapter 1 for full characterization). (FIORIO; LÓPEZ; ROSSI, 2017)

5.4.3. Catalytic investigations

Catalytic deoxygenation reactions

A typical procedure for the deoxygenation reactions is as follows: substrate (1 mmol), ligand (0.02 mmol), Au/SiO₂ (1 mol%) and 2 mL of solvent were added to a modified Fischer–Porter 100 mL glass reactor in a glove box. The reactor was purged five times with H₂, leaving the vessel at 6 bar. The resulting mixture was vigorously stirred using Teflon-coated magnetic stir, temperature was maintained at the desired temperature with an oil bath on a hot stirring plate connected to a digital controller (ETS-D5 IKA). After the desired time, the catalyst was removed by centrifugation and the products were analyzed by GC with an internal standard to determine the conversion of substrate and the selectivity for the product.

Recycling experiment

A magnetic version of the catalyst was prepared for the recycling experiments, as previously described. (JACINTO et al., 2008) (FIORIO; LÓPEZ; ROSSI, 2017) After each catalytic experiment under the above typical reaction conditions, the catalyst was recovered by putting a magnet on the wall of the reactor. The used catalyst was washed two times with isopropyl alcohol, dried in vacuo and subsequently exposed to the reaction conditions again. The product obtained after magnetic separation was analyzed by GC with an internal standard to determine the conversion and selectivity.

Scale-up hydrogenation of trans-stilbene oxide

20 mmol of trans-stilbene oxide, Au/SiO₂ (0.01 mmol Au), triethylphosphite **L20** (1 eq.), and 10 mL of isopropyl alcohol were added to a reactor (Parr Instrument Company, 40 mL capacity, series 5000). After sealing

the reactor and degassed internal air, H₂ was introduced until 3 MPa. Then, the mixture was extensively stirred (1000 rpm.) at 100 °C for 24 h. The product was obtained after removal of solvent.

Product Analysis of Catalytic Experiments

GC analyses were carried out with a Shimadzu GC-2010 equipped with a RTX-5 column (30 m x 0.25 mm x 0.25 mm) and a FID detector. Method: T_i = 40 °C, T_f = 200 °C, 17 min. Internal standard: biphenyl. The conversion and selectivity were determined from the total amount of detected products and reactant.(SCANLON; WILLIS, 1985)

5.5. REFERENCES

ALMORA-BARRIOS, N. et al. Concerted Chemoselective Hydrogenation of Acrolein on Secondary Phosphine Oxide Decorated Gold Nanoparticles. **ACS Catalysis**, v. 7, n. 6, p. 3949–3954, 2 jun. 2017.

ASAKO, S. et al. Molybdenum-Catalyzed Stereospecific Deoxygenation of Epoxides to Alkenes. **Advanced Synthesis & Catalysis**, v. 358, n. 24, p. 3966–3970, 22 dez. 2016.

BARANOV, A. I. et al. **Chemical Modelling**. Cambridge: Royal Society of Chemistry, 2015. v. 12

BARRIO, L. et al. A density functional theory study of the dissociation of H₂ on gold clusters: Importance of fluxionality and ensemble effects. **The Journal of Chemical Physics**, v. 125, n. 16, p. 164715, 28 out. 2006.

BUS, E.; MILLER, J. T.; VAN BOKHOVEN, J. A. Hydrogen Chemisorption on Al₂O₃-Supported Gold Catalysts. **The Journal of Physical Chemistry B**, v.

109, n. 30, p. 14581–14587, ago. 2005.

CANO, I. et al. Air-Stable Gold Nanoparticles Ligated by Secondary Phosphine Oxides for the Chemoselective Hydrogenation of Aldehydes: Crucial Role of the Ligand. **Journal of the American Chemical Society**, v. 136, n. 6, p. 2520–2528, 12 fev. 2014.

CANO, I. et al. Air-Stable Gold Nanoparticles Ligated by Secondary Phosphine Oxides as Catalyst for the Chemoselective Hydrogenation of Substituted Aldehydes: a Remarkable Ligand Effect. **Journal of the American Chemical Society**, v. 137, n. 24, p. 7718–7727, 24 jun. 2015.

CHEN, G. et al. Interfacial electronic effects control the reaction selectivity of platinum catalysts. **Nature Materials**, v. 15, n. 5, p. 564–569, 25 jan. 2016.

COONEY, K. D. et al. A Priori Assessment of the Stereoelectronic Profile of Phosphines and Phosphites. **Journal of the American Chemical Society**, v. 125, n. 14, p. 4318–4324, abr. 2003.

DONG, Y. et al. Tailoring Surface Frustrated Lewis Pairs of $\text{In}_2\text{O}_3-x(\text{OH})_y$ for Gas-Phase Heterogeneous Photocatalytic Reduction of CO_2 by Isomorphous Substitution of In^{3+} with Bi^{3+} . **Advanced Science**, v. 1700732, p. 1700732, 12 mar. 2018.

ERNST, J. B. et al. Tunable Heterogeneous Catalysis: N-Heterocyclic Carbenes as Ligands for Supported Heterogeneous Ru/K- Al_2O_3 Catalysts To Tune Reactivity and Selectivity. **Journal of the American Chemical Society**, v. 138, n. 34, p. 10718–10721, 31 ago. 2016.

ERNST, J. B. et al. Molecular Adsorbates Switch on Heterogeneous Catalysis: Induction of Reactivity by N-Heterocyclic Carbenes. **Journal of the American Chemical Society**, v. 139, n. 27, p. 9144–9147, 12 jul. 2017.

FEDOROV, A. et al. Silica-Supported Cu Nanoparticle Catalysts for Alkyne Semihydrogenation: Effect of Ligands on Rates and Selectivity. **Journal of the American Chemical Society**, v. 138, n. 50, p. 16502–16507, 21 dez. 2016.

FIORIO, J. L. et al. Accessing Frustrated Lewis Pair Chemistry through Robust Gold@N-Doped Carbon for Selective Hydrogenation of Alkynes. **ACS Catalysis**, v. 8, n. 4, p. 3516–3524, 6 abr. 2018.

FIORIO, J. L.; LÓPEZ, N.; ROSSI, L. M. Gold–Ligand-Catalyzed Selective Hydrogenation of Alkynes into cis -Alkenes via H₂ Heterolytic Activation by Frustrated Lewis Pairs. **ACS Catalysis**, v. 7, n. 4, p. 2973–2980, 7 abr. 2017.

GHUMAN, K. K. et al. Illuminating CO₂ reduction on frustrated Lewis pair surfaces: investigating the role of surface hydroxides and oxygen vacancies on nanocrystalline In₂O_{3-x}(OH)_y. **Physical Chemistry Chemical Physics**, v. 17, n. 22, p. 14623–14635, 2015.

GHUMAN, K. K. et al. Photoexcited Surface Frustrated Lewis Pairs for Heterogeneous Photocatalytic CO₂ Reduction. **Journal of the American Chemical Society**, v. 138, n. 4, p. 1206–1214, 3 fev. 2016.

GONZÁLEZ-GÁLVEZ, D. et al. Phosphine-Stabilized Ruthenium Nanoparticles: The Effect of the Nature of the Ligand in Catalysis. **ACS Catalysis**, v. 2, n. 3, p. 317–321, 2 mar. 2012.

GREB, L. et al. Metal-free Catalytic Olefin Hydrogenation: Low-Temperature H₂ Activation by Frustrated Lewis Pairs. **Angewandte Chemie International Edition**, v. 51, n. 40, p. 10164–10168, 1 out. 2012.

HAMMER, B.; NORSKOV, J. K. Why gold is the noblest of all the metals. **Nature**, v. 376, n. 6537, p. 238–240, jul. 1995.

HAN, Y.-P. et al. Lewis Acid Catalyzed Dehydrogenative Coupling of Tertiary Propargylic Alcohols with Quinoline N -Oxides. **The Journal of Organic Chemistry**, v. 82, n. 3, p. 1697–1704, 3 fev. 2017.

JACINTO, M. J. et al. Recoverable rhodium nanoparticles: Synthesis, characterization and catalytic performance in hydrogenation reactions. **Applied Catalysis A: General**, v. 338, n. 1–2, p. 52–57, 2008.

LARI, G. M. et al. Hybrid Palladium Nanoparticles for Direct Hydrogen Peroxide Synthesis: The Key Role of the Ligand. **Angewandte Chemie International Edition**, v. 56, n. 7, p. 1775–1779, 6 fev. 2017.

LI, G. et al. Experimental and Mechanistic Understanding of Aldehyde Hydrogenation Using Au 25 Nanoclusters with Lewis Acids: Unique Sites for Catalytic Reactions. **Journal of the American Chemical Society**, v. 137, n. 45, p. 14295–14304, 18 nov. 2015.

LI, G.; JIN, R. Gold Nanocluster-Catalyzed Semihydrogenation: A Unique Activation Pathway for Terminal Alkynes. **Journal of the American Chemical Society**, v. 136, n. 32, p. 11347–11354, 13 ago. 2014.

LI, S.-S. et al. Heterogeneous Gold-Catalyzed Selective Semireduction of Alkynes using Formic Acid as Hydrogen Source. **Advanced Synthesis & Catalysis**, v. 358, n. 9, p. 1410–1416, 28 abr. 2016.

LIANG, S.; HAMMOND, G. B.; XU, B. Supported gold nanoparticles catalyzed cis-selective semihydrogenation of alkynes using ammonium formate as the reductant. **Chem. Commun.**, v. 52, n. 35, p. 6013–6016, 2016.

LIU, C. et al. One-Pot Synthesis of Au 11 (PPh 2 Py) 7 Br 3 for the Highly Chemoselective Hydrogenation of Nitrobenzaldehyde. **ACS Catalysis**, v. 6, n. 1, p. 92–99, 4 jan. 2016.

LIU, S.-S. et al. Gold supported on titania for specific monohydrogenation of dinitroaromatics in the liquid phase. **Green Chemistry**, v. 16, n. 9, p. 4162, 2014a.

LIU, X. et al. Synthesis of thermally stable and highly active bimetallic Au-Ag nanoparticles on inert supports. **Chemistry of Materials**, v. 21, n. 2, p. 410–418, 2009.

LIU, X. et al. Gold-Catalyzed Direct Hydrogenative Coupling of Nitroarenes To Synthesize Aromatic Azo Compounds. **Angewandte Chemie International Edition**, v. 53, n. 29, p. 7624–7628, 14 jul. 2014b.

LIU, Z.-P.; HU, P. Mechanism of H₂ metabolism on Fe-only hydrogenases. **The Journal of Chemical Physics**, v. 117, n. 18, p. 8177–8180, 8 nov. 2002.

LOU, S.; JIANG, H. Theoretical study of adsorption of organic phosphines on transition metal surfaces. **Molecular Physics**, v. 116, n. 7–8, p. 944–955, 18 abr. 2018.

LU, G. et al. Gold catalyzed hydrogenations of small imines and nitriles: enhanced reactivity of Au surface toward H₂ via collaboration with a Lewis base. **Chem. Sci.**, v. 5, n. 3, p. 1082–1090, 2014.

MAKOSCH, M. et al. Organic Thiol Modified Pt/TiO₂ Catalysts to Control Chemoselective Hydrogenation of Substituted Nitroarenes. **ACS Catalysis**, v. 2, n. 10, p. 2079–2081, 5 out. 2012.

MARSHALL, S. T. et al. Controlled selectivity for palladium catalysts using self-assembled monolayers. **Nature Materials**, v. 9, n. 10, p. 853–858, 12 out. 2010.

MITSDOME, T. et al. One-step Synthesis of Core-Gold/Shell-Ceria Nanomaterial and Its Catalysis for Highly Selective Semihydrogenation of Alkynes. **Journal of the American Chemical Society**, v. 137, n. 42, p. 13452–13455, 28 out. 2015.

NAKAGIRI, T.; MURAI, M.; TAKAI, K. Stereospecific Deoxygenation of Aliphatic Epoxides to Alkenes under Rhenium Catalysis. **Organic Letters**, v. 17, n. 13, p. 3346–3349, 2 jul. 2015.

NOUJIMA, A. et al. Selective Deoxygenation of Epoxides to Alkenes with Molecular Hydrogen Using a Hydrotalcite-Supported Gold Catalyst: A Concerted Effect between Gold Nanoparticles and Basic Sites on a Support. **Angewandte Chemie International Edition**, v. 50, n. 13, p. 2986–2989, 21 mar. 2011.

NOYORI, R. Asymmetric Catalysis: Science and Opportunities (Nobel Lecture)
Copyright© The Nobel Foundation 2002. We thank the Nobel Foundation,

Stockholm, for permission to print this lecture. **Angewandte Chemie International Edition**, v. 41, n. 12, p. 2008, 17 jun. 2002.

ORTUÑO, M. A.; LÓPEZ, N. Creating Cavities at Palladium–Phosphine Interfaces for Enhanced Selectivity in Heterogeneous Biomass Conversion. **ACS Catalysis**, v. 9, n. 21, p. 6138–6145, 8 jun. 2018.

REN, D. et al. An Unusual Chemoselective Hydrogenation of Quinoline Compounds Using Supported Gold Catalysts. **Journal of the American Chemical Society**, v. 134, n. 42, p. 17592–17598, 24 out. 2012.

SCANLON, J. T.; WILLIS, D. E. Calculation of flame ionization detector relative response factors using the effective carbon number concept. **Journal of Chromatographic Science**, v. 23, p. 333–340, 1985.

SCHOENBAUM, C. A.; SCHWARTZ, D. K.; MEDLIN, J. W. Controlling the Surface Environment of Heterogeneous Catalysts Using Self-Assembled Monolayers. **Accounts of Chemical Research**, v. 47, n. 4, p. 1438–1445, 15 abr. 2014.

SEGURA, Y.; LÓPEZ, N.; PÉREZ-RAMÍREZ, J. Origin of the superior hydrogenation selectivity of gold nanoparticles in alkyne + alkene mixtures: Triple- versus double-bond activation. **Journal of Catalysis**, v. 247, n. 2, p. 383–386, 2007.

STEPHAN, D. W. The broadening reach of frustrated Lewis pair chemistry. **Science**, v. 354, n. 6317, p. aaf7229–aaf7229, 9 dez. 2016.

STRATAKIS, M.; GARCIA, H. Catalysis by Supported Gold Nanoparticles: Beyond Aerobic Oxidative Processes. **Chemical Reviews**, v. 112, n. 8, p. 4469–4506, 8 ago. 2012.

TAKALE, B. S. et al. Exclusive Chemoselective Reduction of Imines in the Coexistence of Aldehydes Using AuNPore Catalyst. **Organic Letters**, v. 16, n. 9, p. 2558–2561, 2 maio 2014a.

TAKALE, B. S. et al. Chemoselective reduction of α,β -unsaturated aldehydes using an unsupported nanoporous gold catalyst. **Chem. Commun.**, v. 50, n. 92, p. 14401–14404, 29 set. 2014b.

TAO, L. et al. Heterogeneous Gold-Catalyzed Selective Reductive Transformation of Quinolines with Formic Acid. **Advanced Synthesis & Catalysis**, v. 357, n. 4, p. 753–760, 9 mar. 2015.

TESCHNER, D. et al. The Roles of Subsurface Carbon and Hydrogen in Palladium-Catalyzed Alkyne Hydrogenation. **Science**, v. 320, n. 5872, p. 86–89, 4 abr. 2008.

URAYAMA, T. et al. Green, Multi-Gram One-Step Synthesis of Core-Shell Nanocomposites in Water and Their Catalytic Application to Chemoselective Hydrogenations. **Chemistry - A European Journal**, v. 22, n. 50, p. 17962–17966, 12 dez. 2016.

VASILIKOGIANNAKI, E. et al. cis-Semihydrogenation of alkynes with amine borane complexes catalyzed by gold nanoparticles under mild conditions. **Chemical Communications**, v. 51, n. 12, p. 2384–2387, 2015.

WANG, L. et al. Solid state frustrated Lewis pair chemistry. **Chemical Science**, v. 9, n. 21, p. 4859–4865, 2018.

WANG, M. et al. Frustrated Lewis Pair Polymers as Responsive Self-Healing Gels. **Journal of the American Chemical Society**, v. 139, n. 40, p. 14232–14236, 11 out. 2017.

WELCH, G. C. et al. Reversible, Metal-Free Hydrogen Activation. **Science**, v. 314, n. 5802, p. 1124–1126, 17 nov. 2006.

WELCH, G. C.; STEPHAN, D. W. Facile heterolytic cleavage of dihydrogen by phosphines and boranes. **Journal of the American Chemical Society**, v. 129, n. 7, p. 1880–1881, 2007.

XIAO, B. et al. Copper Nanocrystal Plane Effect on Stereoselectivity of Catalytic

Deoxygenation of Aromatic Epoxides. **Journal of the American Chemical Society**, v. 137, n. 11, p. 3791–3794, 25 mar. 2015.

YAN, M. et al. Nanoporous gold catalyst for highly selective semihydrogenation of alkynes: remarkable effect of amine additives. **Journal of the American Chemical Society**, v. 134, n. 42, p. 17536–17542, 2012.

YE, R. et al. Supported Au Nanoparticles with N -Heterocyclic Carbene Ligands as Active and Stable Heterogeneous Catalysts for Lactonization. **Journal of the American Chemical Society**, v. 140, n. 11, p. 4144–4149, 21 mar. 2018.

YU, L. et al. Gold-Catalyzed Reductive Transformation of Nitro Compounds Using Formic Acid: Mild, Efficient, and Versatile. **ChemSusChem**, v. 8, n. 18, p. 3029–3035, 2015.

ZHANG, Y. et al. Nano-gold catalysis in fine chemical synthesis. **Chemical Reviews**, v. 112, n. 4, p. 2467–2505, 2012.

6. CHAPTER 4

Accessing frustrated Lewis pair chemistry through robust Gold@N-doped carbon for selective hydrogenation of alkynes

"Accepted version of article reproduced with permission from [Fiorio, J. L.; Gonçalves, R. V.; Neto-Teixeira, E.; Ortuño, M. A.; López, N.; Rossi, L. M. Accessing Frustrated Lewis Pair Chemistry through Robust Gold@N- Doped Carbon for Selective Hydrogenation of Alkynes. **ACS Catalysis**, 2018, 8, 3516–3524] Copyright [2018] American Chemical Society." The written permission from the editor is given in Appendices A1. The published article can be accessed in the link: DOI: [10.1021/acscatal.8b00806](https://doi.org/10.1021/acscatal.8b00806) ([ACS Articles on Request](#)).

Abstract

Pyrolysis of Au(OAc)₃ in the presence of phenanthroline over TiO₂ furnishes a highly active and selective Au nanoparticle (NP) catalyst embedded in a nitrogen-doped carbon support, Au@N-doped carbon/TiO₂ catalyst. Parameters such as pyrolysis temperature, type of support and nitrogen ligands and Au:ligand molar ratios were systematically investigated. Highly selective hydrogenation of numerous structurally diverse alkynes proceeded in moderate to excellent yield under mild conditions. The high selectivity toward the industrially important alkene substrates, functional group tolerance and the high recyclability makes the catalytic system unique. Both high activity and selectivity

are correlated with a frustrated Lewis pairs interface formed by the combination of gold and nitrogen atoms of N-doped carbon that can serve as a basic site to promote the heterolytic activation of H₂ under very mild conditions. In comparison to previous gold hydrogenation catalysts, where N-containing ligands were added externally, the present “full heterogeneous” and recyclable catalyst makes the whole process environmentally and economically attractive.

6.1.MOTIVATION

Alkenes have an extensive range of applications from intermediates in the chemicals industry to their primary use as co-monomers in the production of polymers. High purity alkene feedstocks (alkyne free) for the polymer industry are obtained by a very fine-tuned catalytic hydrogenation process; the challenging selective hydrogenation of impurities (alkyne to alkene), while inhibiting the hydrogenation of the alkene to the alkane step and double-bond isomerization. (TROTUŞ; ZIMMERMANN; SCHÜTH, 2014) The semihydrogenation of alkynes to alkenes is also known as a valuable synthetic strategy for drug design.(SHELDON; BEKKUM, 2001) Typically, platinum group metal catalysts are very active for hydrogenations, but they usually suffer from the lack of selectivity to alkenes.(KYRIAKOU et al., 2012):(TESCHNER et al., 2008) Approaches to improve the chemoselectivity relied on addition of ligands,(ZHAO; FU; ZHENG, 2017):(CHEN; RODIONOV, 2016) usually nitrogen, phosphorus, sulfur or addition of a second less active metal.(LÓPEZ; VARGAS-FUENTES, 2012):(VILÉ et al., 2016b) In the context of hydrogenations, gold was less explored,(MITSUDOME; KANEDA,

2013);(STRATAKIS; GARCIA, 2012) but is expected to be intrinsically selective for hydrogenation of triple bonds in alkyne–alkene mixtures, because the preferential adsorption of only one of these components, the alkyne.(SEGURA; LÓPEZ; PÉREZ-RAMÍREZ, 2007) Nevertheless, gold-based catalyst still suffers from the lack of activity, mainly due to limited ability to dissociate molecular hydrogen (H_2), which usually is the rate-limiting step.(KYRIAKOU et al., 2012) Cooperation between the coordinatively unsaturated Au atoms on the Au NPs and the acid–base pair site on Al_2O_3 ,(SHIMIZU et al., 2009);(BUS; MILLER; VAN BOKHOVEN, 2005) basic sites on hydroxyapatite(NUJJIMA et al., 2011);(NUJJIMA et al., 2012) and on ceria(MITSUDOME et al., 2015);(URAYAMA et al., 2016) has been suggested as a strategy for the H_2 dissociation to yield a H^+/H^- pair at the metal–support interface, which is then transferred to the organic moiety. Such heterolytic H_2 splitting has been proposed to occur on pure oxides,(ALBANI et al., 2017; TEJEDA-SERRANO et al., 2017; ZHANG et al., 2017) on gold complexes,(CAMPOS, 2017; COMAS-VIVES et al., 2006; COMAS-VIVES; UJAQUE, 2013) or due to a cooperation between gold and adsorbed basic ligands.(ALMORA-BARRIOS et al., 2017; CANO et al., 2014, 2015; FIORIO; LÓPEZ; ROSSI, 2017; LI et al., 2015; LU et al., 2014a; REN et al., 2012) We have recently systematically studied the activation of gold via the heterolytic dissociation of H_2 based on the adsorption of nitrogen-containing bases on gold surfaces.(FIORIO; LÓPEZ; ROSSI, 2017) The activation of H_2 was proposed to occur at the metal-ligand interface forming a tight ion pair induced by a frustrated Lewis pair (FLP) like structure,(GHUMAN et al., 2015, 2016b; STEPHAN, 2015b, 2016; WELCH et al., 2006) which was able to promote the heterolytic activation of H_2 , allowing a high activity and

selectivity for the hydrogenation of alkynes into alkenes. In the proposed mechanism, identified by DFT, the H₂ molecule splits forming a quaternary N center (amine protonation) and a hydride on the gold surface; both H⁻ and H⁺ were then transferred to the organic moiety in a *syn*-fashion controlled by electrostatic interactions.

Nitrogen-doped carbon materials affect the catalytic activity and selectivity of transition metals significantly, such as cobalt,(WESTERHAUS et al., 2013)(LIU et al., 2016c) nickel,(PISIEWICZ et al., 2016) palladium,(BI et al., 2016)(CHEN et al., 2017b) ruthenium,(CUI et al., 2016) and iron/iron oxide based catalysts.(JAGADEESH et al., 2013)(LIU et al., 2017) The incorporation of nitrogen atoms in the carbon architecture combined with metal nanoparticles have enabled application in a wide range of catalytic reactions including reductions, oxidations and H₂ generation.(HE et al., 2016)(CAO et al., 2017) N-doped carbon structures have also emerged in a plethora of hydrogenation reactions.(WESTERHAUS et al., 2013)(JAGADEESH et al., 2013)(CHEN et al., 2016a)(CHEN et al., 2015) More interestingly, a heterolytic H₂ activation has been invoked to explain the hydrogenation reaction mechanism.(VILÉ et al., 2015)(FORMENTI et al., 2017)(CHEN et al., 2016d) Although it is not explicit in the previous studies, it is likely that the metal-N-doped carbon interface can be understood as a FLP, with active participation of the support basic nitrogen atoms in the H₂ activation. Based on our interest in this concept, we decided to explore the synthesis of gold nanoparticles supported on N-doped carbon supports for studies in selective hydrogenations. The main advantage with respect to previous studies(FIORIO; LÓPEZ; ROSSI, 2017) is to avoid the

addition of external ligands, in large excess, for the activation of gold surfaces via FLP, making the whole process environmentally and economically attractive.

6.2. RESULTS AND DISCUSSION

We commenced our study by preparing a series of gold catalysts inspired by the method developed by Beller's group for the preparation of Ni, Co and Fe-catalysts. (WESTERHAUS et al., 2013); (JAGADEESH et al., 2013); (CHEN et al., 2015); (JAGADEESH et al., 2015a); (JAGADEESH et al., 2015b) The gold catalysts were prepared by pyrolysis of the gold precursor at different temperatures in the range from 200 to 800 °C in the presence of 1,10-phenanthroline (L1) and TiO₂ support under N₂ atmosphere (Figure 22).

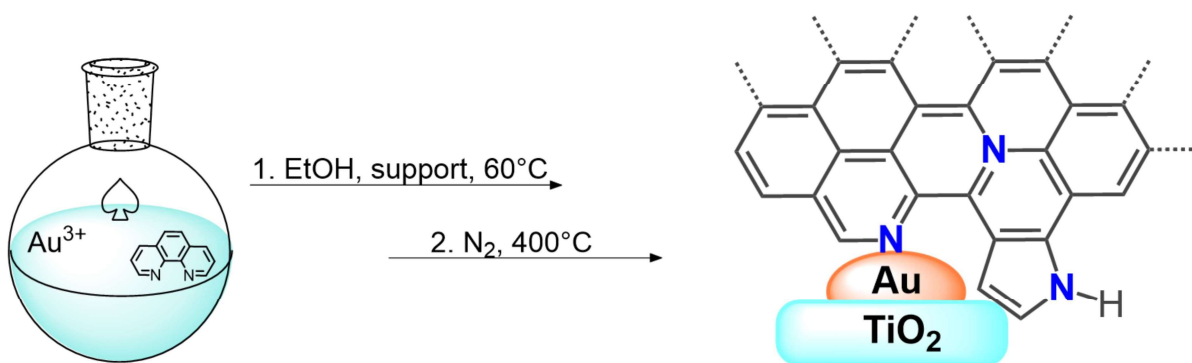


Figure 22. Schematic illustration of the synthesis of Au@N-doped carbon/TiO₂ catalysts.

The thermal behavior TGA-DTG of the Au-L1/TiO₂ material under N₂ indicated that the pyrolysis proceeds in a multi-stage fashion (Figure 23).

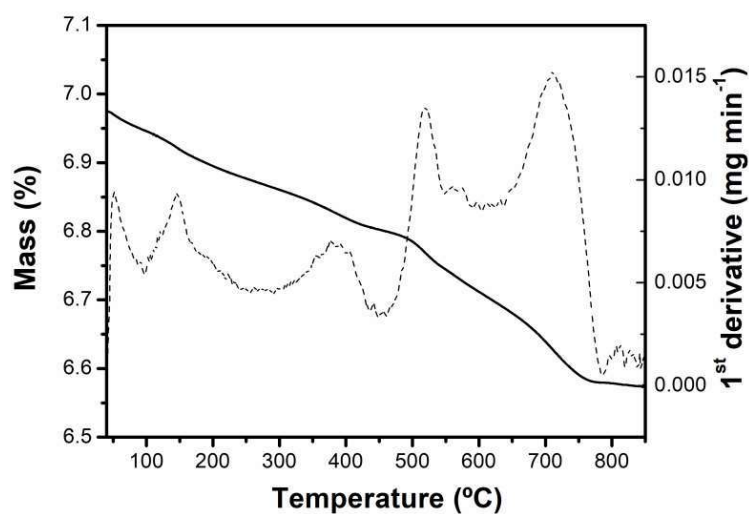
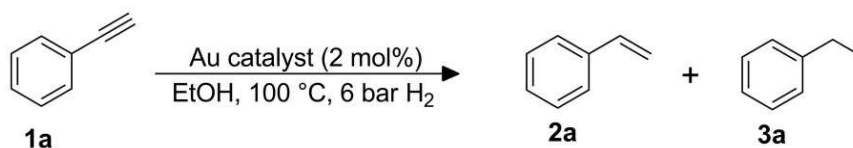


Figure 23. TGA (solid) and DTG (dashed) profile of the precursor Au-L1/TiO₂ under N₂.

We studied the influence of the pyrolysis temperature on the catalytic activity of the various materials obtained for the benchmark hydrogenation of phenylacetylene **1a** using molecular hydrogen (H₂) (Table 14). The material pyrolyzed at 200 °C led to 51% of conversion of **1a** (Table 14, entry 1). The best activity was obtained by performing the pyrolysis at 400 °C (Table 14, entry 2). On increasing the pyrolysis temperature to 600 °C and 800 °C, the activity of the resulting catalyst decreased significantly (Table 14, entry 3 and 4).

Table 14. Catalytic activity in the hydrogenation of phenylacetylene of Au@N-doped carbon catalysts obtained from Au-L1/TiO₂ after pyrolysis at different temperatures.^a



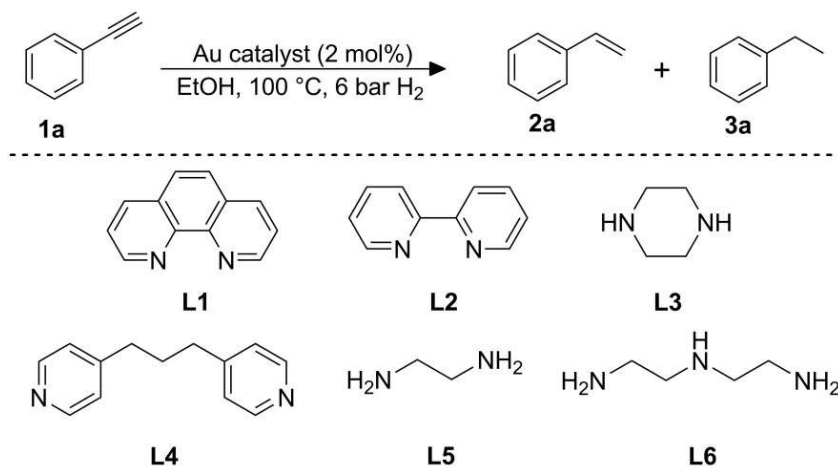
Entry	Pyrolysis temperature (°C)	Conversion of 1a (%)	Yield of 2a (%)
1	200	51	>99
2	400	100	>99
3	600	27	>99
4	800	5	65

^aReaction conditions: 0.14 mmol **1a**, 2 mol% of Au@N-doped catalyst, 2 mL of ethanol, 100 °C, 6 bar H₂, 20 h. ^bDetermined by GC using internal standard technique.

We next studied the influence of the N-containing ligands on the stabilization and catalytic activity of the various materials obtained after pyrolysis at 400 °C (Table 15). Among the different N-containing ligands tested, 1,10-phenanthroline (L1) was found to give the most-active system (Table 15, entry 1), resulting in a catalyst that exhibited superior reactivity in comparison with those obtained from other ligands such as 2,2'-bipyridine (L2), ethylenediamine (L5), diethylenetriamine (L6) (Table 15, entries 2, 5 and 6). The catalyst obtained using piperazine (L4) showed the lowest activity (Table 15, entry 3). Moreover, the model reaction does not occur to any extent in the presence of the material not submitted to pyrolysis (Table 15, entry 7). Notably, the catalyst prepared without addition of any ligand (Au/TiO₂) showed significant low catalytic activity (Table 15, entry 8), and no conversion was observed with a

material obtained via pyrolysis of the support with 1,10-phenantroline (L1/TiO₂) but without the gold precursor (Table 15, entry 9).

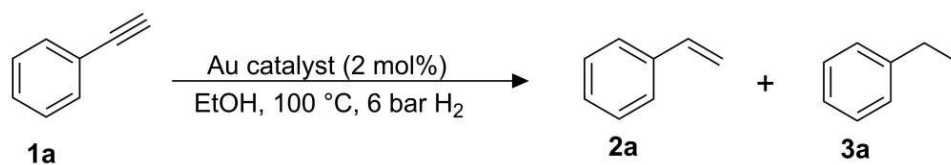
Table 15. Catalytic activity in the hydrogenation of phenylacetylene of Au@N-doped carbon catalysts obtained with different N-containing ligands, after pyrolysis at 400 °C.^a



Entry	Catalyst precursor	Conversion of 1a (%)	Yield of 2a (%)
1	Au-L1/TiO ₂	100	>99 (95)
2	Au-L2/TiO ₂	47	88
3	Au-L3/TiO ₂	8	79
4	Au-L4/TiO ₂	18	94
5	Au-L5/TiO ₂	65	93
6	Au-L6/TiO ₂	17	89
7 ^c	Au-L1/TiO ₂	0	-
8	Au/TiO ₂	4	>99
9	L1/TiO ₂	0	-

^aReaction conditions: 0.14 mmol of **1a**, 2 mol% of Au catalyst, 2 mL of ethanol, 100 °C, 6 bar of H₂, 20 h. ^bDetermined by GC using internal standard technique; numbers in parenthesis refer to isolated yield. ^cCatalyst not pyrolyzed.

We further investigated the potential effect of supports (C, CeO₂, MgO, Fe₃O₄, SiO₂ and TiO₂) in the catalytic activity (Table 16). The catalysts based on carbon, cerium oxide, iron oxide and magnesium oxide (Table 16, entries 1–4) showed low conversion ($\leq 10\%$) of **1a**. Although the catalyst supported on silica reaches 71% of conversion (Table 16, entry 5), the fully hydrogenated product **3a** was formed. Titanium dioxide proved to be the best support (Table 16, entry 6) under the studied conditions. Gold precursor influence in the catalytic activity was also evaluated, the catalyst prepared using gold acetate (Table 16, entry 6) showed the best result, full conversion of **1a**, a slightly decrease in catalytic activity was noticed when using hydrogen tetrachloroaurate(III) (68% of conversion of **1a**, Table 16, entry 7) or potassium dicyanoaurate(I) (90% of conversion of **1a**, Table 16, entry 8). An increase in the Au:L1 molar ratio from 1:2 to 1:5 or 1:10 lead to complete loss of catalytic activity (Table 16, entries 9 and 10).

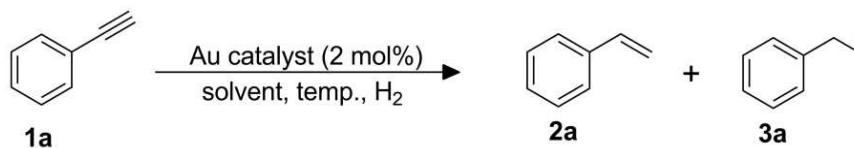
Table 16. Effect of catalysts support in the hydrogenation of phenylacetylene **1a**.^a

Entry	Support	Gold precursor	Au:L1 ratio	Conversion of 1a (%)	Selectivity to 2a (%)
1	Au-L1/C			5	>99
2	Au-L1/CeO ₂			6	>99
3	Au-L1/MgO	Au(OAc) ₃	1:2	4	>99
4	Au-L1/Fe ₃ O ₄			3	>99
5	Au-L1/SiO ₂			71	65
6	Au-L1/TiO ₂			100	>99
7	Au-L1/TiO ₂	H AuCl ₄		68	>99
8	Au-L1/TiO ₂	K Au(CN) ₂		90	>99
9	Au-L1/TiO ₂	Au(OAc) ₃	1:5	0	-
10	Au-L1/TiO ₂	Au(OAc) ₃	1:10	0	-

^aReaction conditions: 1 mmol of **1a**, 2 mol% of Au catalyst, 2 mL of ethanol, 100 °C, 6 bar of H₂, 20 h. ^bDetermined by GC using internal standard technique.

After a further survey of common reaction parameters (solvent, reaction temperature, molecular hydrogen pressure; Tables 17), the best reaction conditions were ethanol as solvent, 6 bar of H₂ at 100 °C.

Table 17. Screening of reaction conditions in the hydrogenation of phenylacetylene **1a**.^a



Entry	Reaction temperature (°C)	Solvent	H ₂ pressure (bar)	Conversion of 1a (%)	Selectivity to 2a (%)
1	100	EtOH	6	100	>99
2	80	EtOH		29	>99
3	60	EtOH		24	>99
4	40	EtOH		4	>99
5	100	Toluene		12	>99
6		DMF		70	>99
7		THF		7	>99
8		Hexane		24	>99
9		1,4-dioxane		17	>99
10		MeCN		<1	>99
11		Et ₃ N		<1	>99
12		Pyridine		<1	>99
13		Diethylamine		<1	>99
14		EtOH	4	92	>99
15		EtOH	2	42	>99

^aReaction conditions: 1 mmol of **1a**, 2 mol% of Au catalyst, 2 mL of ethanol, temperature, 6 bar of H₂, 20 h. ^bDetermined by GC using internal standard technique.

The most active catalytic material obtained by pyrolysis at 400 °C was characterized in detail. The active catalyst contains 1.1 wt% Au, 0.7 wt% C and 0.2 wt% N, as determined by elemental analysis and FAAS. Images by scanning transmission electron microscopy (STEM) of the material pyrolyzed with the L1 ligand revealed the formation of Au NPs with a mean diameter of 4.5 nm, in addition, a few larger particles of 10 nm were observed occasionally (Figure 24a–c). In complete contrast, the catalyst prepared without the presence of the ligand, a significant increase in the gold NPs size was observed, with a mean diameter of ~17 nm (Figure 24d–f).

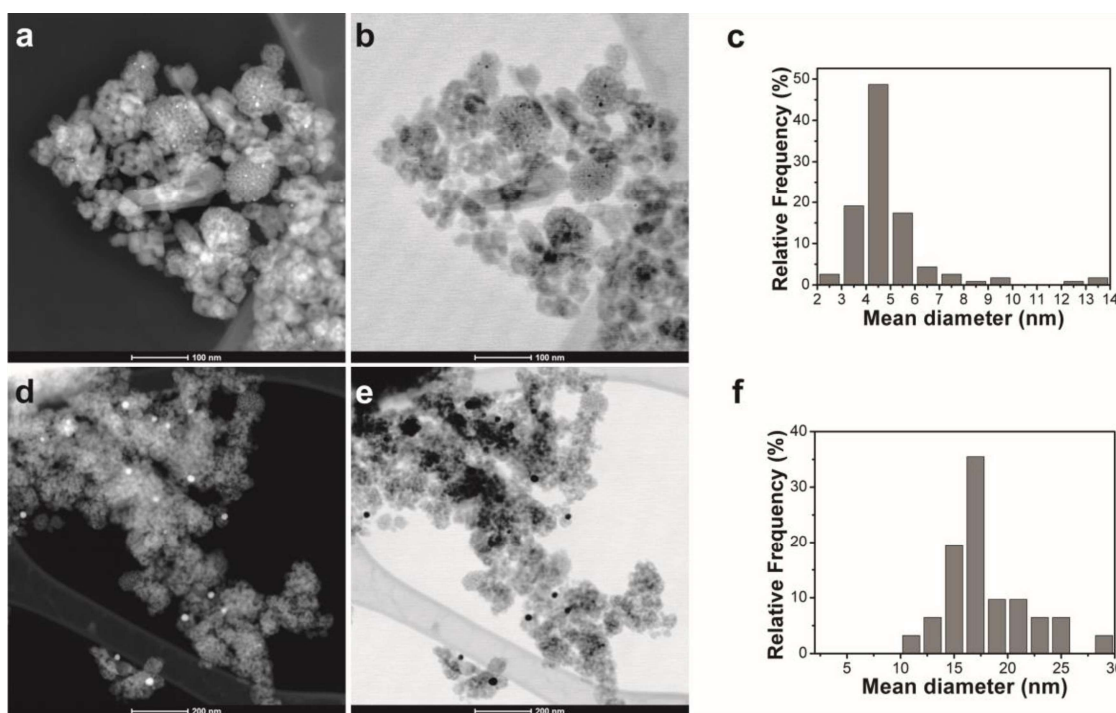


Figure 24. HAADF and STEM bright field images of Au-L1/TiO₂ (a and b), and Au/TiO₂ (d and e). The respective particle size distribution histograms (c and f). Both catalysts were prepared via pyrolysis at 400 °C for 2 h under N₂ flow.

The X-ray diffraction (XRD) pattern corresponding to Bragg diffractions of Au (200) at 44°, Au (220) at 65°, or Au (311) at 78°, confirmed the metal reductions and anatase as the predominant phase without significant phase conversion after thermal treatment (Figure 25a). UV-Vis diffuse reflectance spectra were recorded for both solids (with and without L1), showing a typical gold SPR band (Figure 25b).

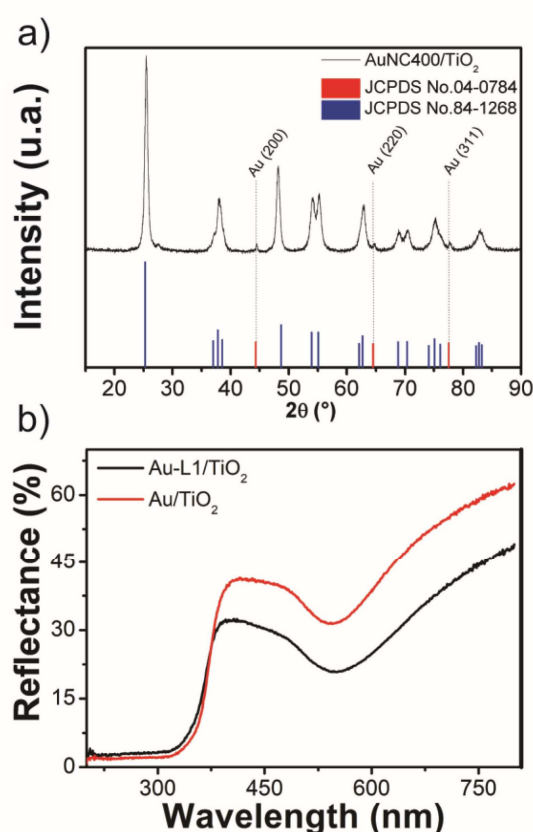


Figure 25. A) XRD pattern of Au-L1/TiO₂; b) UV-Vis diffuse reflectance spectra (UV-Vis DRS) of Au-L1/TiO₂ and Au/TiO₂. All characterized catalysts were prepared via pyrolysis at 400 °C for 2 h under N₂ flow.

EDX spectrum imaging (elemental mapping) of the Au-L1/TiO₂ material after pyrolysis at 400 °C provided clear evidence for the presence of carbon deposited on the surface of the Au NPs (Figure 27b). No conclusive information

on the location of nitrogen in the sample could be obtained, due to the overlap of the majoritarian Ti signal at 0.452 keV with the N signal at 0.392 keV (Figure 26).

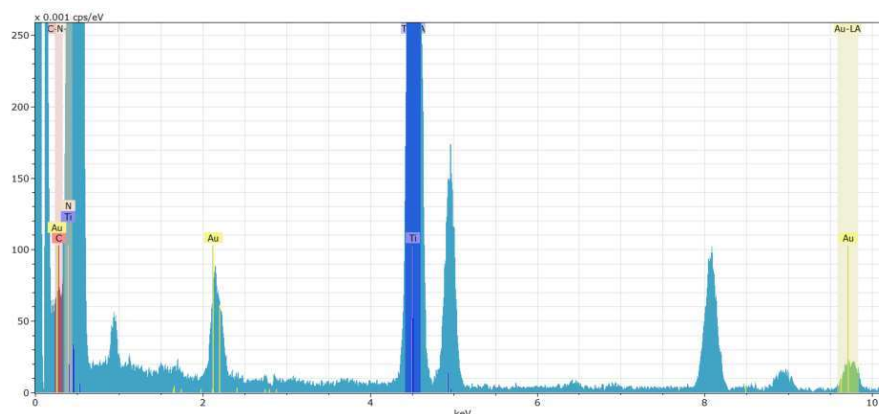


Figure 26. EDX spectrum from the Au@N-doped carbon catalyst.

The type of N-doping was investigated in more detail by X-ray photoelectron spectroscopy (XPS). The XPS survey spectrum of catalytic material obtained by pyrolysis at 400 °C revealed that the surface of the sample contains Au, C, Ti, N and O. The Au 4f spectrum exhibit two peaks centered at binding energy 87.0 eV and 83.3 eV, which correspond to the Au⁰ oxidation state(WANG et al., 2015)(ZHAN et al., 2016) (Figure 27c). Valuable information was obtained by analysis of the binding energy peak of the N 1s region (Figure 26d). The N 1s spectrum of the most active Au@N-doped carbon catalyst (pyrolysis at 400 °C) was fitted with three components located at binding energies of 399.5, 400 and 401.3 eV. The peak at 401.3 eV can be attributed to graphitic nitrogen, while the peak at 399.5 eV can be attributed to the pyridinic nitrogen species.(DUAN et al., 2015; GUO et al., 2016; HE et al., 2016)

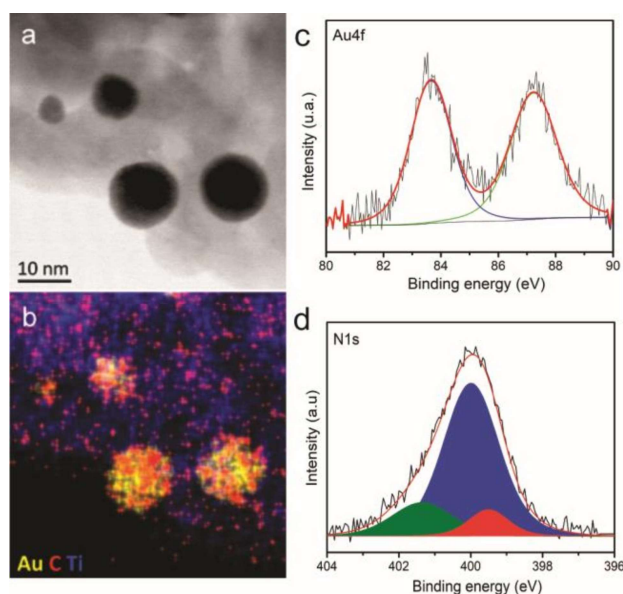


Figure 27. (a) Bright field STEM image of a representative area of the Au@N-doped carbon catalyst (Au-L1/TiO₂ material after pyrolysis at 400 °C) and (b) corresponding EDX elemental maps. Carbon appear as the red spots deposited mostly on the yellow gold particles. (c) Au 4f XPS spectra and (d) N 1s XPS spectra for Au-L1/TiO₂ material after pyrolysis at 400 °C.

However, the peak at 400 is more difficult to attribute, as it can be both a result of Au-N interaction or due to pyrrolic nitrogen species, very often present in N-doped carbon systems,(CHEN et al., 2016a) and also present in the XPS N1s spectrum of the sample L1/TiO₂ (without gold) (Figure 28). The 1,10-phenanthroline ligand adsorbed on TiO₂ (L1/TiO₂ without gold) displays only one nitrogen species at 399.4 eV (Figure 28), typically of a pyridinic nitrogen atom (free ligand).

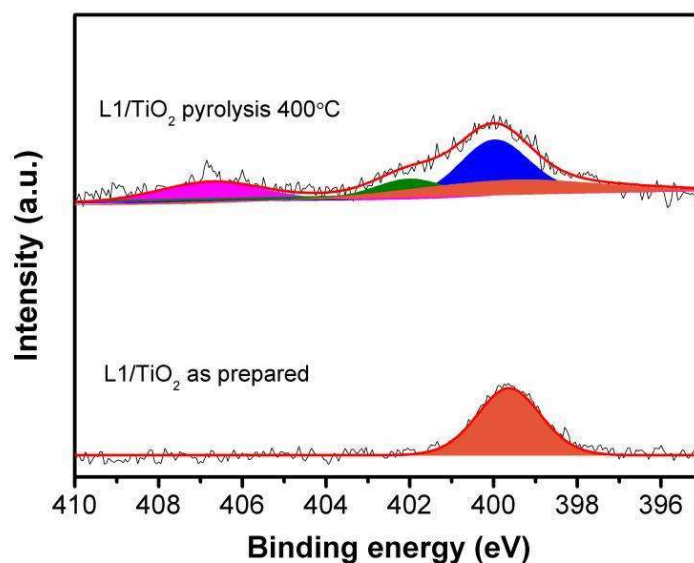


Figure 28. XPS spectra of N1s region of L1/TiO₂ (without gold) as prepared and after pyrolysis.

This component at ca. 400 eV was found in all catalysts prepared by pyrolysis with other ligands (L2–L6) at 400 °C (Figure 29). The as-prepared catalyst precursor Au-L1/TiO₂ (before pyrolysis) displays two nitrogen species at 399.3 and 399.8 eV (Figure 28), which are tentatively attributed to pyridinic nitrogen atoms of free ligand and of the ligand coordinated and/or adsorbed on gold (Au-N), respectively.

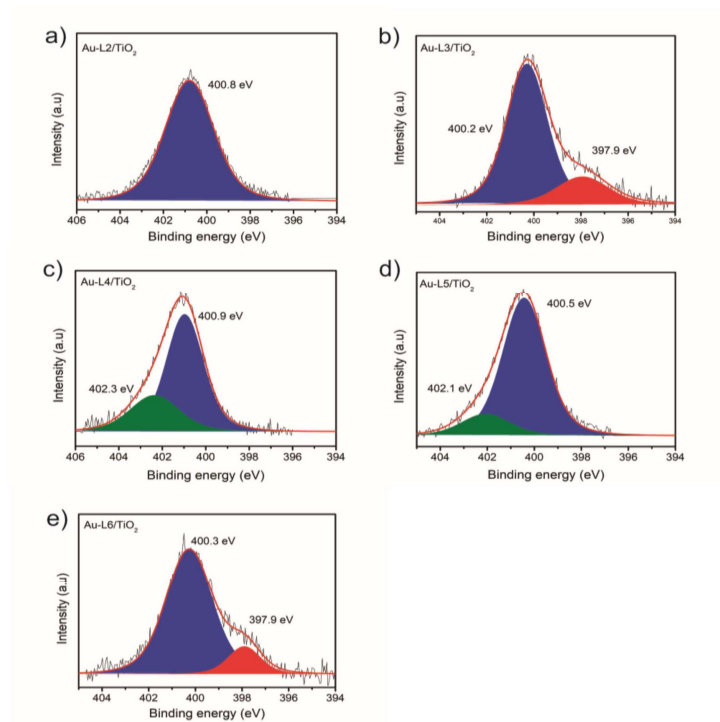


Figure 29. XPS spectra of N1s region of the catalyst prepared by pyrolysis at 400 °C a)Au-L2/TiO₂; b)Au-L3/TiO₂; c)Au-L4/TiO₂; d)Au-L5/TiO₂; e)Au-L6/TiO₂.

The N 1s spectrum of L1/TiO₂, Au-L1/TiO₂ and Au@N-doped carbon/TiO₂ catalysts prepared at 200, 400, 600 and 800 °C disclosed different nitrogen species (Figure 30). The 1,10-phenanthroline ligand adsorbed on TiO₂ (L1/TiO₂ without gold) displays only one nitrogen species at 399.4 eV, typically of a pyridinic nitrogen atom (free ligand). The as-prepared catalyst precursor Au-L1/TiO₂ (before pyrolysis) displays two nitrogen species at 399.3 and 399.8 eV, which are tentatively attributed to pyridinic nitrogen atoms of free ligand and of the ligand coordinated and/or adsorbed on gold (Au-N), respectively. It is worth to note that the solid was purple after analysis, indicating reduction of gold(III) acetate to gold(0). The catalyst prepared at 200 °C displays the same two nitrogen species shifted to 399 and 400 eV. The N 1s spectrum of the most

active Au@N-doped carbon catalyst prepared at 400 °C was fitted with three components located at binding energies of 398.8, 399.8 and 401.0 eV. The peak at 401.0 eV can be attributed to graphite nitrogen, while the peak at 398.8 eV can be attributed to the pyridinic nitrogen species. The component at ca. 400 eV in the Au@N-doped carbon catalysts, which can then be assigned to pyrrolic N atoms formed after pyrolysis, gains intensity with the increase of pyrolysis temperature, suggesting an increase of defects in the graphene-like structure. Besides the differences in the concentration of N species present, the less active catalysts prepared at 600 and 800 °C contain less nitrogen than the catalyst prepared at 400 °C.

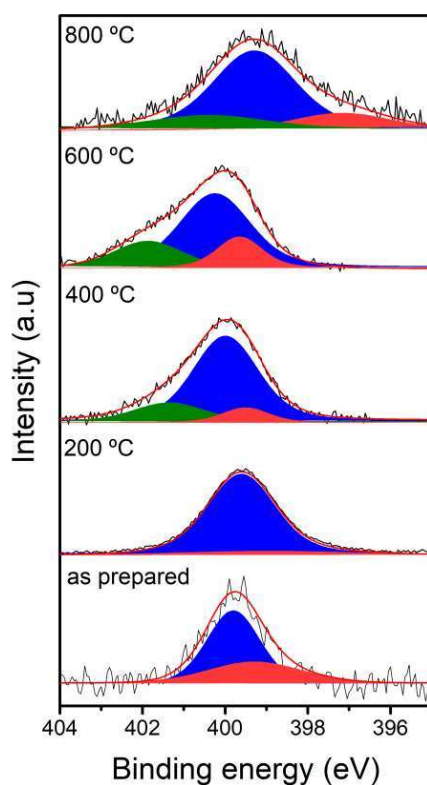


Figure 30. XPS spectra of N1s region of the Au-L1/TiO₂ material freshly-prepared and after pyrolysis at 200, 400, 600 and 800 °C under N₂.

The kinetic study shown in Figure 31 indicates full conversion of **1a** to **2a** in about 8 hours and suppression of further hydrogenation of **2a** to **3a**, even at long reaction times. It is worth to note that a sixty-fold reaction rate enhancement was observed when comparing the catalytic activity of similar Au catalysts prepared with **L1** (Figure 31b) (reaction rate = 0.273 mmol g_{cat}⁻¹ h⁻¹) or without any ligand (Figure 31c) (reaction rate = 0.00472 mmol g_{cat}⁻¹ h⁻¹). In order to further examine the stability as well as recyclability of the “fully heterogeneous” catalytic material, the hydrogenation of **1a** was repeated up to ten times (Figure 31d) using the same catalysts portion without any further treatment or ligand addition. A hot filtration test (Figure 29e) revealed that the obtained activity is not related to any leaching of the catalytically active metal (no remaining activity in the supernatant).

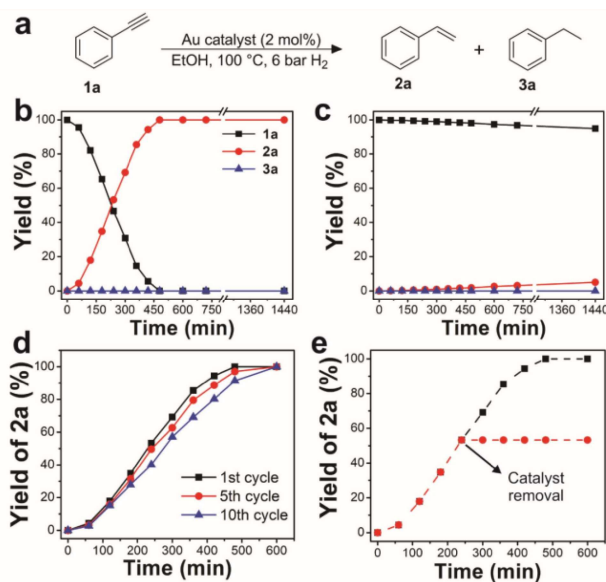


Figure 31. (a) Time course of hydrogenation of phenylacetylene **1a** catalyzed by (b) Au@N-doped carbon/TiO₂ catalyst and (c) Au/TiO₂ catalyst; (d) Recycling experiments using the Au@N-doped carbon/TiO₂ catalyst; (e) Hot filtration test to determine homogeneous catalysis contribution in hydrogenation of **1a**. Reaction conditions: 0.14 mmol of **1a**, 2 mol% of Au, 2 mL of ethanol, 100 °C, 6 bar of H₂.

As depicted in Figure 32, the desired product styrene **2a** was obtained in a 99% yield even after ten runs and no significant loss of activity was observed (see also Figure 31d).

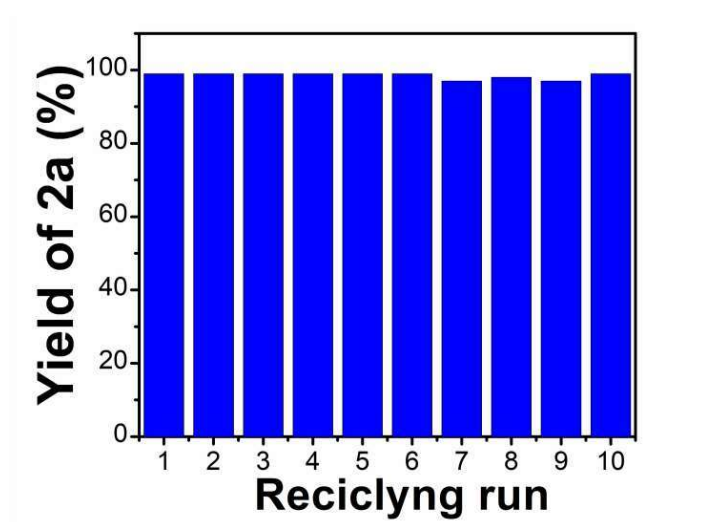


Figure 32. Catalyst recycling of the hydrogenation of phenylacetylene catalyzed by Au@N-doped carbon/TiO₂ catalyst. Reaction conditions: 1 mmol 1a, 2 mol% of Au, 2 mL of ethanol, 100 °C, 6 bar H₂.

This high selectivity for the alkene **2a** is an intrinsic property of our catalyst and it was not observed for the well-known Pd Lindlar catalyst (Pd/CaCO₃ + Pb(OCOCH₃)₂ + quinoline), which produces **3a** at high conversions (Figure 30).

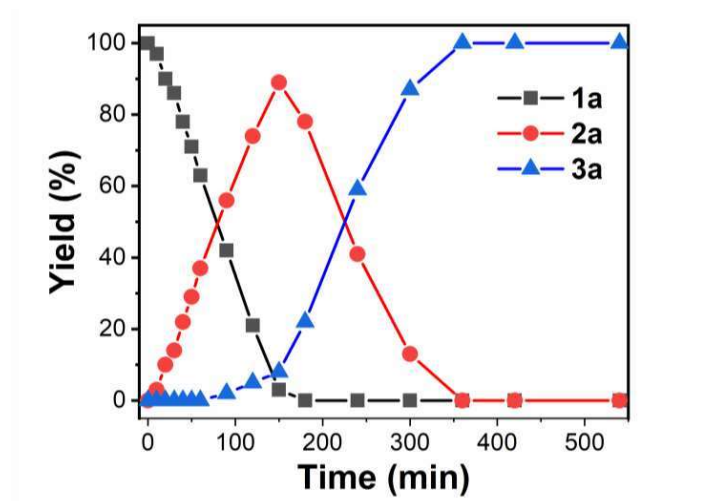


Figure 33. Time course of hydrogenation of phenylacetylene catalyzed by Lindlar catalyst. Reactions conditions: 4 mmol of **1a**, 0.25 mol% Pd, 4 mL of hexane, 0.2 mL of quinoline, 100 °C, 6 bar of H₂.

ICP AES analysis of the recycling experiments indicated no undesired leaching processes of gold occurred during the course of the catalytic transformation. Furthermore, no aggregation of Au NPs was observed by STEM of the recycled catalyst after the tenth recycle (Figure 31).

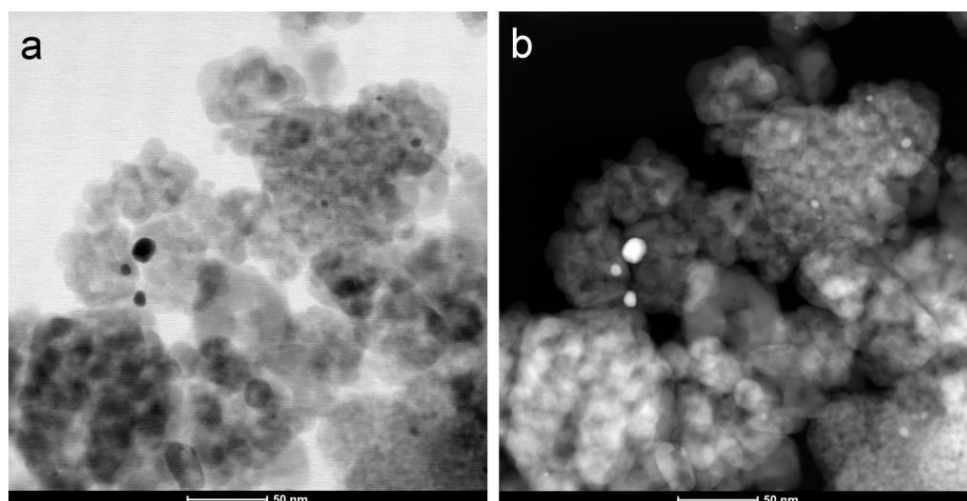
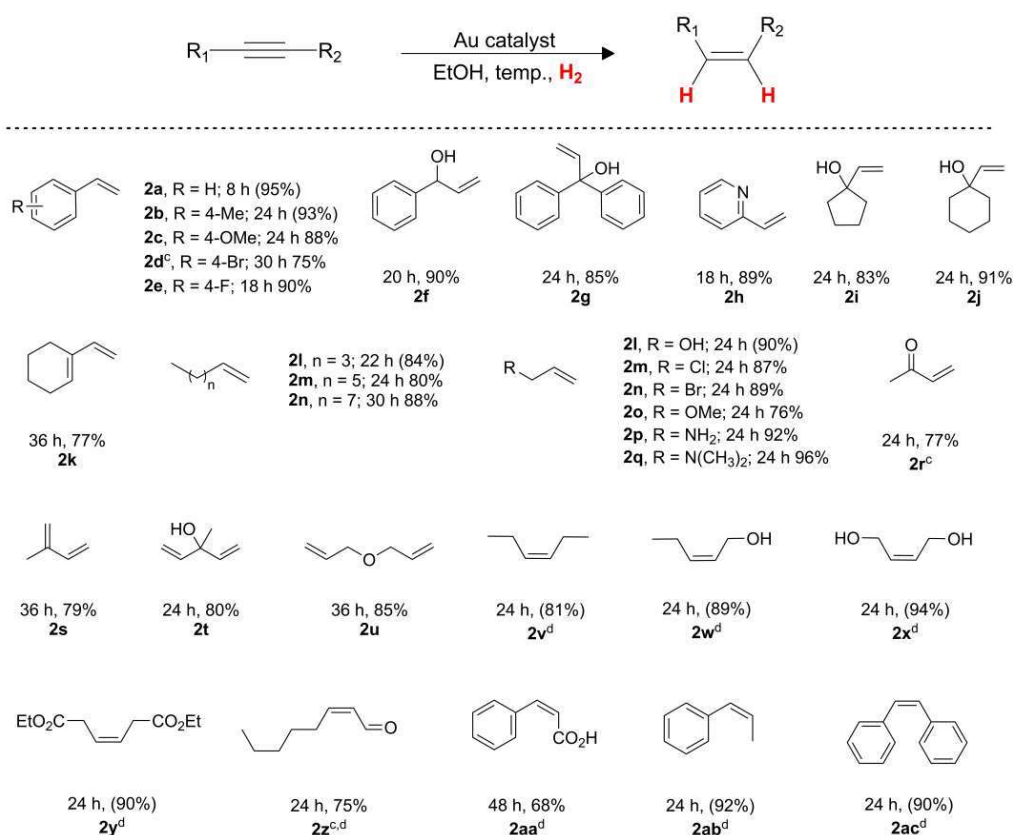


Figure 34. STEM bright field (a) and HAADF (b) images of the Au@N-doped carbon/TiO₂ catalyst after the tenth hydrogenation cycle.

Since Au@N-doped carbon/TiO₂ catalyst (Au-L1/TiO₂ pyrolyzed at 400 °C) displayed the best activity for the production of styrene, it was explored in the scope study under the optimized conditions. A variety of terminal and internal alkynes was readily hydrogenated to the desired alkene and *cis*-alkene with moderate to excellent yield (Table 18) and, notably, different from what occurred with other transition metals, without any over-reduction to alkane. *cis*-Control was also reported to be a consequence of FLP. Moreover, both electron-deficient substituents, such as esters (**2ab**) and carboxylic acids (**2ad**) moieties, and electron-rich groups, for example, amino (**2s** and **2t**) and methoxy (**2c** and **2o**), were tolerated well. The developed catalyst was even able to reduce only the alkyne unit in molecules with alkene moieties (**2k**, **2v**, **2w** and **2x**), without any detectable concurrent reduction of the alkene moieties both in the parent and product molecules. The results depicted in Table 18 confirmed that a broad range of sensitive and reducible functional groups, including halide (**2d**, **2e**, **2p**, and **2q**), ketones (**2u**) and aldehydes (**2ac**), were tolerated in the alkyne hydrogenation process. With an increase in H₂ pressure (10 bar H₂), (*Z*)-alkenes were mostly formed from internal alkynes (**2y-2af**). The catalyst system was also applicable for scaled-up conditions, where 5 mmol of **1a** (0.51 g) was successfully converted into the alkene **2a** (0.49 g, 94%). Considering full conversion, the turnover number (TON) of 1700 was reached, with a TOF of approximately 70 mol mol⁻¹ h⁻¹.

Table 18. Au@N-doped carbon/TiO₂ catalyst for the semihydrogenation of alkynes to alkenes.^{a,b}



^aReaction conditions: 0.14 mmol of alkyne, 2 mol% of Au-L1/TiO₂ catalyst, 2 mL of ethanol at 100 °C, 6 bar of H₂. ^bGC yields are shown; values in parentheses refer to isolated yields. Selectivity was >99%. ^c8 bar of H₂. ^d80 °C. ^e10 bar of H₂.

Such a TOF value is an order of magnitude higher than the values reported for heterogeneous gold-based catalysts using molecular hydrogen as hydride source and without the use of ligands. Furthermore, this TOF is also high when taking into account values for systems using other sources of hydride and ligands to boost the catalytic activity (Table 19).

Table 19. Summary of results reported for semihydrogenation of alkynes with heterogeneous gold-based catalyst with and without addition of ligands.

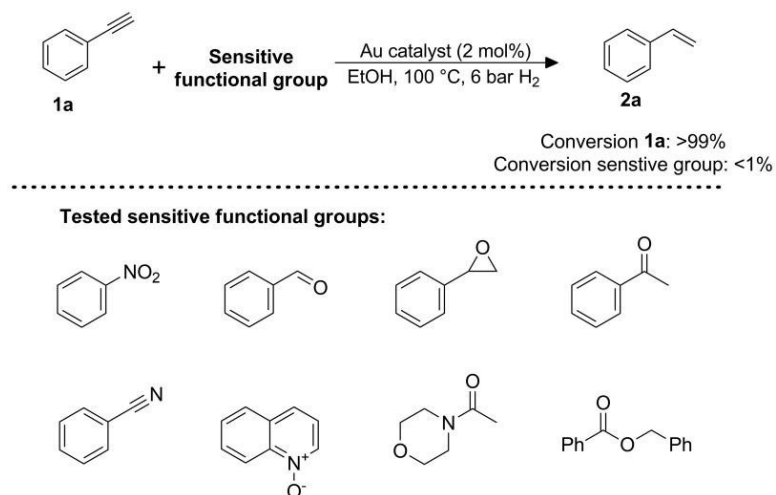
Catalyst	Condition	Hydride source	TOF (h ⁻¹)	Ref.
Au@N-doped carbon/TiO ₂	6 bar H ₂ , 100 °C, 8 h	H ₂	6.25	This work
Au@N-doped carbon/TiO ₂	30 bar H ₂ , 100 °C, 24 h	H ₂	70	This work
Au@CeO ₂	30 bar H ₂ , r.t., 12 h	H ₂	0.833	(MITSUDOME et al., 2015)
Au _{>99} Ag ₁ NPore	8 bar H ₂ , 90 °C, diethylamine, 24 h	H ₂	0.833	(TAKALE et al., 2016)
Au ₂₅ (SR) ₁₈ /TiO ₂	20 bar H ₂ , 100 °C, pyridine, 20 h	H ₂	0.985	(LI; JIN, 2014)
Au/SiO ₂	6 bar H ₂ , 80 °C, piperazine, 5 h	H ₂	20	(FIORIO; LÓPEZ; ROSSI, 2017a)
Au NPore	PhMe ₂ SiH, 35 °C, pyridine, 6 h	PhMe ₂ SiH	8.33	(YAN et al., 2012)
Au/TiO ₂	HCOONH ₄ , 80 °C, 6 h	HCOONH ₄	33.3	(LIANG; HAMMOND; XU, 2016)

The TOF value was calculated in the format of mol **2a** mol⁻¹ metal h⁻¹. The amount of metal is based on the moles of metal components involved.

To further check the chemoselectivity of the developed catalyst, we performed experiments using **1a** as substrate in the presence of diverse sensitive functionalized molecules (Table 20). Total chemoselectivity was observed for the reduction of the model alkyne in the presence of potentially reducible groups such as nitro, aldehydes, epoxides, ketones, nitriles, esters,

heteroaromatic *N*-oxides and amide, since not even traces of conversion of these functional groups were detected.

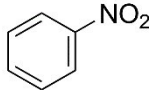
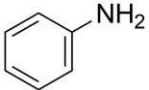
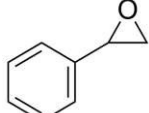
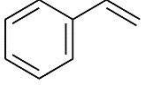
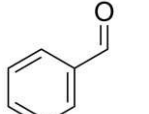
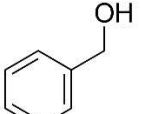
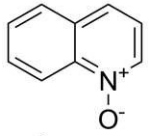
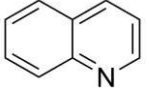
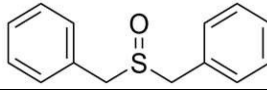
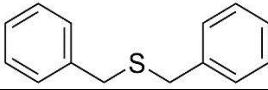
Table 20. Selective hydrogenation of **1a** in the presence of molecules with other reducible functional groups by Au@N-doped carbon/TiO₂ catalyst.^a



^aReaction conditions: 0.14 mmol **1a**, 0.14 mmol of sensitive molecule, 2 mol% of Au catalyst, 2 mL of ethanol, 24 h, 100 °C, 6 bar H₂. Conversion was determined by GC using internal standard technique.

In the absence of the alkyne, some of those functional groups such as epoxides, nitro, aldehydes, heteroaromatic *N*-oxides, and sulfoxides can be efficiently reduced too (Table 21).

Table 21. Selective hydrogenation of other functional groups by Au@N-doped carbon/TiO₂ catalyst.^a

Entry	Substrate	Product	Conversion (%) ^b	Selectivity (%) ^b
1 ^c			>99	>99
2			>99	>99
3			>99	>99
4 ^d			>99	>99
5			>99	>99

^aReaction conditions: 0.14 mmol of substrate, 2 mol% of Au, 2 mL of ethanol, 24 h, 110°C and 15 bar of H₂. ^bDetermined by GC using internal standard technique. ^c8 bar of H₂. ^d10 bar of H₂.

Based on the experimental results and previous ascertain, we believe that pyridinic, graphitic and pyrrolic N atoms play a pivotal role in boosting the catalytic activity of our gold-based catalyst. The reactivity pattern displayed by the Au@N-doped carbon catalyst, prepared via pyrolysis of Au-L1/TiO₂, allows us to postulate that H₂ activation may proceed by a heterolytic pathway, due to the interaction of Au NPs and the nitrogen atoms of the N-doped carbon around the metallic nanoparticles, following the concept of frustrated Lewis pair (FLP) interface suggested before for Au NPs and externally added N-containing ligands. (FIORIO; LÓPEZ; ROSSI, 2017) This type of H₂ activation at N-doped

carbon supports was previously described for Pd,(VILÉ et al., 2015) boron-nitrogen co-doped graphene,(SUN et al., 2016) and Co catalyst.(FORMENTI et al., 2017) The introduction of N atoms might affect the properties of the supported catalyst, such as tunable acid–base character at the support surface, which could cause a better interaction of metal–support–reactant, as well as charge transfer phenomena at the metal–support junction.(HE et al., 2016)

6.3. CONCLUSIONS

We have prepared, for the first time, a N-doped carbon supported gold-based catalyst that exhibited excellent activity and selectivity for the hydrogenation of alkynes to alkenes, in a broad scope of substrates, at mild reaction condition. The intriguing structure of the novel gold heterogeneous catalyst, which could be understood as frustrated Lewis pairs (FLP) interfaces according to computational studies, enables the heterolytic activation of molecular hydrogen, boosting gold catalytic activity while avoiding addition of external ligands to improve activity and selectivity. The graphitization of the ligand ensures that it is present on the surface and not removed by the solvent or the reactants, which explains the robustness of the material under reaction conditions. We demonstrated that the heterolytic dissociation of H₂ can occur in a fully-heterogeneous catalyst, which will be economically and environmentally attractive. The Au@N-doped carbon catalyst tolerates other reducible functional groups, including C–C double bonds, nitro, aldehydes, epoxides, ketones, nitriles, esters, heteroaromatic *N*-oxides, and amides, and can be recycled without loss of activity. The surface-FLP concept is in its infancy when

compared to main group-FLP(STEPHAN, 2016)(STEPHAN, 2015a) and transition metal-based FLP,(CHAPMAN; HADDOW; WASS, 2011) but has shown many interesting features. The expansion of this concept for a broad range of applications in the field of heterogeneous catalysis is encouraged. New reactivity patterns, not limited to activation of H₂, will be soon explored.

6.4. EXPERIMENTAL SECTION

6.4.1. Materials and methods

The metal precursor Au(OAc)₃ was purchased from Alfa Aesar. Amines were purchased from Sigma-Aldrich. Supports TiO₂ (anatase, particle size <25nm) and CeO₂ (particle size <25nm) were obtained from Sigma Aldrich and MgO was purchased from Synth. The SiO₂ support was obtained by a method previously described in literature.(JACINTO et al., 2008) The glass reactor was thoroughly cleaned with aqua regia (HCl:HNO₃ = 3:1 v/v), pure water, and dried in an oven prior to use. Unless otherwise stated, all other reagents used for the support and catalysts preparation were of analytical grade, purchased from Sigma-Aldrich and used as received

Metal content in the catalysts were measured by FAAS analysis, on a Shimadzu AA-6300 spectrophotometer using an Au hollow cathode lamp (Photron). Metal leaching into the supernatant solution was measured by inductively coupled plasma optical emission spectrometry measurements, performed on a Spectro Arcos ICP OES. X-ray diffraction (XRD) of the samples was recorded using a Rigaku miniflex diffractometer with Cu K α radiation (λ =

1.54 Å) at a 2θ range from 20 to 90° with a 0.02° step size and measuring time of 5 s per step.

The morphology of the catalysts was investigated by the acquisition of high-angle annular dark field (HAADF) and bright field (BF) images using an aberration corrected scanning transmission electron microscope (STEM) FEI Titan Themis³ 60-300 operating at 300 kV. Samples were prepared by directly applying the catalyst powder onto standard TEM grids. X-ray energy dispersive spectrum images (XED-SI) were acquired using an Espirit system (Bruker) for compositional mapping. Electron probes of ca. 0.2 nm were used to guarantee sufficient current density at each sample point to obtain statistically significant X-ray counts for the elements of interest. SIs were acquired by scanning an area of interest of the sample with pixel size of ca. 0.2 nm and a total dwell time of 0.6 s/pixel. Complete XED-spectra were acquired at each SI pixel in the 0-20 keV energy range.

X-ray photoelectron spectroscopy (XPS) were performed using synchrotron radiation with a photon energy of 3000 eV at SXS beamline on the Brazilian Synchrotron Light Laboratory (LNLS, Campinas-Brazil, Proposal number 20170205). The operating pressure in the ultra-high vacuum chamber (UHV) during the analysis was 10^{-8} Pa. The XPS high resolution spectra were recorded at constant pass energy of 50 eV with a 0.05 eV per step, while the survey scan was taken at 50 eV pass energy with a 0.5 eV per step.

6.4.2. Catalyst preparation

Procedure to preparation of Au-L/Support

Typically, Au(OAc)₃ (19.0 mg, 0.05 mmol) and amine ligand (18.0 mg, 0.1 mmol) (molar ratio Au:L = 1:2) were stirred in 20 mL of ethanol for approximately 5 minutes at 60 °C. The support was then added, and the mixture was stirred for more 30 min. After, the solvent was dried at the rotavapor. The as obtained solid was ground to a fine powder and then pyrolyzed in the desired temperature in an oven at a rate of 20 °C per minute and held at temperature for 2 hours under nitrogen atmosphere.

6.4.3. Catalytic procedures

General procedure for hydrogenation of alkynes

Unless otherwise stated a typical procedure for the semihydrogenation of alkynes is as follows: alkyne (0.14 mmol), Au catalyst (2 mol % Au), and 2 mL of solvent were placed in a modified Fischer–Porter 100 mL glass reactor. The reactor was purged five times with H₂, leaving the vessel at 6 bar. The resulting mixture was vigorously stirred, and the temperature was maintained with an oil bath. After the desired time, the catalyst was removed by centrifugation and the products were analyzed by GC with an internal standard to determine the conversion of alkyne and the selectivity for alkene. To determine the isolated yield of the obtained products, after the reaction was complete, the solvent was evaporated, and the crude reaction mixture was

purified by column chromatography on silica gel to afford corresponding alkenes. ^1H confirmed the purity of the isolated products.

Recycling experiment

For the recycle experiments, after each catalytic experiment under the above typical reaction conditions, the catalyst was recovered from the reaction system by centrifugation. The used catalyst was tested again under identical reaction conditions just by adding to the reactor a new amount of substrate and solvent. The product obtained after centrifugation was analyzed by GC with an internal standard to determine the conversion and selectivity.

Scale-up hydrogenation of alkynes

Alkyne (5 mmol), Au catalyst (2 mol% Au), and 10 mL of ethanol were added to a glass-lined stainless-steel reactor (Parr Instrument Company, 75 mL capacity, Series 5000 Multiple Reactor System). After sealing the reactor and degassed internal air, H_2 was introduced until 30 bar. Then, the mixture was extensively stirred (1000 rpm) at 100 °C for 24 h. The catalyst was removed by centrifugation, and the products were analyzed by GC with an internal standard to determine the conversion and the selectivity. To determine the isolated yield of the obtained product, after the reaction was complete, the solvent was evaporated, and the crude reaction mixture was purified by column chromatography on silica gel.

6.5. REFERENCES

- ALBANI, D. et al. Semihydrogenation of Acetylene on Indium Oxide: Proposed Single-Ensemble Catalysis. **Angewandte Chemie International Edition**, v. 56, n. 36, p. 10755–10760, 28 ago. 2017.
- ALMORA-BARRIOS, N. et al. Costless Derivation of Dispersion Coefficients for Metal Surfaces. **Journal of Chemical Theory and Computation**, v. 10, n. 11, p. 5002–5009, 11 nov. 2014.
- ALMORA-BARRIOS, N. et al. Concerted Chemoselective Hydrogenation of Acrolein on Secondary Phosphine Oxide Decorated Gold Nanoparticles. **ACS Catalysis**, v. 7, n. 6, p. 3949–3954, 2 jun. 2017.
- ÁLVAREZ-MORENO, M. et al. Managing the Computational Chemistry Big Data Problem: The ioChem-BD Platform. **Journal of Chemical Information and Modeling**, v. 55, n. 1, p. 95–103, 26 jan. 2015.
- ARNDT, S.; RUDOLPH, M.; HASHMI, A. S. K. Gold-based frustrated Lewis acid/base pairs (FLPs). **Gold Bulletin**, v. 50, n. 3, p. 267–282, 13 set. 2017.
- BI, Q.-Y. et al. Dehydrogenation of Formic Acid at Room Temperature: Boosting Palladium Nanoparticle Efficiency by Coupling with Pyridinic-Nitrogen-Doped Carbon. **Angewandte Chemie International Edition**, v. 55, n. 39, p. 11849–11853, 19 set. 2016.
- BUS, E.; MILLER, J. T.; VAN BOKHOVEN, J. A. Hydrogen Chemisorption on Al₂O₃-Supported Gold Catalysts. **The Journal of Physical Chemistry B**, v. 109, n. 30, p. 14581–14587, ago. 2005.
- CAMPOS, J. Dihydrogen and Acetylene Activation by a Gold(I)/Platinum(0) Transition Metal Only Frustrated Lewis Pair. **Journal of the American Chemical Society**, v. 139, n. 8, p. 2944–2947, 13 mar. 2017.
- CANO, I. et al. Air-Stable Gold Nanoparticles Ligated by Secondary Phosphine Oxides for the Chemoselective Hydrogenation of Aldehydes: Crucial Role of the Ligand. **Journal of the American Chemical Society**, v. 136, n. 6, p. 2520–2528, 12 fev. 2014.
- CANO, I. et al. Air-Stable Gold Nanoparticles Ligated by Secondary Phosphine Oxides as Catalyst for the Chemoselective Hydrogenation of Substituted Aldehydes: a Remarkable Ligand Effect. **Journal of the American Chemical Society**, v. 137, n. 24, p. 7718–7727, 24 jun. 2015.
- CAO, Y. et al. Metal/Porous Carbon Composites for Heterogeneous Catalysis: Old Catalysts with Improved Performance Promoted by N-Doping. **ACS**

- Catalysis**, v. 7, n. 12, p. 8090–8112, 27 dez. 2017.
- CHAPMAN, A. M.; HADDOW, M. F.; WASS, D. F. Frustrated Lewis Pairs beyond the Main Group: Synthesis, Reactivity, and Small Molecule Activation with Cationic Zirconocene–Phosphinoaryloxy Complexes. **Journal of the American Chemical Society**, v. 133, n. 45, p. 18463–18478, 16 nov. 2011.
- CHEN, F. et al. Selective Catalytic Hydrogenation of Heteroarenes with N - Graphene-Modified Cobalt Nanoparticles (Co₃O₄-Co/NGr@ α -Al₂O₃). **Journal of the American Chemical Society**, v. 137, n. 36, p. 11718–11724, 16 set. 2015.
- CHEN, F. et al. Stable and Inert Cobalt Catalysts for Highly Selective and Practical Hydrogenation of C≡N and C=O Bonds. **Journal of the American Chemical Society**, v. 138, n. 28, p. 8781–8788, 20 jul. 2016a.
- CHEN, T.; RODIONOV, V. O. Controllable Catalysis with Nanoparticles: Bimetallic Alloy Systems and Surface Adsorbates. **ACS Catalysis**, v. 6, n. 6, p. 4025–4033, 3 jun. 2016.
- CHEN, Z. et al. Merging Single-Atom-Dispersed Silver and Carbon Nitride to a Joint Electronic System via Copolymerization with Silver Tricyanomethanide. **ACS Nano**, v. 10, n. 2, p. 3166–3175, 2016b.
- CHEN, Z. et al. Stabilization of Single Metal Atoms on Graphitic Carbon Nitride. **Advanced Functional Materials**, v. 27, n. 8, p. 1605785, fev. 2017.
- COMAS-VIVES, A. et al. Single-Site Homogeneous and Heterogeneous Gold(III) Hydrogenation Catalysts: Mechanistic Implications. **Journal of the American Chemical Society**, v. 128, n. 14, p. 4756–4765, abr. 2006.
- COMAS-VIVES, A.; UJAQUE, G. Unraveling the Pathway of Gold(I)-Catalyzed Olefin Hydrogenation: An Ionic Mechanism. **Journal of the American Chemical Society**, v. 135, n. 4, p. 1295–1305, 30 jan. 2013.
- CUI, X. et al. Highly selective hydrogenation of arenes using nanostructured ruthenium catalysts modified with a carbon–nitrogen matrix. **Nature Communications**, v. 7, p. 11326, 2016.
- DUAN, J. et al. Heteroatom-Doped Graphene-Based Materials for Energy-Relevant Electrocatalytic Processes. **ACS Catalysis**, v. 5, n. 9, p. 5207–5234, 4 set. 2015.
- FIORIO, J. L.; LÓPEZ, N.; ROSSI, L. M. Gold–Ligand-Catalyzed Selective Hydrogenation of Alkynes into cis -Alkenes via H₂ Heterolytic Activation by Frustrated Lewis Pairs. **ACS Catalysis**, v. 7, n. 4, p. 2973–2980, 7 abr. 2017.
- FORMENTI, D. et al. Co-based heterogeneous catalysts from well-defined α -

diimine complexes: Discussing the role of nitrogen. **Journal of Catalysis**, v. 351, p. 79–89, jul. 2017.

GHUMAN, K. K. et al. Illuminating CO₂ reduction on frustrated Lewis pair surfaces: investigating the role of surface hydroxides and oxygen vacancies on nanocrystalline In₂O_{3-x}(OH)_y. **Physical Chemistry Chemical Physics**, v. 17, n. 22, p. 14623–14635, 2015.

GHUMAN, K. K. et al. Photoexcited Surface Frustrated Lewis Pairs for Heterogeneous Photocatalytic CO₂ Reduction. **Journal of the American Chemical Society**, v. 138, n. 4, p. 1206–1214, 3 fev. 2016.

GRIMME, S. Semiempirical GGA-type density functional constructed with a long-range dispersion correction. **Journal of Computational Chemistry**, v. 27, n. 15, p. 1787–1799, 30 nov. 2006.

GU, J. et al. Nitrogen-doped carbon supports with terminated hydrogen and their effects on active gold species: a density functional study. **Phys. Chem. Chem. Phys.**, v. 16, n. 46, p. 25498–25507, 2014.

GUO, D. et al. Active sites of nitrogen-doped carbon materials for oxygen reduction reaction clarified using model catalysts. **Science**, v. 351, n. 6271, p. 361–365, 22 jan. 2016.

HE, L. et al. Synthesis, Characterization, and Application of Metal Nanoparticles Supported on Nitrogen-Doped Carbon: Catalysis beyond Electrochemistry. **Angewandte Chemie International Edition**, v. 55, n. 41, p. 12582–12594, 4 out. 2016.

HENKELMAN, G.; JÓNSSON, H. Improved tangent estimate in the nudged elastic band method for finding minimum energy paths and saddle points. **The Journal of Chemical Physics**, v. 113, n. 22, p. 9978–9985, 8 dez. 2000.

JACINTO, M. J. et al. Recoverable rhodium nanoparticles: Synthesis, characterization and catalytic performance in hydrogenation reactions. **Applied Catalysis A: General**, v. 338, n. 1–2, p. 52–57, 2008.

JAGADEESH, R. V. et al. Nanoscale Fe₂O₃-Based Catalysts for Selective Hydrogenation of Nitroarenes to Anilines. **Science**, v. 342, n. 6162, p. 1073–1076, 29 nov. 2013.

JAGADEESH, R. V et al. Cobalt-based nanocatalysts for green oxidation and hydrogenation processes. **Nature Protocols**, v. 10, n. 6, p. 916–926, 2015a.

JAGADEESH, R. V et al. Hydrogenation using iron oxide – based nanocatalysts for the synthesis of amines. **Nature Protocols**, v. 10, n. 4, p. 548–557, 2015b.

KRESSE, G.; FURTHMÜLLER, J. Efficiency of ab-initio total energy

calculations for metals and semiconductors using a plane-wave basis set. **Computational Materials Science**, v. 6, n. 1, p. 15–50, jul. 1996.

KRESSE, G.; HAFNER, J. Ab initio molecular dynamics for liquid metals. **Physical Review B**, v. 47, n. 1, p. 558–561, 1 jan. 1993.

KRESSE, G.; JOUBERT, D. From ultrasoft pseudopotentials to the projector augmented-wave method. **Physical Review B**, v. 59, n. 3, p. 1758–1775, 15 jan. 1999.

KYRIAKOU, G. et al. Isolated Metal Atom Geometries as a Strategy for Selective Heterogeneous Hydrogenations. **Science**, v. 335, n. 6073, p. 1209–1212, 9 mar. 2012.

LI, G. et al. Experimental and Mechanistic Understanding of Aldehyde Hydrogenation Using Au₂₅ Nanoclusters with Lewis Acids: Unique Sites for Catalytic Reactions. **Journal of the American Chemical Society**, v. 137, n. 45, p. 14295–14304, 18 nov. 2015.

LI, G.; JIN, R. Gold Nanocluster-Catalyzed Semihydrogenation: A Unique Activation Pathway for Terminal Alkynes. **Journal of the American Chemical Society**, v. 136, n. 32, p. 11347–11354, 13 ago. 2014.

LIU, W. et al. Single-atom dispersed Co–N–C catalyst: structure identification and performance for hydrogenative coupling of nitroarenes. **Chemical Science**, v. 7, n. 9, p. 5758–5764, 2016.

LIU, W. et al. Discriminating Catalytically Active Fe–N–C Species of Atomically Dispersed Fe–N–C Catalyst for Selective Oxidation of the C–H Bond. **Journal of the American Chemical Society**, v. 139, n. 31, p. 10790–10798, 9 ago. 2017.

LÓPEZ, N.; VARGAS-FUENTES, C. Promoters in the hydrogenation of alkynes in mixtures: insights from density functional theory. **Chem. Commun.**, v. 48, n. 10, p. 1379–1391, 2012.

LU, G. et al. Gold catalyzed hydrogenations of small imines and nitriles: enhanced reactivity of Au surface toward H₂ via collaboration with a Lewis base. **Chem. Sci.**, v. 5, n. 3, p. 1082–1090, 2014.

MAKOV, G.; PAYNE, M. C. Periodic boundary conditions in ab initio calculations. **Physical Review B**, v. 51, n. 7, p. 4014–4022, 15 fev. 1995.

MITSUDOME, T. et al. One-step Synthesis of Core-Gold/Shell-Ceria Nanomaterial and Its Catalysis for Highly Selective Semihydrogenation of Alkynes. **Journal of the American Chemical Society**, v. 137, n. 42, p. 13452–13455, 28 out. 2015.

- MITSUDOME, T.; KANEDA, K. Gold nanoparticle catalysts for selective hydrogenations. **Green Chemistry**, v. 15, n. 10, p. 2636, 2013.
- MONKHORST, H. J.; PACK, J. D. Special points for Brillouin-zone integrations. **Physical Review B**, v. 13, n. 12, p. 5188–5192, 15 jun. 1976.
- NOUJIMA, A. et al. Selective Deoxygenation of Epoxides to Alkenes with Molecular Hydrogen Using a Hydrotalcite-Supported Gold Catalyst: A Concerted Effect between Gold Nanoparticles and Basic Sites on a Support. **Angewandte Chemie International Edition**, v. 50, n. 13, p. 2986–2989, 21 mar. 2011.
- NOUJIMA, A. et al. Unique catalysis of gold nanoparticles in the chemoselective hydrogenolysis with H₂: cooperative effect between small gold nanoparticles and a basic support. **Chemical Communications**, v. 48, n. 53, p. 6723, 2012.
- ORTUÑO, M. **Au-NC Collection home page**. Disponível em: <<https://iochem-bd.iciq.es/browse/handle/100/8776>>.
- PERDEW, J. P.; BURKE, K.; ERNZERHOF, M. Generalized Gradient Approximation Made Simple. **Physical Review Letters**, v. 77, n. 18, p. 3865–3868, 28 out. 1996.
- PISIEWICZ, S. et al. Synthesis of Nickel Nanoparticles with N-Doped Graphene Shells for Catalytic Reduction Reactions. **ChemCatChem**, v. 8, n. 1, p. 129–134, jan. 2016.
- REN, D. et al. An Unusual Chemoselective Hydrogenation of Quinoline Compounds Using Supported Gold Catalysts. **Journal of the American Chemical Society**, v. 134, n. 42, p. 17592–17598, 24 out. 2012.
- SEGURA, Y.; LÓPEZ, N.; PÉREZ-RAMÍREZ, J. Origin of the superior hydrogenation selectivity of gold nanoparticles in alkyne + alkene mixtures: Triple- versus double-bond activation. **Journal of Catalysis**, v. 247, n. 2, p. 383–386, 2007.
- SHELDON, R. A.; BEKKUM, H. VAN. **Fine Chemicals through Heterogeneous Catalysis**. [s.l.: s.n.].
- SHIMIZU, K. et al. Chemoselective Hydrogenation of Nitroaromatics by Supported Gold Catalysts: Mechanistic Reasons of Size- and Support-Dependent Activity and Selectivity. **The Journal of Physical Chemistry C**, v. 113, n. 41, p. 17803–17810, 15 out. 2009.
- STEPHAN, D. W. Frustrated Lewis pairs: From concept to catalysis. **Accounts of Chemical Research**, v. 48, n. 2, p. 306–316, 2015a.
- STEPHAN, D. W. Frustrated Lewis Pairs. **Journal of the American Chemical**

- Society**, v. 137, n. 32, p. 10018–10032, 19 ago. 2015b.
- STEPHAN, D. W. The broadening reach of frustrated Lewis pair chemistry. **Science**, v. 354, n. 6317, p. aaf7229–aaf7229, 9 dez. 2016.
- STRATAKIS, M.; GARCIA, H. Catalysis by Supported Gold Nanoparticles: Beyond Aerobic Oxidative Processes. **Chemical Reviews**, v. 112, n. 8, p. 4469–4506, 8 ago. 2012.
- SUN, X. et al. Designing graphene as a new frustrated Lewis pair catalyst for hydrogen activation by co-doping. **Phys. Chem. Chem. Phys.**, v. 18, n. 16, p. 11120–11124, 2016.
- SYOMIN, D. et al. Identification of Adsorbed Phenyl (C₆H₅) Groups on Metal Surfaces: Electron-Induced Dissociation of Benzene on Au(111). **The Journal of Physical Chemistry B**, v. 105, n. 35, p. 8387–8394, set. 2001.
- TAKALE, B. S. et al. Unsupported Nanoporous Gold Catalyst for Chemoselective Hydrogenation Reactions under Low Pressure: Effect of Residual Silver on the Reaction. **Journal of the American Chemical Society**, v. 138, n. 32, p. 10356–10364, 17 ago. 2016.
- TEJEDA-SERRANO, M. et al. Synthesis of Supported Planar Iron Oxide Nanoparticles and Their Chemo- and Stereoselectivity for Hydrogenation of Alkynes. **ACS Catalysis**, v. 7, n. 5, p. 3721–3729, 5 maio 2017.
- TESCHNER, D. et al. The Roles of Subsurface Carbon and Hydrogen in Palladium-Catalyzed Alkyne Hydrogenation. **Science**, v. 320, n. 5872, p. 86–89, 4 abr. 2008.
- TROTUŞ, I.-T.; ZIMMERMANN, T.; SCHÜTH, F. Catalytic Reactions of Acetylene: A Feedstock for the Chemical Industry Revisited. **Chemical Reviews**, v. 114, n. 3, p. 1761–1782, 12 fev. 2014.
- URAYAMA, T. et al. Green, Multi-Gram One-Step Synthesis of Core-Shell Nanocomposites in Water and Their Catalytic Application to Chemoselective Hydrogenations. **Chemistry - A European Journal**, v. 22, n. 50, p. 17962–17966, 12 dez. 2016.
- VILÉ, G. et al. A Stable Single-Site Palladium Catalyst for Hydrogenations. **Angewandte Chemie International Edition**, v. 54, n. 38, p. 11265–11269, 14 set. 2015.
- VILÉ, G. et al. Advances in the Design of Nanostructured Catalysts for Selective Hydrogenation. **ChemCatChem**, v. 8, n. 1, p. 21–33, jan. 2016.
- WANG, L. et al. Design and Preparation of Supported Au Catalyst with Enhanced Catalytic Activities by Rationally Positioning Au Nanoparticles on

Anatase. **The Journal of Physical Chemistry Letters**, v. 6, n. 12, p. 2345–2349, 18 jun. 2015.

WELCH, G. C. et al. Reversible, Metal-Free Hydrogen Activation. **Science**, v. 314, n. 5802, p. 1124–1126, 17 nov. 2006.

WESTERHAUS, F. A. et al. Heterogenized cobalt oxide catalysts for nitroarene reduction by pyrolysis of molecularly defined complexes. **Nature Chemistry**, v. 5, n. 6, p. 537–543, 12 maio 2013.

YAN, M. et al. Nanoporous gold catalyst for highly selective semihydrogenation of alkynes: remarkable effect of amine additives. **Journal of the American Chemical Society**, v. 134, n. 42, p. 17536–17542, 2012.

ZHAN, W. et al. A Sacrificial Coating Strategy Toward Enhancement of Metal–Support Interaction for Ultrastable Au Nanocatalysts. **Journal of the American Chemical Society**, v. 138, n. 49, p. 16130–16139, 14 dez. 2016.

ZHAN, W. et al. Surfactant-Assisted Stabilization of Au Colloids on Solids for Heterogeneous Catalysis. **Angewandte Chemie International Edition**, v. 56, n. 16, p. 4494–4498, 10 abr. 2017.

ZHANG, S. et al. Solid frustrated-Lewis-pair catalysts constructed by regulations on surface defects of porous nanorods of CeO₂. **Nature Communications**, v. 8, n. May, p. 15266, 18 maio 2017.

ZHAO, Y.; FU, G.; ZHENG, N. Shaping the selectivity in heterogeneous hydrogenation by using molecular modification strategies: Experiment and theory. **Catalysis Today**, v. 279, p. 36–44, jan. 2017.

7. GENERAL CONCLUSIONS

The interest in gold catalysis increased a lot after the pioneering studies by Haruta, Hutchings, Rossi and others, mainly due to the unique performance and extraordinary selectivity for oxidations compared to other noble metals. However, there are comparatively few studies on gold as hydrogenation catalyst, probably because it was anticipated a low activity compared to platinum group metals due to the unfavorable chemisorption of molecular hydrogen. We started our studies by showing that gold can be a highly active and selective hydrogenation catalyst due to a unique promotion effect of nitrogen-containing bases. The inactive gold nanoparticles supported on silica become highly active for the selective hydrogenation of alkyne into cis-alkenes using H₂ as the hydrogen source in the presence of nitrogen or phosphorus containing ligands. These ligands play a key role by opening a new channel for the heterolytic dissociation of molecular hydrogen by the formation of a frustrated Lewis pair. Theoretical calculations highlighted that molecular hydrogen dissociation occurs at the ligand-gold interface generating a tight-ion pair that can be selectively transferred to the adsorbed alkyne in a *syn*-fashion controlled by electrostatic interactions. The promotional effect by P and N-containing ligands may have implications for gold catalysis while stimulating more applications in the field of selective hydrogenations, while the versatile synthetic concept presented can be transferrable to trace back the properties of other metallic nanoparticles.

Regarding the effect of capping ligands on the catalytic activation of colloidal gold nanoparticles by frustrated Lewis pair methodology, our studies demonstrated that the presence of an organic moiety adsorbed at the metal nanoparticle surface (nanoparticles prepared with different stabilizers) influences the amine ligand-to-metal key interactions during the formation of the FLP interface, therefore, the capping ligands cannot be simply ignored. Once the FLPs can be formed, the catalytic system enables the highly selective semihydrogenation of various alkynes mild reaction conditions.

Even though the ligands play a key role by opening a new channel for the heterolytic dissociation of molecular hydrogen, application in large scale was limited by the high amount of amine needed plus product purification step. The development of a gold catalyst embedded in a nitrogen carbon-doped structure catalyst was performed for the selective hydrogenation of alkynes, where the system is based on an easy graphitization process that renders the labile ligand into a capping shell bound to the nanoparticle. As ligands employed can be relatively simple, the pyrolysis ensures the presence of active N centers that allows the selective and robust chemistry. The main advantage with respect to our previous study is to avoid the addition of external ligands, in large excess, for the activation of gold surfaces via FLP, making the whole process environmentally and economically attractive. Besides, the main reason to investigate gold, when compared to the most commonly used transition metals, is the intrinsically high selectivity in the alkyne to alkene conversion and the tolerance to many functional groups for reaction under mild conditions.

8. PERSPECTIVES

The concept of FLP can certainly be used and an attempt to activate and improve catalytic activity of other metals with poor activity in hydrogenation reactions, such as copper and silver-based catalysts, and should be a key focus for future investigations. By combining metallic nanoparticles of these metals with ligands, a significant increased catalytic activity might be achieved. It should be emphasized that studies to date have focused almost exclusively on gold catalysts. Alongside investigation of the application of the developed catalytic systems in challenging hydrogenation reaction may be achievable, making possible the selective hydrogenation of nitriles, ketones, aldehydes, sulfones, etc. An enormous scope for development of doped carbon materials either with nitrogen, boron or phosphorus remains. This strategy might result in the successful development of catalysts with tuned activity when compared to non-doped carbon materials. Furthermore, introducing dopant atoms in a carbon matrix may also affect the size and electronic properties of the catalysts, allowing the synthesis of single metal atom catalyst thus leading to materials with superior activity in a wide plethora of reactions. Moreover, systematic investigation to clarify and maybe identify the active site architecture in order to choose the most appropriate synthesis/treatment route, which could furnish the catalyst with full selectivity towards one specific product, would lead to the ultimate development of industrially important target product.

APPENDICES

Appendice A1. Permissions

Permissions ACS Catalysis

Chapter 1:



RightsLink®



Home



Help



Email Support



Jhonatan Florio



Gold-Ligand-Catalyzed Selective Hydrogenation of Alkynes into cis-Alkenes via H₂ Heterolytic Activation by Frustrated Lewis Pairs

Author: Jhonatan L. Florio, Núria López, Liane M. Rössi

Publication: ACS Catalysis

Publisher: American Chemical Society

Date: Apr 1, 2017

Copyright © 2017, American Chemical Society

PERMISSION/LICENSE IS GRANTED FOR YOUR ORDER AT NO CHARGE

This type of permission/license, instead of the standard Terms & Conditions, is sent to you because no fee is being charged for your order. Please note the following:

- Permission is granted for your request in both print and electronic formats, and translations.
- If figures and/or tables were requested, they may be adapted or used in part.
- Please print this page for your records and send a copy of it to your publisher/graduate school.
- Appropriate credit for the requested material should be given as follows: "Reprinted (adapted) with permission from (COMPLETE REFERENCE CITATION). Copyright (YEAR) American Chemical Society." Insert appropriate information in place of the capitalized words.
- One-time permission is granted only for the use specified in your request. No additional uses are granted (such as derivative works or other editions). For any other uses, please submit a new request.

[BACK](#)

[CLOSE WINDOW](#)

Chapter 4:



RightsLink®



Home



Help



Email Support



Jhonatan Florio ▾



Accessing Frustrated Lewis Pair Chemistry through Robust Gold@N-Doped Carbon for Selective Hydrogenation of Alkynes

Author: Jhonatan Luiz Florio, Renato Vitalino Gonçalves, Erico Teixeira-Neto, et al

Publication: ACS Catalysis

Publisher: American Chemical Society

Date: Apr 1, 2018

Copyright © 2018, American Chemical Society

PERMISSION/LICENSE IS GRANTED FOR YOUR ORDER AT NO CHARGE

This type of permission/license, instead of the standard Terms & Conditions, is sent to you because no fee is being charged for your order. Please note the following:

- Permission is granted for your request in both print and electronic formats, and translations.
- If figures and/or tables were requested, they may be adapted or used in part.
- Please print this page for your records and send a copy of it to your publisher/graduate school.
- Appropriate credit for the requested material should be given as follows: "Reprinted (adapted) with permission from (COMPLETE REFERENCE CITATION). Copyright (YEAR) American Chemical Society." Insert appropriate information in place of the capitalized words.
- One-time permission is granted only for the use specified in your request. No additional uses are granted (such as derivative works or other editions). For any other uses, please submit a new request.

[BACK](#)

[CLOSE WINDOW](#)

Letter of the editor (ACS Catal.):

De: **Jones, Christopher W** <christopher.jones@chbe.gatech.edu> 
Assunto: RE: Reuse/Republication of the Entire Work in Theses
Data: 20 de fevereiro de 2020 05:14
Para: Liane Marcia Rossi <lrossi@iq.usp.br>
Cc: Williams, Rhea <R_Williams@acs.org>



Liane-

Permission to use these chapters in the thesis is granted.

The Word version or "just-accepted manuscript" (JAM) can be used in the university repository, but not the galley proof PDF version.

The tentative citation format will be OK: "Accepted version of article reproduced with permission from [FULL REFERENCE CITATION]. Copyright [YEAR] American Chemical Society."

Thanks.
Chris

From: Liane Marcia Rossi <lrossi@iq.usp.br>
Sent: Tuesday, February 18, 2020 4:07 PM
To: Jones, Christopher W <christopher.jones@chbe.gatech.edu>
Cc: Jhonatan Luiz Fiorio <jhonatan@iq.usp.br>
Subject: Reuse/Republication of the Entire Work in Theses

Dear Prof. C. W. Jones,

We would like to ask permission to use the Post-print versions of the following papers on the Thesis of the first-author Jhonatan L. Fiorio:

Fiorio, J. L.; López, N.; Rossi, L. M. Gold–Ligand-Catalyzed Selective Hydrogenation of Alkynes into cis-Alkenes via H₂ Heterolytic Activation by Frustrated Lewis Pairs. **ACS Catalysis**, 2017, 7, 2973 - 2980.

Fiorio, J. L.; Gonçalves, R. V.; Neto-Teixeira, E.; Ortuño, M. A.; López, N.; Rossi, L. M. Accessing Frustrated Lewis Pair Chemistry through Robust Gold@N-Doped Carbon for Selective Hydrogenation of Alkynes. **ACS Catalysis**, 2018, 8, 3516–3524.

We already obtained the permission via RightsLink, but since the Thesis will be send to the university repository, which is mandatory for us, we do need you additional consent (the author should secure written confirmation (via letter or email) from the respective ACS journal editor(s) to avoid potential conflicts with journal prior publication*/embargo policies).

According the the publisher policy (consulted in Sherpa Romeo - attached file), we understood that we cannot use the final PDF, but the Pre-print or Post-print (embargo 12 month) version can be used in the Thesis, which will be archived in the university repository. Can you please confirm this information?

Can you also instruct us on the correct sentence to be added in the beginning of the chapter. Should be like this: "Post-print version reproduced with permission from [FULL REFERENCE CITATION.] Copyright [YEAR] American Chemical Society." ?

Many thanks for your time and help.

Best regards,



Liane M. Rossi
Laboratório de Nanomateriais e Catálise
Instituto de Química
Universidade de São Paulo
Av. Prof. Lineu Prestes 748 sl. 1265
05508-000 São Paulo SP Brasil
Tel. + 55 11 30919143 (office)
+55 11 30912181 (lab)
<http://www.lianerossi.org>

Permission RSC:

Chapter 2:



Marketplace™

Order Number: 1009709

Order Date: 18 Dec 2019

Payment Information

Jhonatan Florio
jhonatham15@hotmail.com
Payment method: Invoice

Billing Address:
Mr. Jhonatan Florio
Sebnitzer Str. 35
Dresden, Saxony 01099
Germany

+49 15171318877
jhonatham15@hotmail.com

Customer Location:
Mr. Jhonatan Florio
Sebnitzer Str. 35
Dresden, Saxony 01099
Germany

Order Details

1. Catalysis Science & Technology

Billing Status:
Open

Order license ID	1009709-1
Order detail status	Completed
ISSN	2044-4761
Type of use	Republish in a thesis/dissertation
Publisher	Royal Society of Chemistry
Portion	Chapter/article

0.00 USD

LICENSED CONTENT

Publication Title	Catalysis Science & Technology	Country	United Kingdom of Great Britain and Northern Ireland
Author/Editor	Royal Society of Chemistry (Great Britain)	Rightholder	Royal Society of Chemistry
Date	01/01/2011	Publication Type	e-Journal
Language	English		

REQUEST DETAILS

Portion Type	Chapter/article	Rights Requested	Main product
Page range(s)	1-8	Distribution	Worldwide
Total number of pages	8	Translation	Original language of publication
Format (select all that apply)	Electronic	Copies for the disabled?	No
Who will republish the content?	Publisher, not-for-profit	Minor editing privileges?	Yes
Duration of Use	Current edition and up to 5 years	Incidental promotional use?	No
Lifetime Unit Quantity	Up to 999		

Currency USD

NEW WORK DETAILS

Title Catalysis at gold-ligand interfaces: a frustrated Lewis pair mechanism for selective reduction reactions

Institution name IQ-USP

Expected presentation date 2019-12-13

Instructor name Liane M. Rossi

ADDITIONAL DETAILS

The requesting person / organization to appear on the license Jhonatan Luiz Florio

REUSE CONTENT DETAILS

Title, description or numeric reference of the portion(s)	Influence of capping ligands on the formation of surface-frustrated Lewis pairs at gold-ligand interfaces	Title of the article/chapter the portion is from	Catalysis at gold-ligand interfaces: a frustrated Lewis pair mechanism for selective reduction reactions
Editor of portion(s)	N/A	Author of portion(s)	Royal Society of Chemistry (Great Britain)
Volume of serial or monograph	N/A	Publication date of portion	2020-01-13
Page or page range of portion	73-98		

Royal Society of Chemistry Special Terms

The Royal Society of Chemistry hereby grants permission for the use of the material specified below in your thesis. Please note that if the material specified below or any part of it appears with credit or acknowledgement to a third party then you must also secure permission from that third party before reproducing that material. Please ensure that the published article carries a credit to The Royal Society of Chemistry in the following format: [Original citation] – Reproduced by permission of The Royal Society of Chemistry and that any electronic version of the work includes a hyperlink to the article on the Royal Society of Chemistry website.

Total Items: 1

Subtotal: 0.00 USD

Order Total: 0.00 USD

Letter of the editor RSC



Customer Sales Support
Thomas Graham House
Science Park, Milton Road
Cambridge CB4 0WF, UK

Tel +44 (0) 1223 420066

Email contracts-copyright@rsc.org

www.rsc.org

Professor Liane M. Rossi
Laboratório de Nanomateriais e Catálise
Instituto de Química
Universidade de São Paulo
Av. Prof. Lineu Prestes 748 sl. 1265
05508-000 São Paulo SP
Brasil

21 February 2020

Dear Professor Rossi

Re: Piperazine-promoted gold-catalyzed hydrogenations: the influence of capping ligands,

Catal. Sci. Technol., 2020, **10**(7), DOI: 10.1039/C9CY02016K

The Royal Society of Chemistry (RSC) hereby grants permission for the use of your paper specified above in the printed and microfilm version of your thesis. You may also make available the paper in the following ways: in your thesis via any website that your university may have for the deposition of theses, via your university's Intranet or via your own personal website. You may include the preprint of the article in your institutional, however we are unable to grant you permission to include the final PDF version of the paper on its own in your institutional repository. The Royal Society of Chemistry is a signatory to the STM Guidelines on Permissions (available on request).

Please note that if the material specified below or any part of it appears with credit or acknowledgement to a third party then you must also secure permission from that third party before reproducing that material.

Please ensure that the thesis includes the correct acknowledgement (see <http://rsc.li/permissions> for details) and a link is included to the paper on the Royal Society of Chemistry's website.

Please also ensure that your co-authors are aware that you are including the paper in your thesis.

Yours sincerely

A handwritten signature in black ink that reads 'Gill Cockhead'.

Gill Cockhead
Contracts & Copyright Executive

Co-authors permission of use



Jhonatan Luiz Fiorio <jhonatan@iq.usp.br>

Fwd: CY-ART-10-2019-002016.R1

hashmi@hashmi.de <hashmi@hashmi.de>
Para: Jhonatan Luiz Fiorio <jhonatan@iq.usp.br>

24 de fevereiro de 2020 17:38

Dear Jhonatan,

Yes, I confirm my consent.
The use of the data from our common paper Catal. Sci. Technol. 2020 is perfectly OK for me.

With kind regards,
Stephen

Zitat von Jhonatan Luiz Fiorio <jhonatan@iq.usp.br>:
[Texto das mensagens anteriores oculto]



Jhonatan Luiz Fiorio <jhonatan@iq.usp.br>

Fwd: CY-ART-10-2019-002016.R1

Camargo, Pedro H C <pedro.camargo@helsinki.fi>
Para: Jhonatan Luiz Fiorio <jhonatan@iq.usp.br>

24 de fevereiro de 2020 17:32

I confirm my consent.

Pedro

From: Jhonatan Luiz Fiorio <jhonatan@iq.usp.br>
Sent: Monday, February 24, 2020 6:30:56 PM
To: Camargo, Pedro H C <pedro.camargo@helsinki.fi>; hashmi@hashmi.de <hashmi@hashmi.de>; matthiasrudolph@oci.uni-heidelberg.de <matthiasrudolph@oci.uni-heidelberg.de>; Eduardo Cesar Melo Barbosa <eduardocmbarbosa07@gmail.com>; Jhon Quiroz <jhonquiroz@gmail.com>
Cc: Liane Marcia Rossi <lrossi@iq.usp.br>
Subject: Fwd: CY-ART-10-2019-002016.R1

[Texto das mensagens anteriores oculto]



Jhonatan Luiz Fiorio <jhonatan@iq.usp.br>

Fwd: CY-ART-10-2019-002016.R1

Eduardo Barbosa <eduardocmbarbosa07@gmail.com>
Para: Jhonatan Luiz Fiorio <jhonatan@iq.usp.br>

25 de fevereiro de 2020 10:46

Dear Jhonatan,

Congratulations on your successful defense,

I grant you permission to use the data published on our paper published on Catalysis Science and Technology towards your thesis.

Best wishes,

Eduardo Barbosa
[Texto das mensagens anteriores oculto]

--

Fwd: CY-ART-10-2019-002016.R1

Danielle Kimie <danielle.kimie@gmail.com>
Para: Jhonatan Luiz Fiorio <jhonatan@iq.usp.br>

25 de fevereiro de 2020 15:15

Dear Jhonatan,

I agree.

Best regards,

Danielle

[Texto das mensagens anteriores oculto]

Fwd: CY-ART-10-2019-002016.R1

Rudolph, Dr. Matthias <matthiasrudolph@oci.uni-heidelberg.de>
Para: Jhonatan Luiz Fiorio <jhonatan@iq.usp.br>

26 de fevereiro de 2020 09:17

Hi Jhonatan,

I confirm that you can use the data no Problem for me.

Greetings Matthias

Von: Jhonatan Luiz Fiorio [jhonatan@iq.usp.br]

Gesendet: Montag, 24. Februar 2020 17:30

An: pedro.camargo@helsinki.fi; hashmi@hashmi.de; Rudolph, Dr. Matthias; Eduardo Cesar Melo Barbosa; Jhon Quiroz

Cc: Liane Marcia Rossi

Betreff: Fwd: CY-ART-10-2019-002016.R1

Dear all,

First, I am grateful for having had the opportunity to work/collaborate with you all!

Last December it happened my PhD defense, and fortunately, I was approved. To submit the PhD thesis to the repository, since I used the data of our paper (Catal. Sci. Technol., 2020), I need the approval of all the authors (see editor's email below for more information). Could you please send me an email confirming your consent?

Best regards,

Jhonatan

----- Mensagem encaminhada -----

De: catalysis (shared) <catalysis@rsc.org<<mailto:catalysis@rsc.org>>>

Data: qua, 19 de fev de 2020 às 07:33

Assunto: RE: CY-ART-10-2019-002016.R1

Para: Liane Marcia Rossi <lrossi@iq.usp.br<<mailto:lrossi@iq.usp.br>>>

[Texto das mensagens anteriores oculto]

Appendice A2. NMR

Additional characterizations of the products

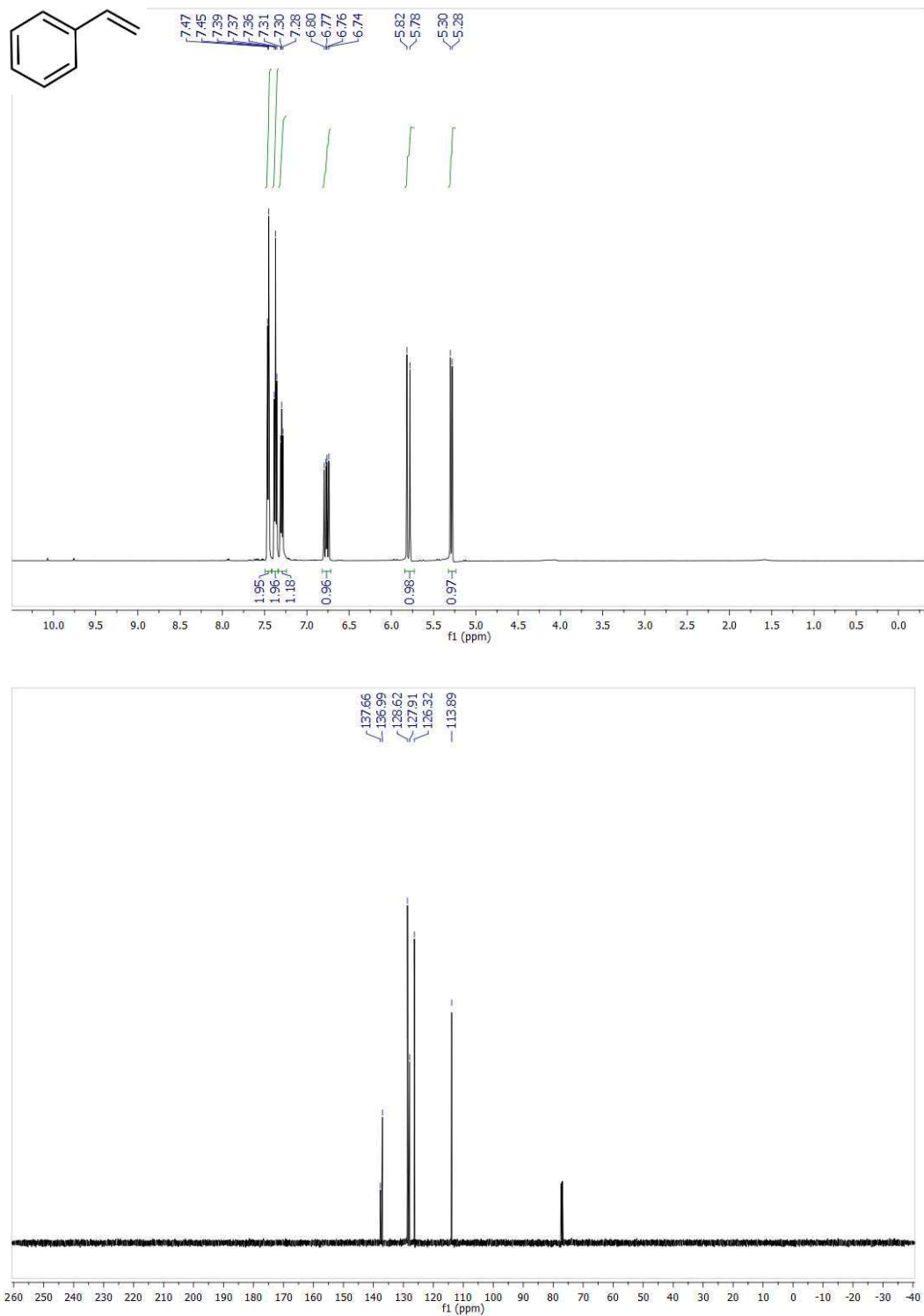


Figure S1. ^1H and ^{13}C NMR Spectrum of 2a

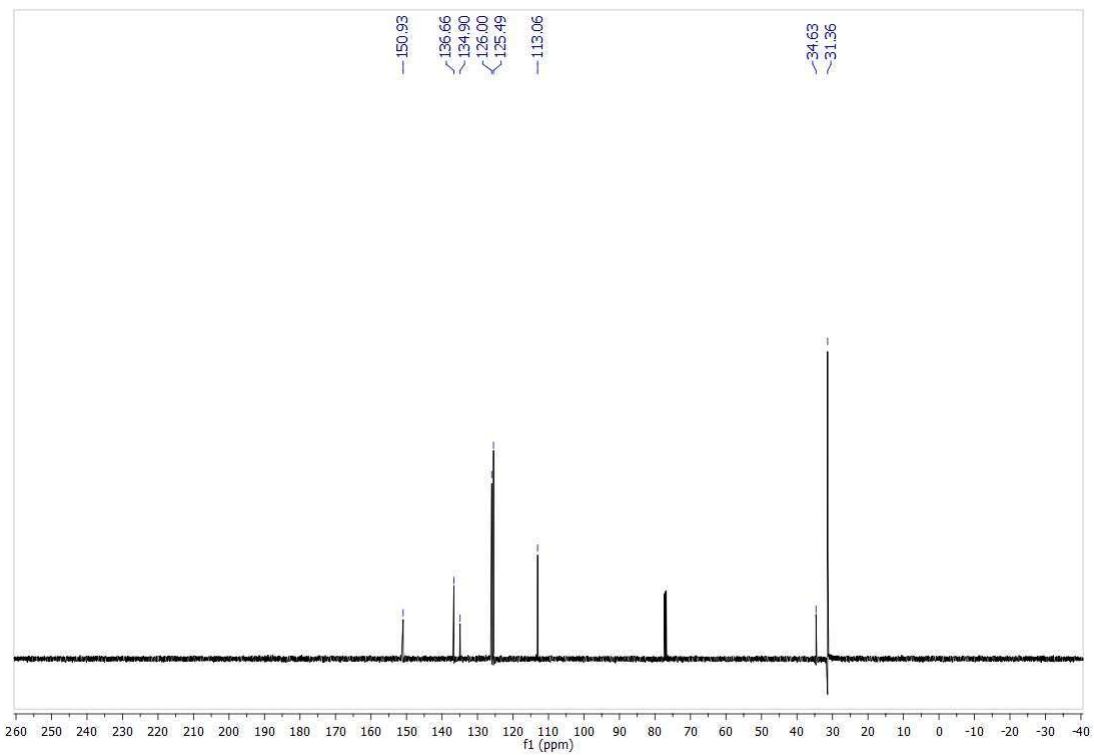
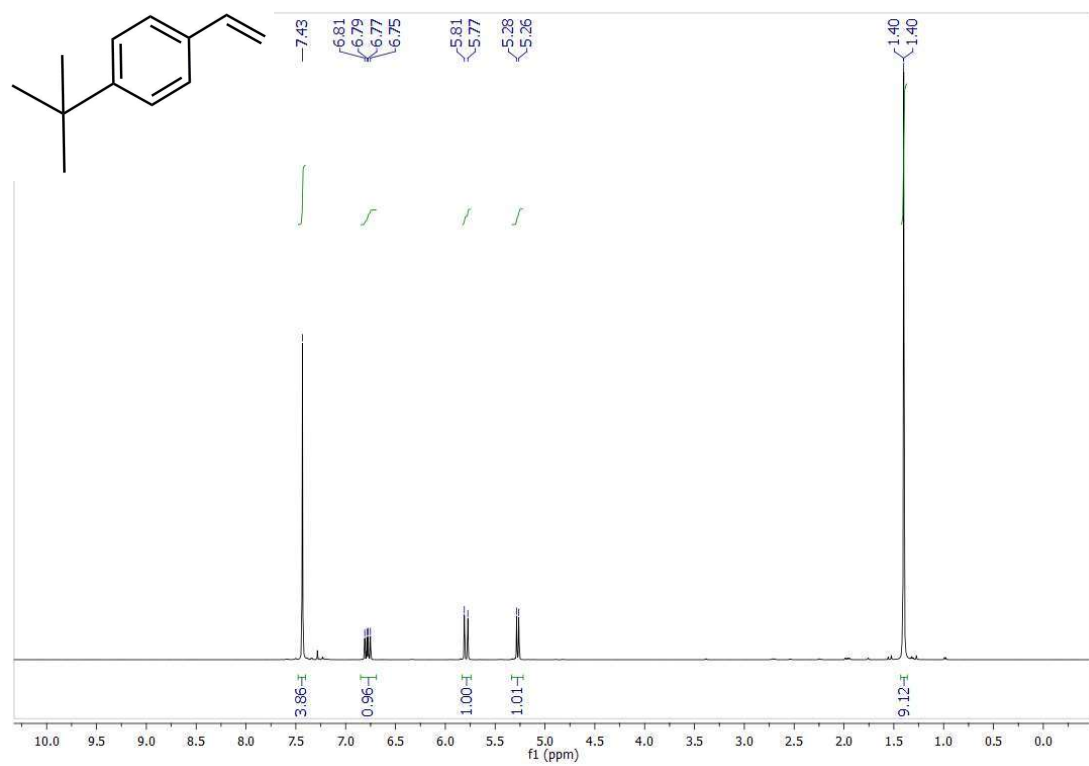


Figure S2. ¹H and ¹³C NMR Spectrum of **2b**

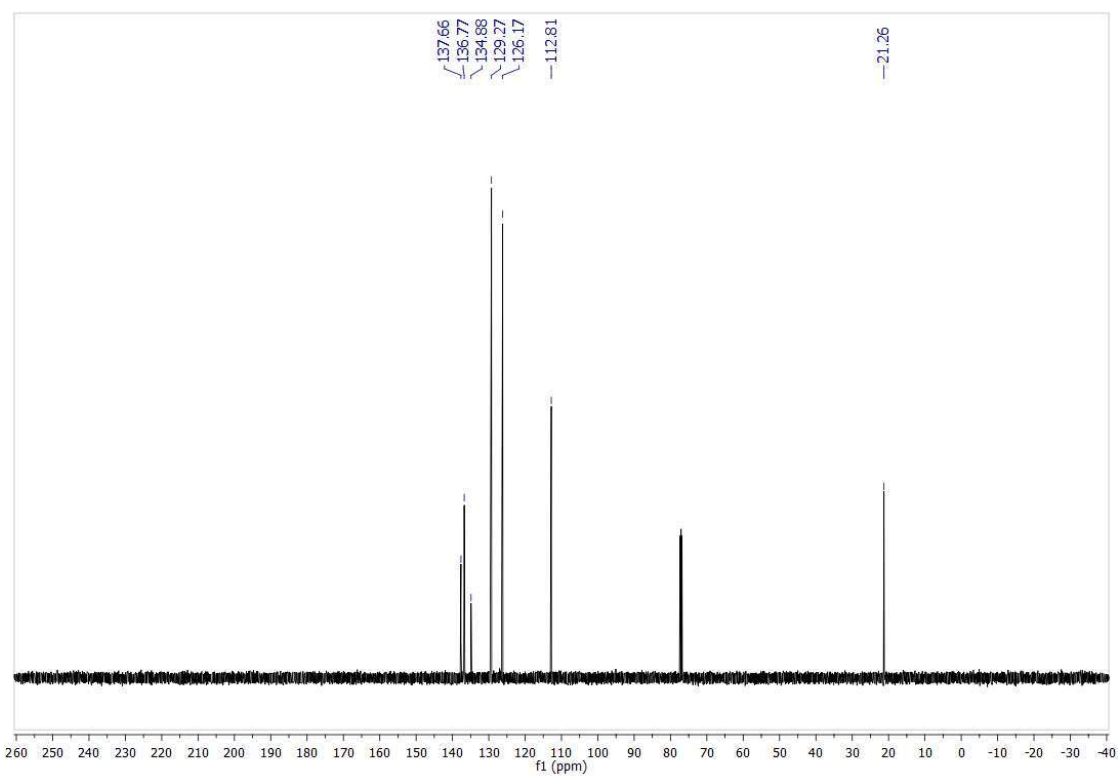
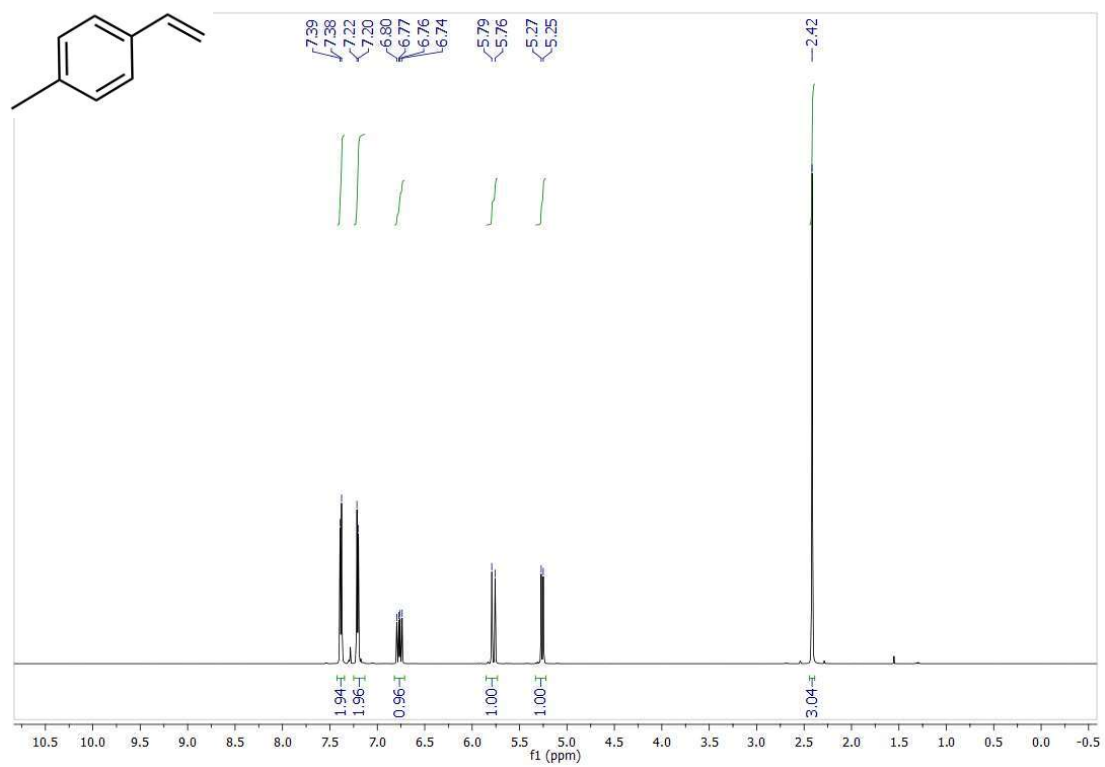


Figure S3. ¹H and ¹³C NMR Spectrum of 2c

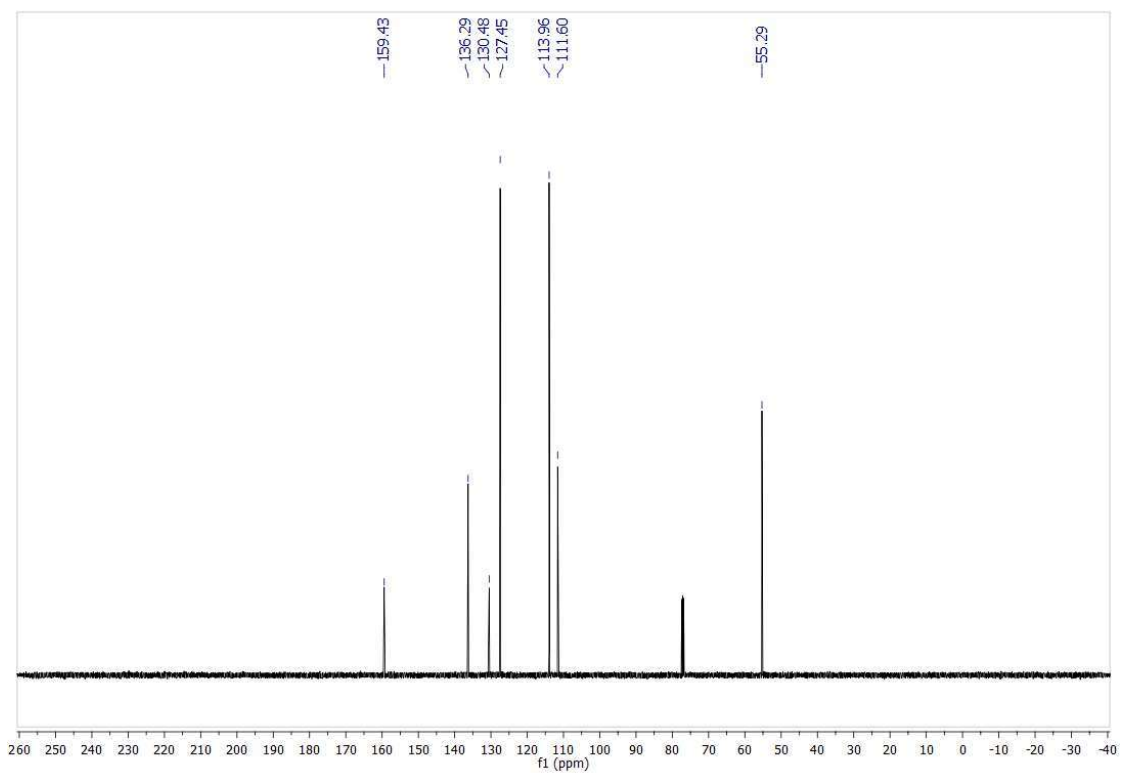
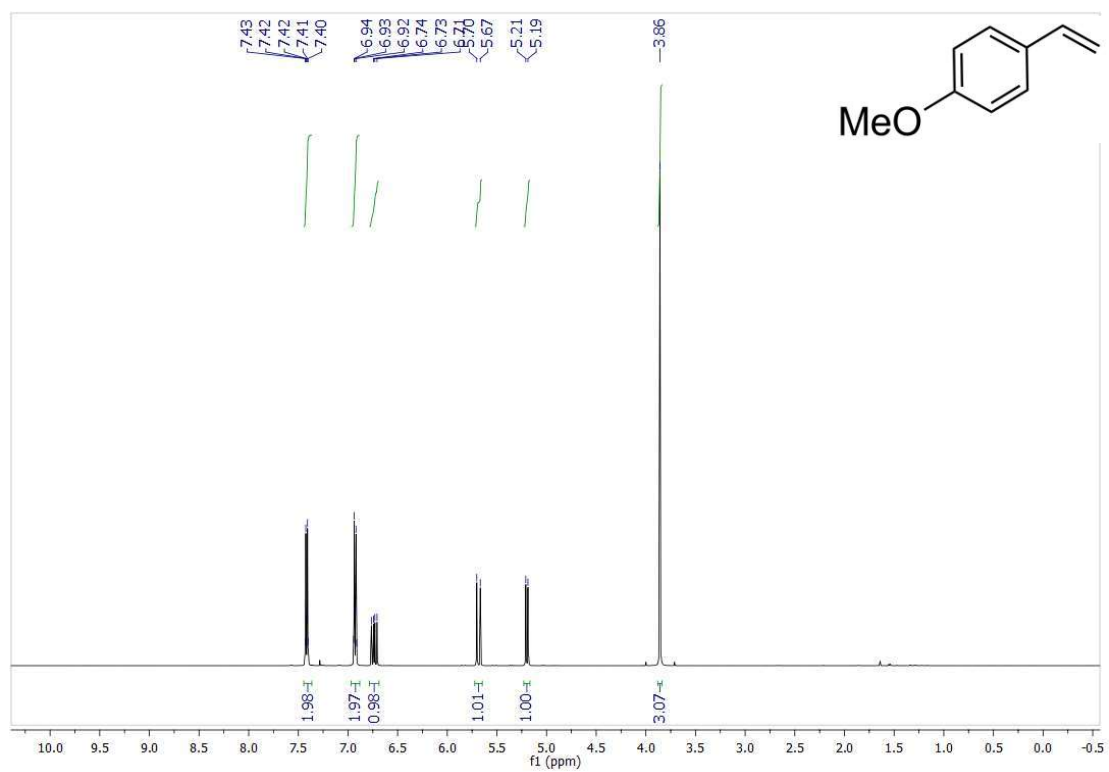


Figure S4. ^1H and ^{13}C NMR Spectrum of 2d

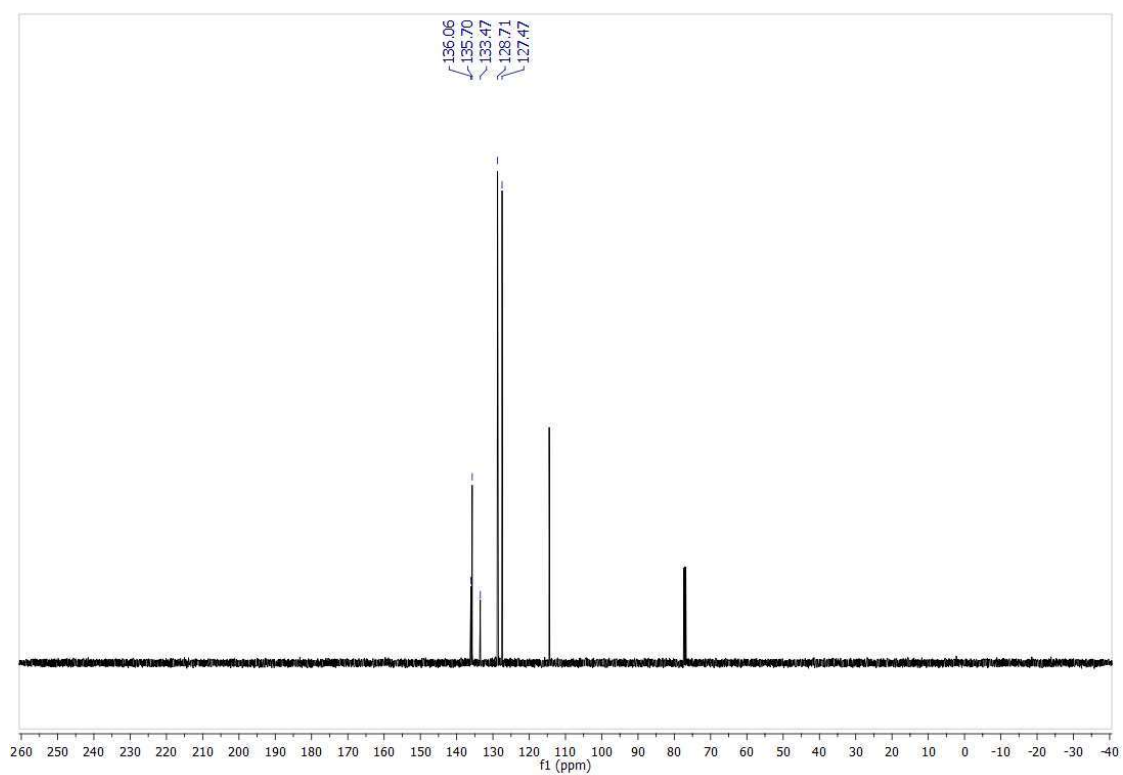
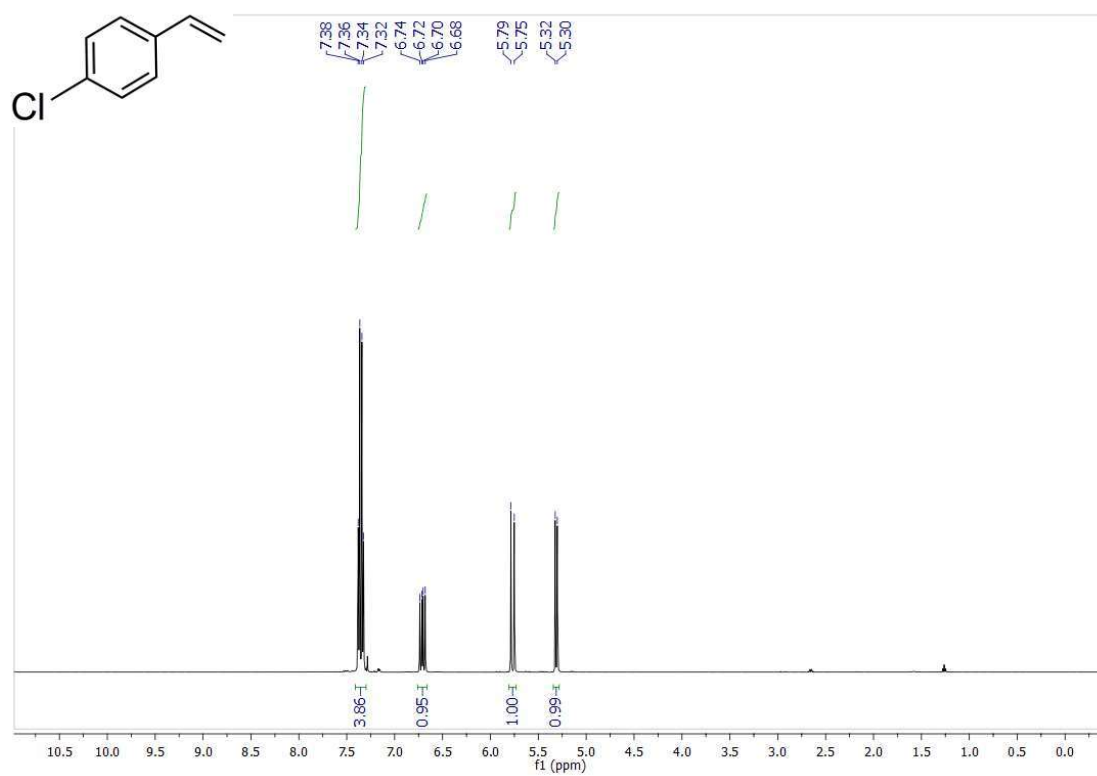


Figure S5. ¹H and ¹³C NMR Spectrum of 2f

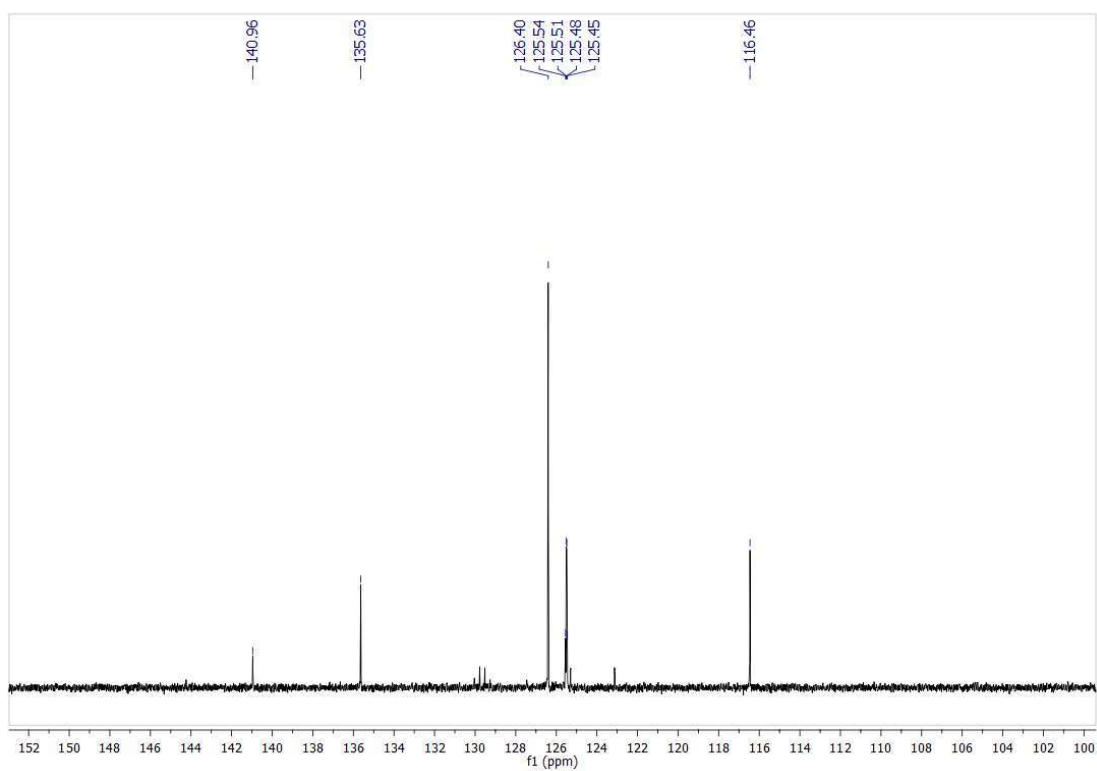
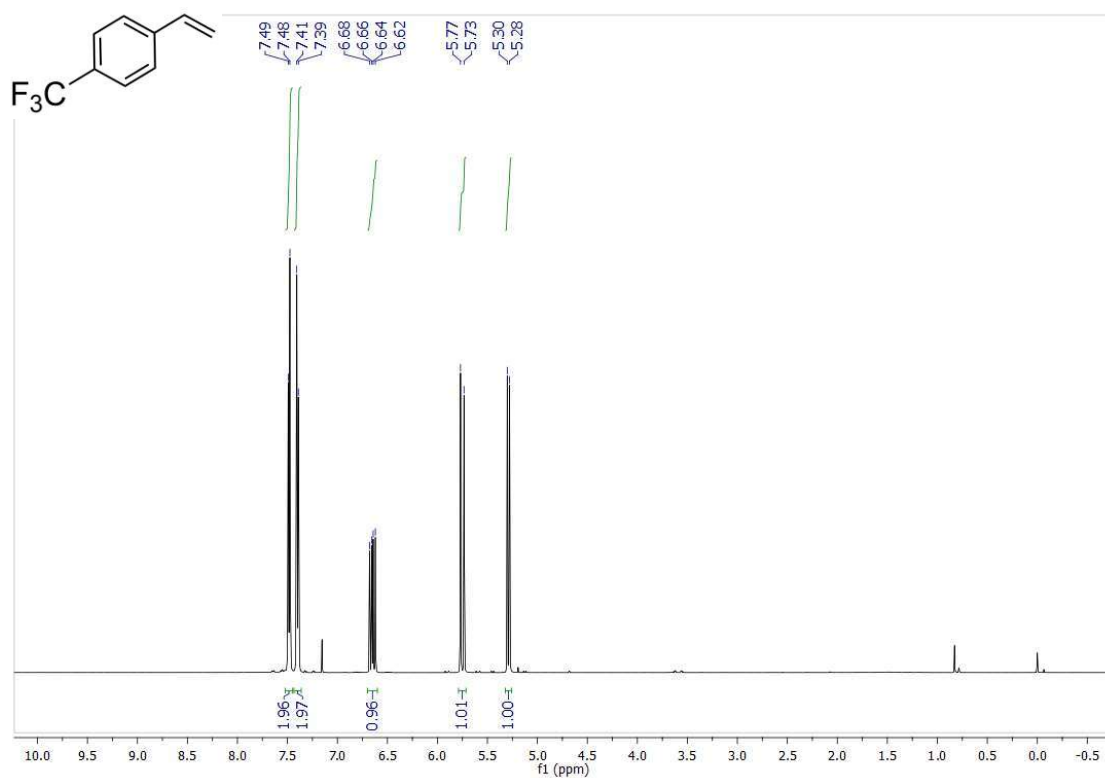


Figure S6. ¹H and ¹³C NMR Spectrum of 2h

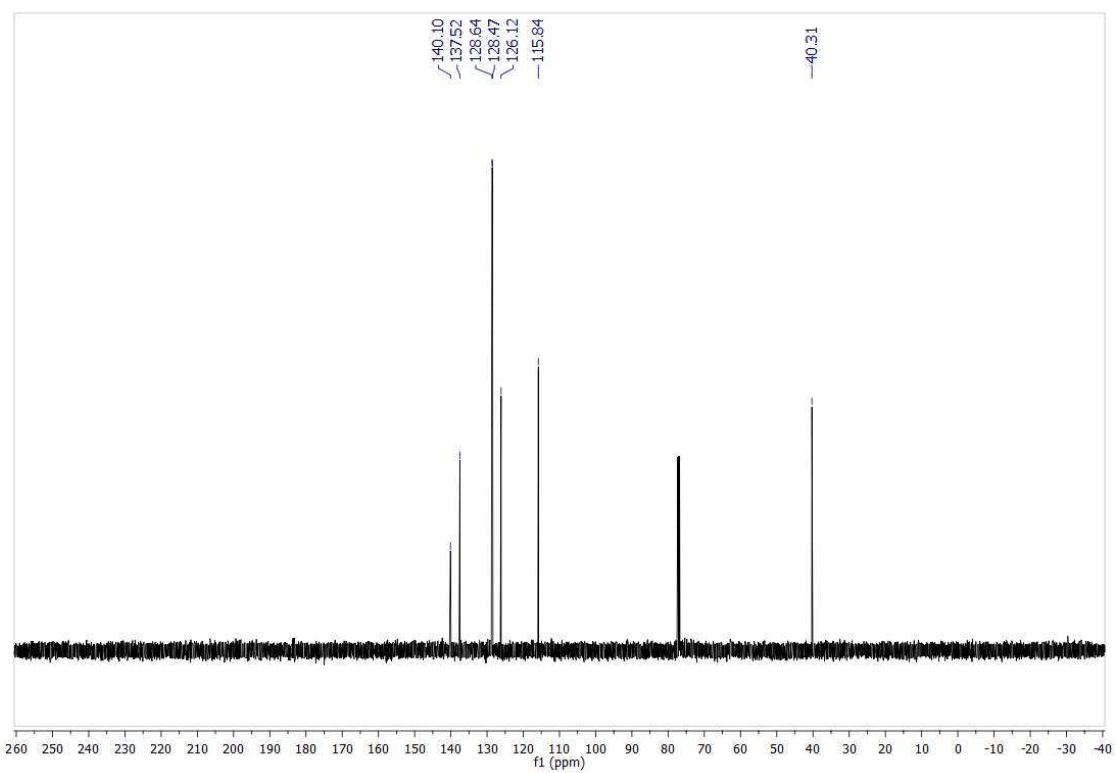
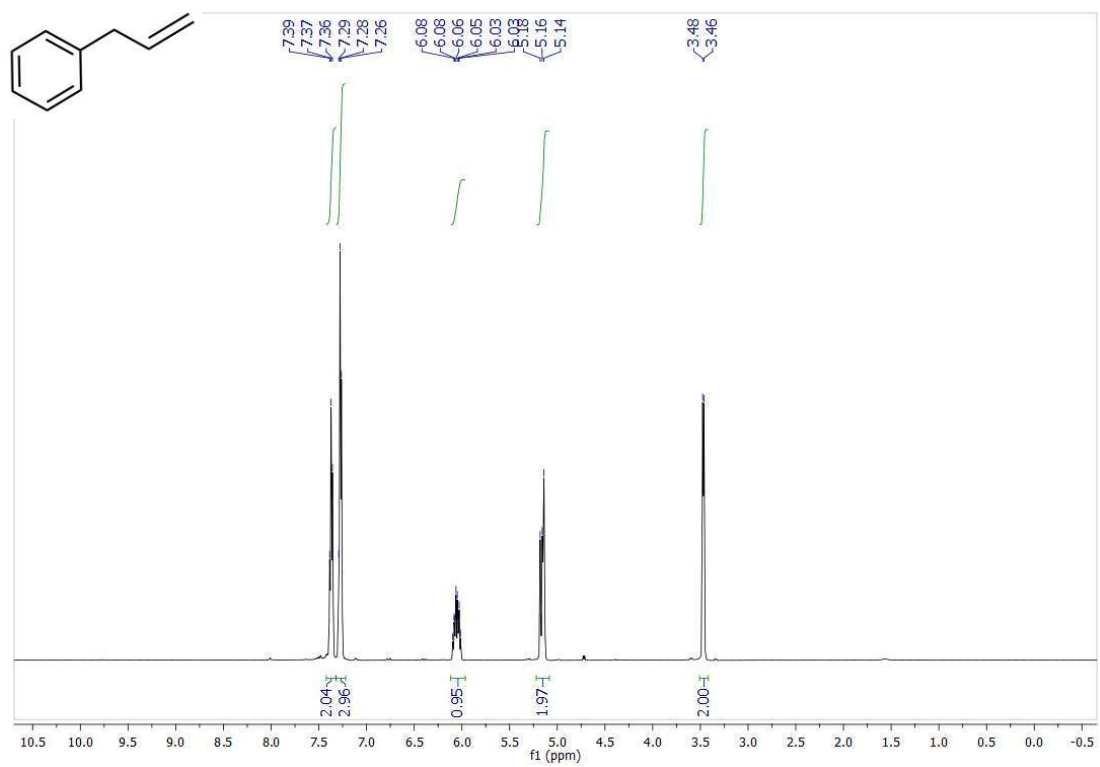


Figure S7. ¹H and ¹³C NMR Spectrum of 2i

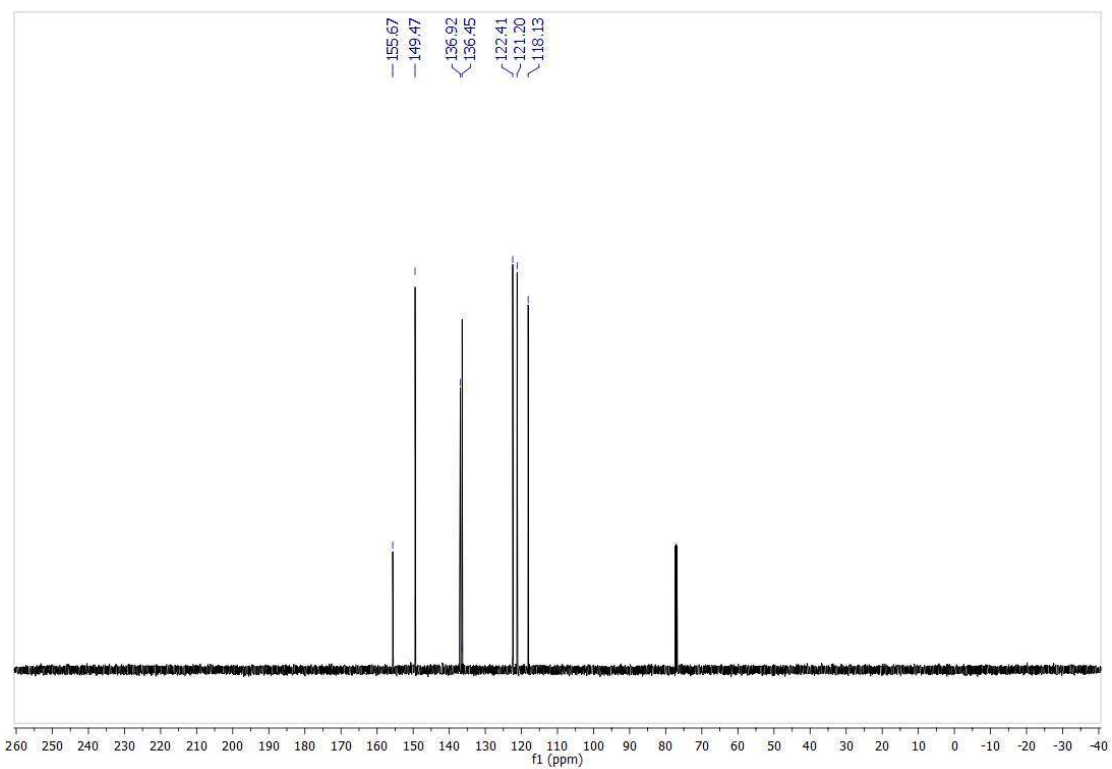
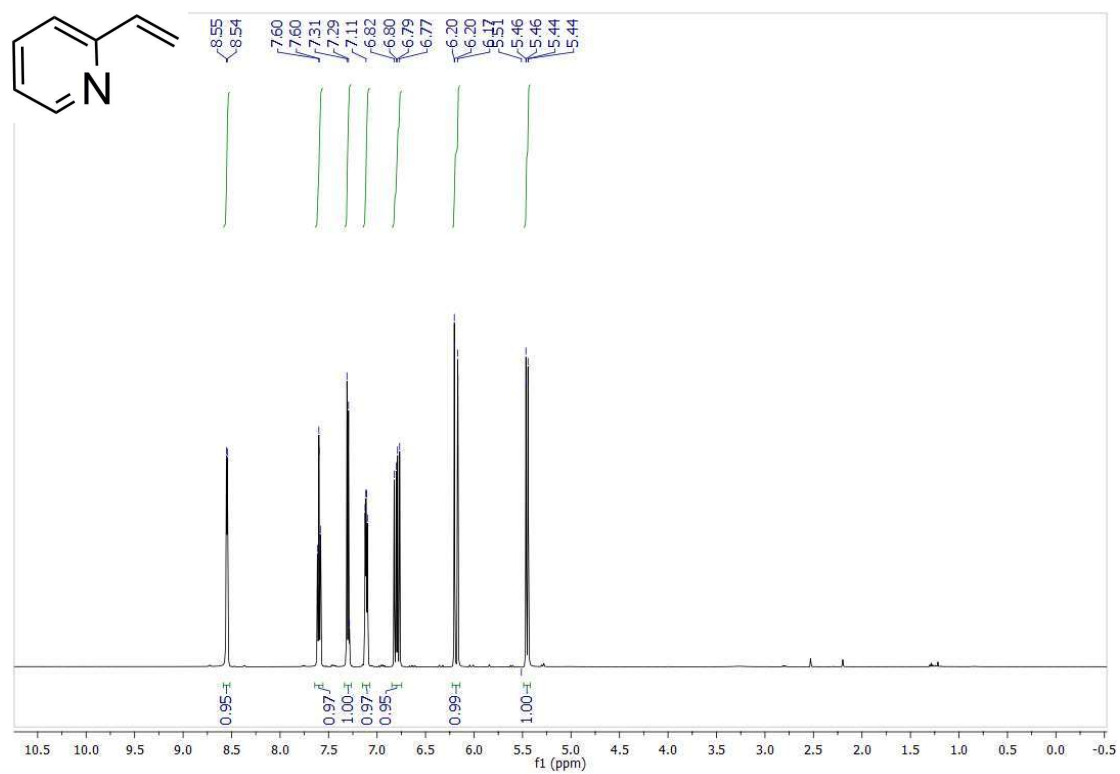


Figure S8. ^1H and ^{13}C NMR Spectrum of 2k

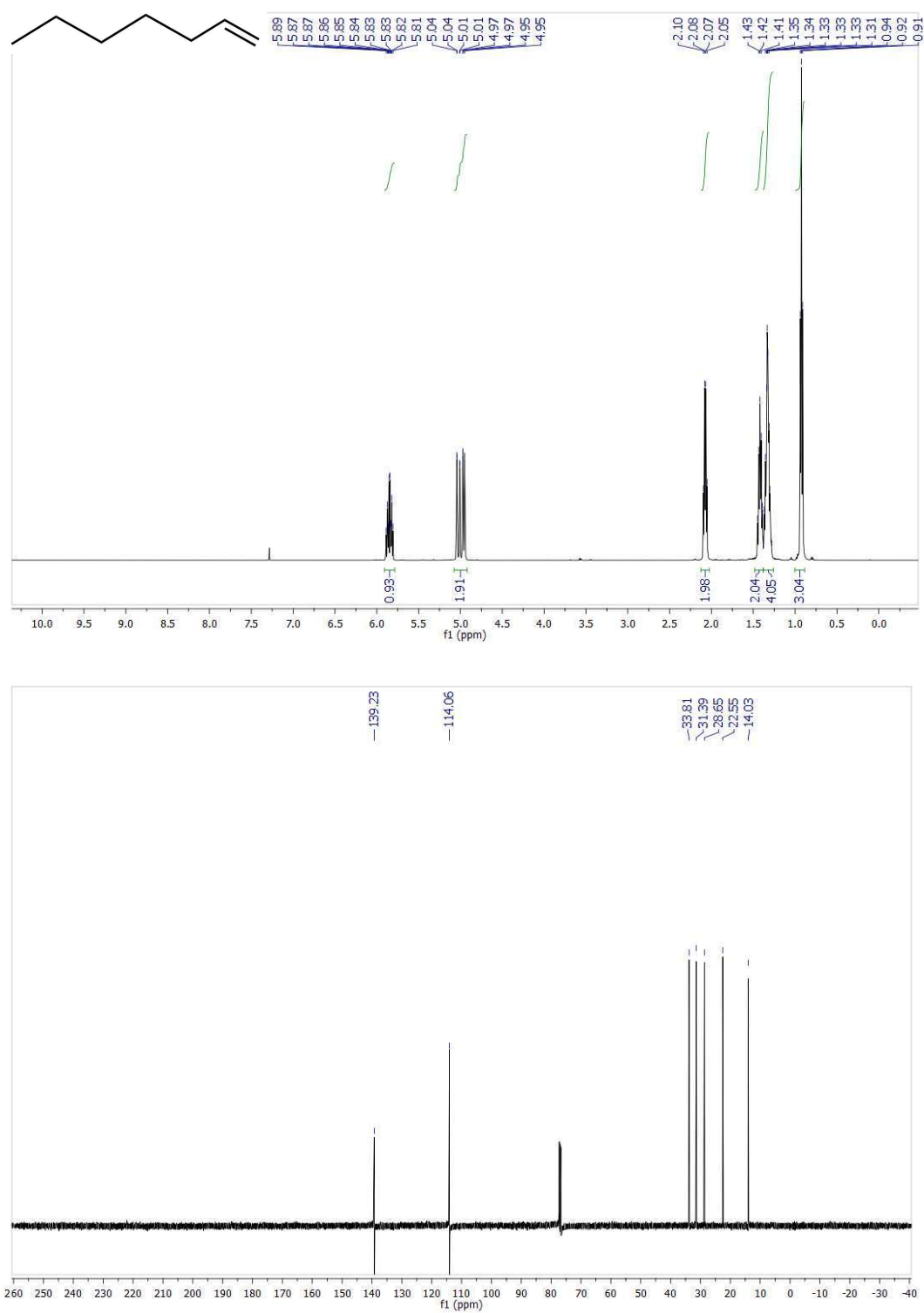


Figure S9. ¹H and ¹³C NMR Spectrum of 2r

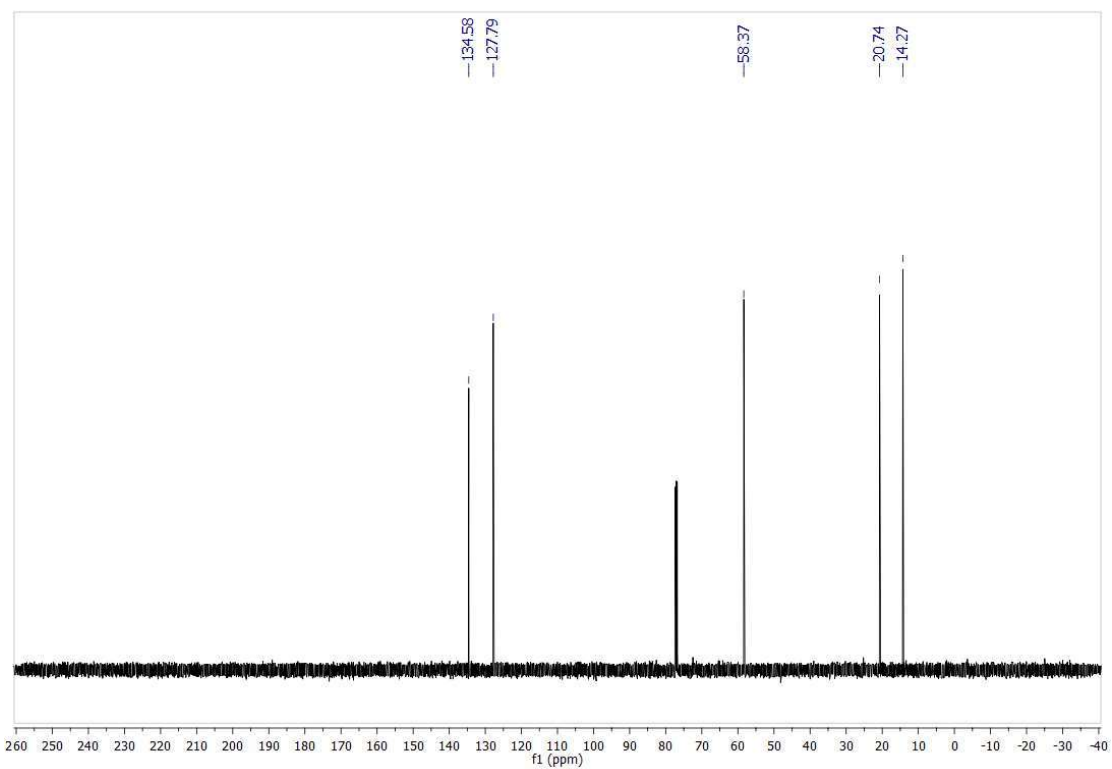
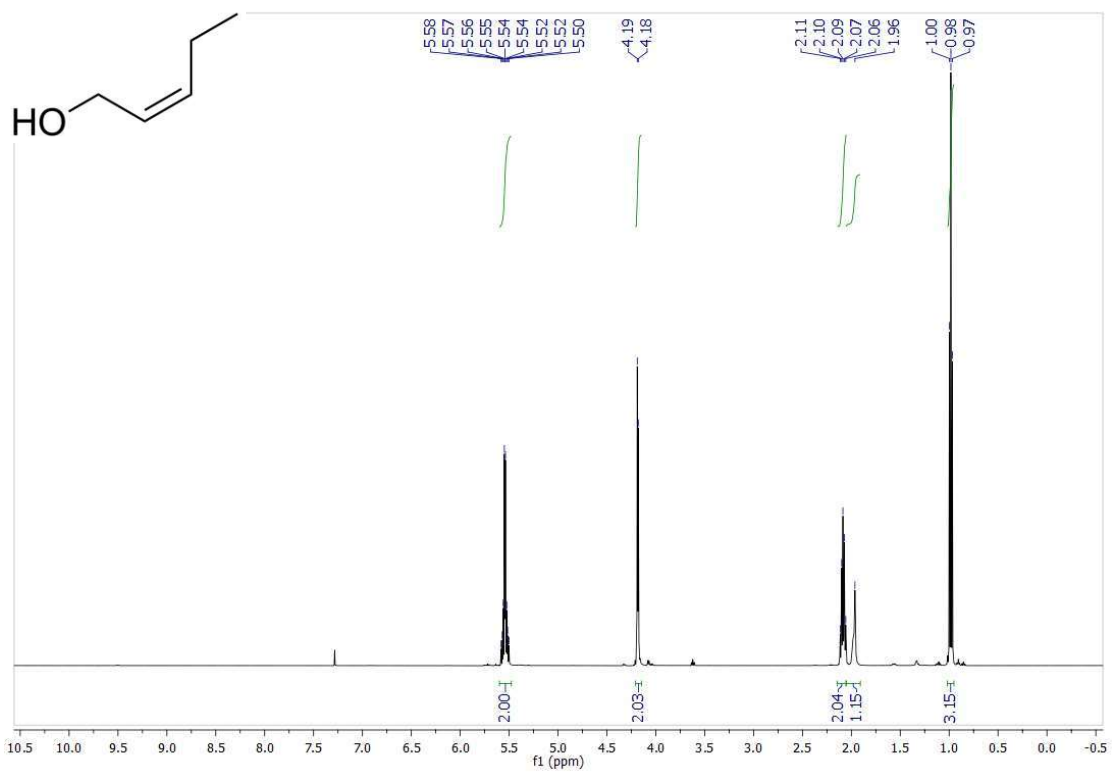


Figure S10. ¹H and ¹³C NMR Spectrum of 2y

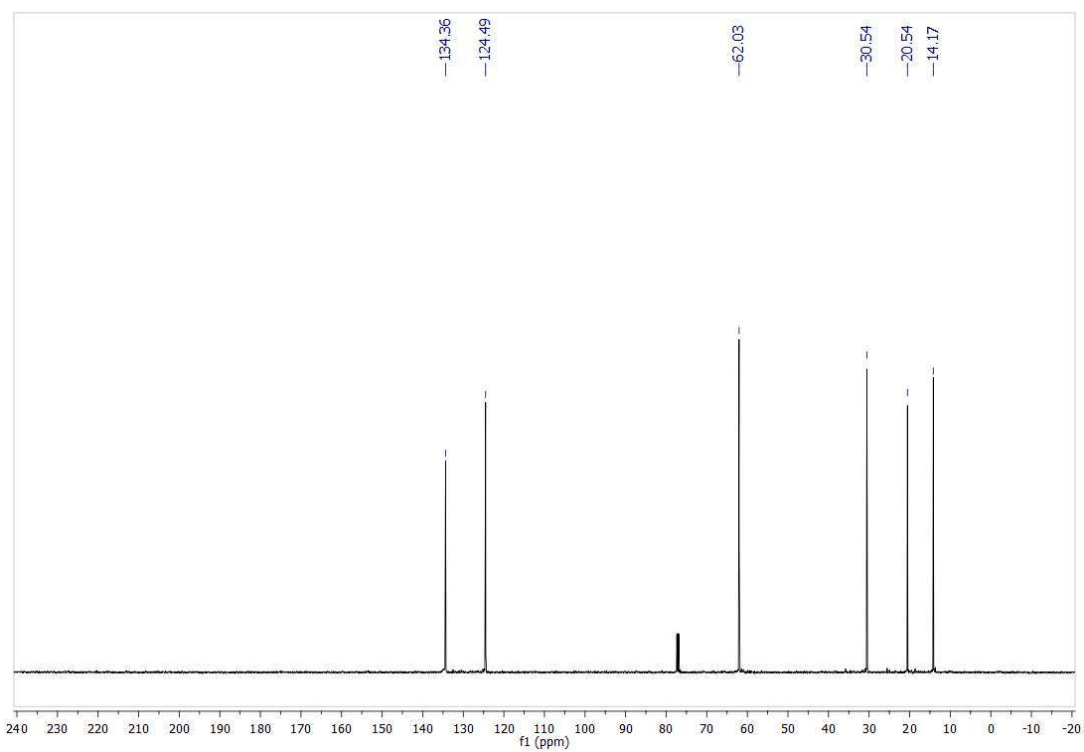
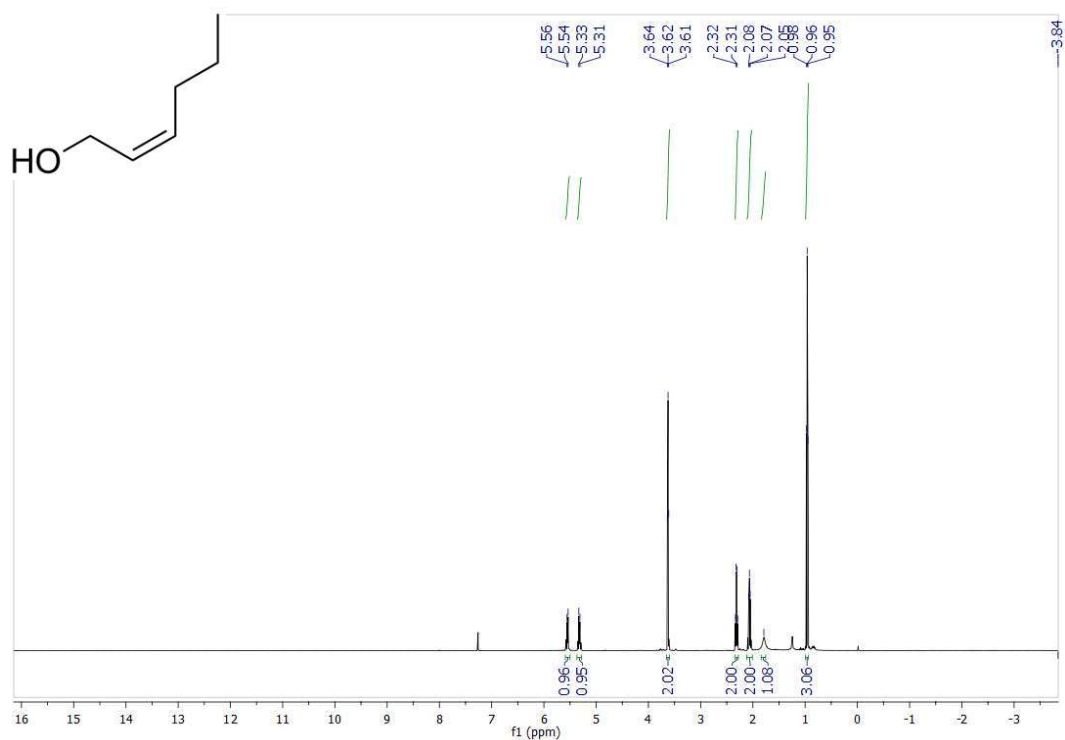


Figure S11. ¹H and ¹³C NMR Spectrum of **2a**

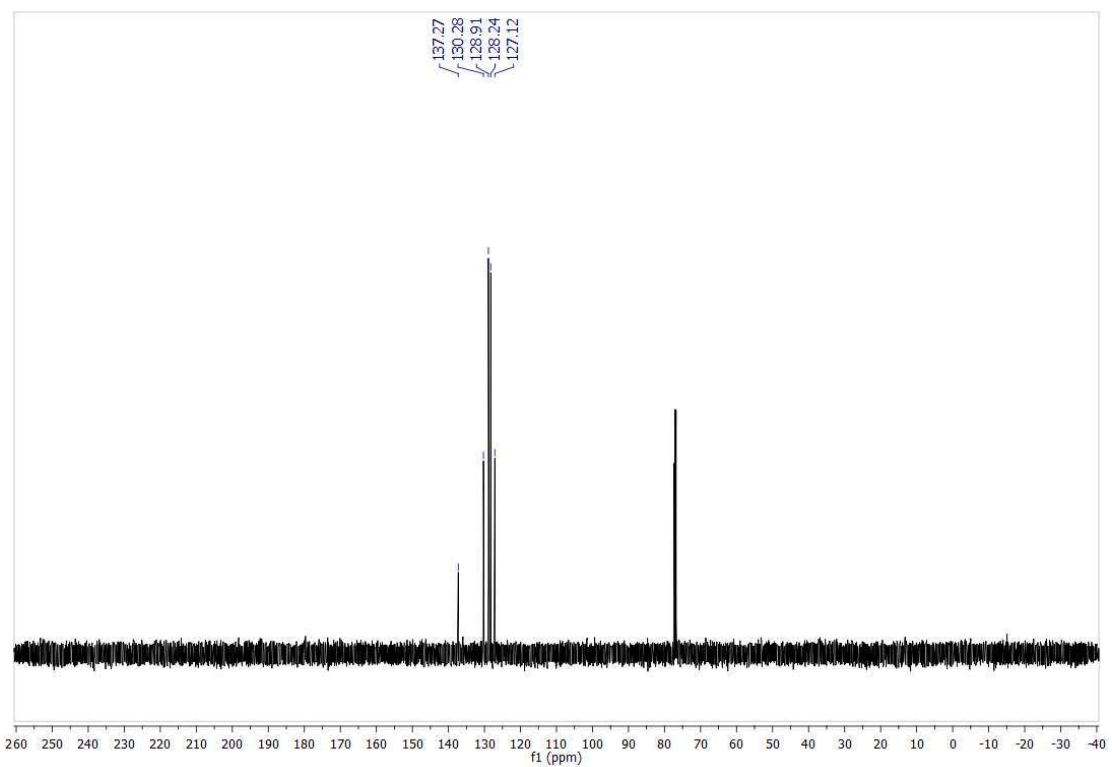
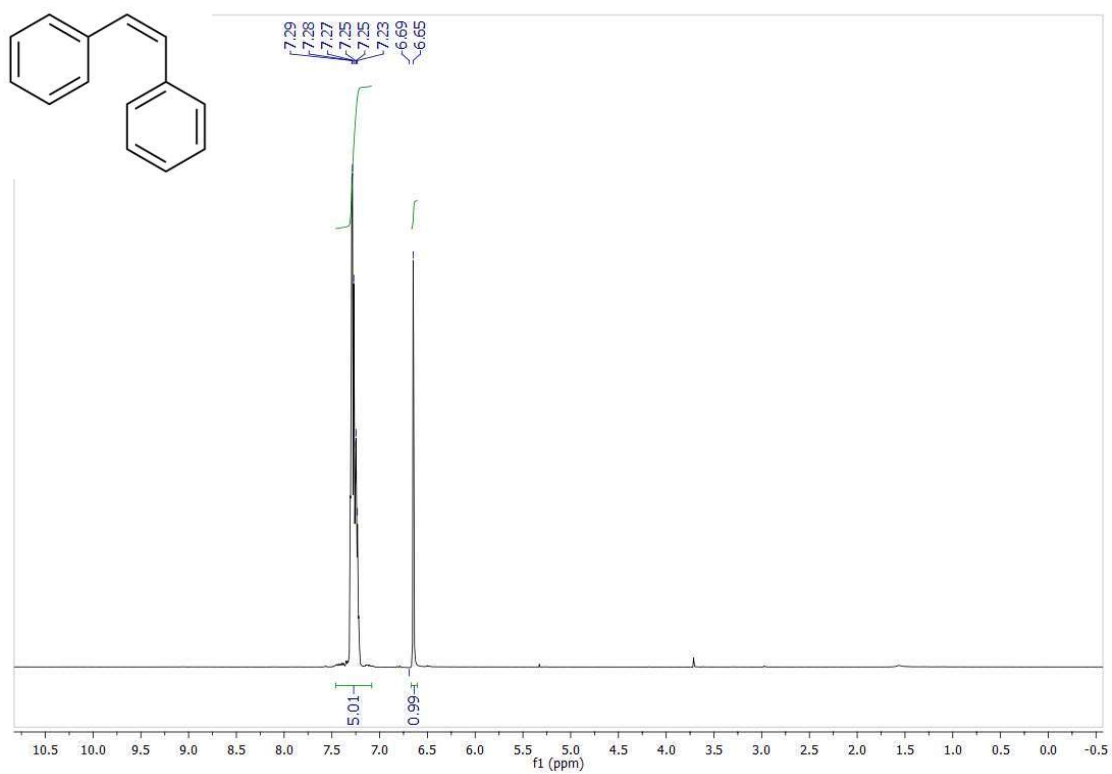


Figure S12. ¹H and ¹³C NMR Spectrum of **2ae**

Appendice A3. Curricular Summary

1. PERSONAL DATA

Name: Jhonatan Luiz Fiorio

Date and place of birth: 25 de fevereiro, Pato Branco – PR.

2. EDUCATION BACKGROUND

Msc. in Bioenergy (2012-2014)

Department of Chemistry, State University of Londrina, Londrina, Brazil

B.S. in Chemistry (2008 - 2011)

Department of Chemistry, Federal University of Technology - Paraná, Pato Branco, Brazil

***Licentiate* in Chemistry (2008 - 2011)**

Department of Chemistry, Federal University of Technology - Paraná, Pato Branco, Brazil

3. MOST RELEVANT SCIENTIFIC RESULTS

Fiorio, J. L.; Silva, F. P da; Gonçalves, R. V.; Teixeira-Neto, E.; Rossi, L. M. Synergic effect of copper-palladium nanoparticle catalyst for selective hydrogenation of alkynes. *Ind. Eng. Chem. Res.*, **2018**, DOI: 10.1021/acs.iecr.8b03627.

Quiroz, J.; Barbosa, E. C. M.; Araujo, T. P.; Fiorio, J. L.; Wang, Y. C.; Mou, T.; Alves, T. V.; Oliveira, D. C.; Wang, B.; Haigh, S. J.; Rossi, L. M.; Camargo, P. H. C. Controlling Reaction Selectivity over Hybrid Plasmonic Nanocatalysts. *Nano Letters*, **2018**, DOI: 10.1021/acs.nanolett.8b03499.

Fiorio, J. L.; Gonçalves, R. V.; Teixeira-Neto, E.; Lopez, N.; Rossi, L. M. Accessing Frustrated Lewis Pair Chemistry through Robust Gold@N-Doped Carbon for Selective Hydrogenation of Alkynes. *ACS Catalysis*, **2018**, DOI: 10.1021/acscatal.8b00806. (Highlighted in Synfacts)

Rossi, L. M.; Fiorio, J. L.; Garcia, M. A. S.; Ferraz, C. P. The role and fate of capping ligands in colloiddally prepared metal nanoparticle catalysts. *Dalton Transactions*, **2018**, DOI: 10.1039/C7DT04728B.

Barbosa, E. C. M.; Fiorio, J. L.; Mou, T.; Wang, B.; Rossi, L. M.; Camargo, P. H. C. Reaction Pathway Dependence in Plasmonic Catalysis: Hydrogenation as a Model Molecular Transformation. *Chemistry - A European Journal*, **2018**, DOI: 10.1002/chem.201705749. (Hot Paper)

Fiorio, J. L.; Lopez, N.; Rossi, L. M. Gold-ligand catalyzed selective hydrogenation of alkynes into cis-alkenes via H₂ heterolytic activation by frustrated Lewis pairs. *ACS Catalysis*, **2017**, DOI: 10.1021/acscatal.6b03441.

Silva, F. P da; Fiorio, J. L.; Rossi, L. M. Tuning the catalytic activity and selectivity of Pd nanoparticles using ligand-modified supports and surfaces. *ACS Omega*, **2017**, DOI: 10.1021/acsomega.7b00836.

Fiorio, J. L.; Gonçalves, R. V.; Teixeira-Neto, E.; Lopez, N.; Rossi, L. M. Design of gold nanoparticle catalysts for chemoselective hydrogenations: N-doped carbon as support. Oral presentation In: GOLD, 2018, Paris. GOLD, 2018.

Fiorio, J. L.; Rossi, L. Highly selective deoxygenation of epoxides over magnetically recoverable gold catalyst. Oral presentation In: 46th World Chemistry Congress, 40a Reunião Anual da Sociedade Brasileira de Química, and IUPAC 49th General Assembly, 2017, São Paulo, Brazil.

Fiorio, J.L.; Lopez, N.; Rossi, L. M. Switching on the Catalytic Activity of Gold for Alkyne Hydrogenation: a frustrated Lewis Pairs approach for Hydrogen Dissociation. Poster presentation In: North American Catalysis Society Meeting 2017 - NAM25, 2017, Denver. North American Catalysis Society Meeting 2017 - NAM25, 2017.

Rossi, L. M.; Silva, F. P.; Fiorio, J.L. Ligand-assisted Preparation of Nanoparticles-supported Catalysts: Taking Advantage of Catalyst Poisoning. Poster presentation In: North American Catalysis Society Meeting 2017 - NAM25, 2017, Denver. North American Catalysis Society Meeting 2017 - NAM25, 2017.

4. INTELLECTUAL PROPERTY: PATENT

Rossi, L. M.; Fiorio, J. L. Heterogeneous catalyst of carbon doped with nitrogen and gold for hydrogenation reactions. 2018, Brazil. Patent: Innovation privilege. Patent protect under the no.: BR1020180049020, Registration institution: INPI - Instituto Nacional da Propriedade Industrial, Deposit: 12/03/2018